

**Osteological analysis of human remains found within passageways  
at the old parish church of St Catherine (known as St Gregory),  
Żejtun (Malta).**

**Debra Jane Camilleri**

**Supervisor: Ms Bernardette Mercieca-Spiteri  
Co-Supervisor: Dr Gianmarco Alberti**

**A dissertation presented to the Faculty of Arts, in the  
University of Malta in part fulfilment of the degree of  
Masters of Archaeological Practice  
July 2022.**



L-Università  
ta' Malta

## **University of Malta Library – Electronic Thesis & Dissertations (ETD) Repository**

The copyright of this thesis/dissertation belongs to the author. The author's rights in respect of this work are as defined by the Copyright Act (Chapter 415) of the Laws of Malta or as modified by any successive legislation.

Users may access this full-text thesis/dissertation and can make use of the information contained in accordance with the Copyright Act provided that the author must be properly acknowledged. Further distribution or reproduction in any format is prohibited without the prior permission of the copyright holder.



L-Università  
ta' Malta

FACULTY/INSTITUTE/CENTRE/SCHOOL Faculty of Arts

Student's I.D. /Code 057016L

Student's Name & Surname Debra Jane Camilleri

Course Masters of Archaeological Practice

Title of Dissertation/Thesis  
Osteological analysis of human remains  
found within passageways at the old parish church of  
St Catherine (Known as St Gregory), Zejtun (Malta).

I am hereby submitting my dissertation/thesis for examination by the Board of Examiners.

  
Signature of Student

DEBRA JANE CAMILLERI  
Name of Student (in Caps)

1 July 2022  
Date

Submission noted.

BERNARDETTE  
MERLIECA-SPITERI  
Principal Supervisor  
(in Caps)

  
Signature

1 July 2022  
Date

## ABSTRACT

The 1969 discovery of commingled human remains found in the hidden rooftop passageways of the 15<sup>th</sup> century old parish of St Catherine's, now known as the Chapel of St Gregory (San Girgor) in Żejtun (Malta), has intrigued locals for decades. Believed to be the remains of victims of an Ottoman attack in the 17<sup>th</sup> century, studies conducted on these remains ten years after being discovered left unanswered questions surrounding their temporal period, population affinity and how they came to be in these passageways.

Demographic analysis (sex, age, and ancestry) using metric and non-metric skeletal analysis is performed in this study, incorporating radiocarbon dating results and extensive archival research. To obtain evidence that the site is not a primary burial, studies are performed on antemortem fractures, postmortem taphonomic processes, and tool marks to rule out interpersonal violence. In addition, using GIS (geographic information systems) software, a 'geographical landscape' on human bone is created to visualize large amounts of osteological data. Femurs are used as base maps on which features are 'mapped' to determine density patterns that provide a spatial representation of data.

This study demonstrates the advantages of using several techniques to understand commingled remains in archaeological and historical settings and encourages the future use of GIS in documenting, collecting, and analysing human remains.

The concluding results show that the remains found in the passageways make up at least ninety-two males and females who are primarily older adults, originally buried elsewhere. Although most of the individuals are of European ancestry, five of the individuals are deemed to be most probably sub-Saharan enslaved persons, substantiated by information found in the parish archives.

*"Doubt is an uncomfortable condition, but certainty is a ridiculous one."*

*Voltaire 1664-1778*

## **ACKNOWLEDGEMENTS**

The guidance of my supervisor, Ms Bernardette Mercieca-Spiteri has been instrumental in the completion of this dissertation and her expertise in the field of osteology is much admired. I am thankful for her reigning me in when needed and for our interesting talks. Thanks also goes to Dr Gianmarco Alberti, co-supervisor, whose sense of humour and knowledge of GIS added a very important and unique aspect to this dissertation.

The sincere interest of many in the conservation and promotion of cultural heritage was the impetus for this dissertation. My gratitude goes to Mr Joseph Magro Conti (former Superintendent) and Mr Kurt Farrugia (present Superintendent) at the Superintendence of Cultural Heritage (SCH) without whose support this study could not have taken place, and SpatialTRAIN for the scholarship. Sincere thanks goes to Kevin Borda, Head of Unit of National Inventory, Archaeology and Research at SCH who was a key guiding figure and source of encouragement, providing the much-needed lab space to analyse the huge collection.

I would like to extend my thanks to the Parish Priest of San Girgor for unrestricted access to the human remains; to Wirt Żejtun President Ruben Abela who provided me with private site access numerous times and who shared his thoughts and knowledge willingly; to Mr Tony Gerardi who manages the Parish archives with the utmost care and Mr Matthew Grima, Heritage Malta who kindly shared the radiocarbon dating results with me. I must thank my colleagues who offered encouragement when the exhaustion set in; my friends and family who spent countless hours listening to me talk about my findings with excitement; and my 'study buddy' who provided encouragement as we ploughed through our own respective piles of research. A final thanks to the Department of Classics and Archaeology and all the professors who made their lectures so very interesting, each having a small part to play in the development of this dissertation. The experience has been rewarding and inspirational to say the least.



The research work in this dissertation is funded by the ESF.04.071 SpatialTRAIN Scholarship Scheme. The scholarship is part-financed by the European Union – European Social Fund (ESF) under Operational Programme II – Cohesion Policy 2014-2020, "Investing in human capital to create more opportunities and promote the well-being of society".



Operational Programme II – European Structural and Investment Funds 2014-2020  
"Investing in human capital to create more opportunities and promote the well-being of society."  
Project part-financed by the European Social Fund  
Co-financing rate: 80% European Union; 20% National Funds



## TABLE OF CONTENTS

ABSTRACT .....	i
ACKNOWLEDGEMENTS.....	ii
TABLE OF CONTENTS .....	iv
LIST OF FIGURES .....	ix
LIST OF TABLES.....	xiii
CHAPTER 1. INTRODUCTION.....	1
1.1 Importance of this study.....	2
1.2 Aims and Objectives .....	3
1.3 Historical Context .....	4
1.4 Construction of the Chapel .....	8
1.5 Discovery of the Passageways and Contents .....	12
CHAPTER 2. LITERATURE REVIEW .....	21
2.1 Commingled Remains.....	21
2.2 Background of Osteological Analysis .....	25
2.3 Burial Settings & Cemeteries.....	26
2.4 Decomposition and Positioning .....	28
2.5 Determining Size of Population.....	29
2.5.1 Fragmentation .....	31
2.5.2 Pair Matching.....	32
2.6 Sexing and Ageing .....	33

2.6.1 Sexing .....	33
2.6.2 Ageing .....	35
2.7 Ancestry .....	39
2.7.1 Cranial Non-Metric and Metric Approaches in Ancestry Estimation .....	39
2.7.2 Postcranial Non-Metric and Metric Approaches .....	43
2.8 Pathology .....	43
2.9 Taphonomy or Trauma?.....	44
2.10 Trauma Analysis and Cut Marks .....	46
2.11 Geographic Information Systems (GIS) .....	48
2.12 Future of Studying Commingled Remains .....	52
<b>CHAPTER 3. METHODOLOGY .....</b>	<b>54</b>
3.1 Establishing MNE and MNI .....	55
3.2 Assessment of Taphonomy and Trauma – GIS-based approach .....	56
3.3 Sexing .....	57
3.3.1 Os Coxae: Non-Metric Analysis .....	59
3.3.2 Sexing Os Coxae: Metric Analysis .....	62
3.4 Sexing: Metric and Non-Metric Analysis of the Crania .....	64
3.5 Mandibles.....	69
3.6 Ageing.....	69
3.6.1 Ageing: Non-Metric Analysis of the Os Coxae .....	70
3.6.2 Ageing: Epiphyseal Fusion .....	73



3.6.3 Ageing: Cranial Sutures .....	77
3.6.4 Ageing Based on Fusion of the Spheno-occipital synchondrosis .....	78
3.6.5 Ageing: Odontology.....	79
3.7 Ancestry Determination .....	80
<b>CHAPTER 4. RESULTS.....</b>	<b>84</b>
4.1 MNE/MNI.....	84
4.2 Bone Representation Index (BRI).....	84
4.3 Sexing, Siding and Ageing of the Os Coxae.....	86
4.2 Dental Assessment .....	88
4.4 Sexing and Ageing of Crania.....	88
4.6 Indices .....	91
4.5 Ancestry Determination using Crania.....	95
4.7 Comparative Analysis.....	97
4.8 Radiocarbon Dating Results .....	98
4.9 Taphonomy and GIS .....	100
<b>CHAPTER 5. DISCUSSION .....</b>	<b>103</b>
5.1 Hidden Passageways and Skeletal Remains .....	104
5.2 Burials in Malta.....	107
5.3 Population .....	109
<b>CONCLUSION.....</b>	<b>120</b>
<b>REFERENCES .....</b>	<b>123</b>

APPENDIX I: Full Inventory and raw data for analyses (Appendix I.A – I.G).....	136
APPENDIX II: Glossary .....	137
APPENDIX III: List of Morphological pelvic traits used for sex determination .....	139
APPENDIX IV: Cranial Landmarks used for non-metric sex estimation.....	140
APPENDIX V: Craniometric Points on the Midsagittal Plane (MSP) .....	141
APPENDIX V: Continued.....	142
APPENDIX VI: Important Indices used for comparative analysis..	143
APPENDIX VII.A: Phases of morphological changes in the Pubic Symphysis – Age estimation using the Suchey-Brooks Method .....	144
APPENDIX VII.B: Suchey-Brooks method: Associated ages with phases to estimate age - based on descriptions of morphological changes in the pubic symphysis.....	145
APPENDIX VIII.A: Morphological changes to the auricular surface – Age estimation .....	146
APPENDIX VIII.B: Auricular surface - Scoring to determine age estimation based on revisions by Buckberry and Chamberlain (2002) .....	146
APPENDIX IX: Cranial suture observation sites and definitions, used to estimate age. ....	147
APPENDIX X: Location of cranial sutures and scoring key to determine age.....	148
APPENDIX XI: Human tooth development following.....	149
APPENDIX XII: Non-metric traits for ancestry determination.....	150

APPENDIX XIII: Ancestry determination measurements utilised, following worksheet and form created by Giles and Elliot (1962) and Gill (1984). .....	151
APPENDIX XIV: List of Bone Elements for San Girgor assemblage with MNE, MNI and BRI. ....	152
APPENDIX XV: Results of indices for those determined to be of sub-Saharan Ancestry. ....	157
APPENDIX XVI: Radiocarbon dating results of samples taken from the human remains at San Girgor (Molnár 2020: 1-5 and 1-2).....	158
APPENDIX XVII: Baptisms and confirmation of enslaved persons 1586 -1693 .....	164

## LIST OF FIGURES

Figure 1. Framed pictures of the discovery from 12 <sup>th</sup> March 1969 showing the sacristan next to the human remains found in Passageway 2 and 3.....	5
Figure 2. Human remains inventoried and logged from the passageways at the Chapel of San Girgor, stacked on wooden shelving units in Passageway 3.....	5
Figure 3. Site Map showing the location of the old parish of St Catherine's, now known as the Chapel of San Girgor in Żejtun.....	6
Figure 4. Old Parish of St Catherine circa 1940s, now known as San Girgor.....	7
Figure 5. Map of south eastern area of Malta showing San Girgor and surrounding bays..	7
Figure 6. Chapel of San Girgor, front facing entrance with cemeteries on the west and south sides .....	8
Figure 7. North side of the Chapel of San Girgor; (a) older entrance now blocked, most likely was an annex to a previously existing chapel;(b) foundations of a smaller chapel visible.....	9
Figure 8. East side of Chapel of San Girgor: (a) lookout windows; (b) buttress; (c) a tower-like structure where the present-day spiral staircase is located.....	9
Figure 9. South side of the Chapel of San Girgor.....	10
Figure 10. East side of Chapel of San Girgor showing buttress fortification on the south-east side.....	10
Figure 11. Close-up of Chapel from above as it is situated today with the location of three passageways; (a) Passageway 1; (b) Passageway 2; (c) Passageway 3 .....	12
Figure 12. Architectural plan of San Girgor .....	13
Figure 13. Roof top of Chapel of San Girgor. Facing west. ....	13
Figure 14. Dome on roof, Chapel of San Girgor. Facing south with views of Birżebbuġa. Arrows indicate: (a) Passageway 2; (b) Passageway 3; (c) external staircase .....	14
Figure 15. Roof of Chapel of San Girgor, facing northwest with views of St Thomas Bay .....	14
Figure 16. West facing, showing external staircase to roof, Chapel of San Girgor .....	15
Figure 17. (a) Trap door to enter the hidden passageways from the roof of the Chapel (b) ledge just below trap door; (c) entrance way to Passageway 1; (d) steps.....	15
Figure 18. Hidden Passageway 1.....	16
Figure 19. Hidden Passageway 2, Blind Corner, Chapel of San Girgor.....	16

Figure 20. Lookout window, Hidden Passageway 2, Chapel of San Girgor .....	17
Figure 21. Hidden Passageway 3, Chapel of San Girgor .....	18
Figure 22. Cross incised into wall, Hidden Passageway 2, Chapel of San Girgor. ....	19
Figure 23. Inscription on wall above window in Passageway 2 ‘Carmelo Zahra 1909’, Chapel of San Girgor .....	19
Figure 24. Inscription on wall in Passageway 2, 'Giovanni Zahra 1909' (or 1969?) opposite previous inscription, Chapel of San Girgor .....	20
Figure 25. Sexual dimorphism in os coxae. Phenice method assessing 3 features on the pubis: (a) subpubic concavity (dorsal side), (b) medial aspect of ischiopubic ramus, and (c) ventral arc .....	60
Figure 26. Sexual dimorphism in the greater sciatic notch.....	61
Figure 27. Landmarks for sexing the os coxae using Ischium-Pubis Index (IPI) .....	63
Figure 28. (a) ID SGR2019/1750 right os coxae, older adult female; (b) ID SGR2019/1746 right os coxae, older adult male. Notice evidence of tool/cut-marks. Anterior view. ....	64
Figure 29. Sex determination using sexually dimorphic features of the cranium with a qualitative scoring system.....	65
Figure 30. (a) ID SGR2019/758 older adult male, European; (b) ID SGR2019/725 adult female, European. ....	66
Figure 31. (a) ID SGR2019/758 older adult male, European; (b) ID SGR2019/1740 adult female, European; (c) ID SGR2019/1785 sub-adult female, European (?). ....	66
Figure 32. Craniometric landmark points .....	68
Figure 33. ID SGR2019/755 adult female, European (?), inferior view. Landmark points shown, used for craniometric analysis. Spheno-occipital synchondrosis used for ageing.. .....	68
Figure 34. (a) ID SGR2019/1614 left os coxae, older adult female; (b) ID SGR2019/1754 left os coxae, adult male, anterior view .....	70
Figure 35. Age determination based on morphological changes of pubic symphysis - using Suchey-Brooks method.....	71
Figure 36. Age estimation based on morphological changes of the auricular surface in males and females .....	73
Figure 37. Age of epiphyseal fusion of various skeletal elements.....	74
Figure 38. (a) ID SGR2019/256 left os coxae, child, male (?), posterior view; (b) ID SGR2019/232 left os coxae, subadult, female, anterior view .....	75

Figure 39. (a) ID SGR2019/100 right femur, subadult; (b) ID SGR2019/128 left femur, subadult. Anterior view.....	76
Figure 40. (a) ID SGR2019/617 right tibia, adult, anterior view; (b) IDSGR2019/1580 left tibia, adult, medial view; (c) ID SGR2019/667 left tibia, subadult, medial view; (d) ID SGR2019/624 left tibia, adult, medial view.....	76
Figure 41. Age estimation using visual inspection of cranial suture closure based on distinct points.....	78
Figure 42. Maxillary and mandibular permanent and deciduous dentition .....	79
Figure 43. (a) ID SGR2019/713; (b) ID SGR2019/1730; (c) ID SGR2019/714; (d) ID SGR2019/754; (e) ID SGR2019/715. Adult sub-Saharan females, frontal view .....	83
Figure 44. Percentage of bone elements represented, based on the MNI of 92.....	85
Figure 45. Graphic representation of age distribution based on os coxae.....	88
Figure 46. Graphic representation of age distribution based on 29 crania.....	90
Figure 47. Morphometric Analysis based on Indices .....	95
Figure 48. Index analysis of five female sub-Saharan crania. ....	97
Figure 49. Timeline chart of radiocarbon dating results for samples from San Girgor assemblage .....	99
Figure 50. Polygons of four views of left and right femur, with proximal, mid-shaft and distal ends presented in separate polygons. ....	101
Figure 51. Polylines representing tool/cut marks on left and right femurs. ....	101
Figure 52. Heat map showing ‘hot spots’ of tool/cut marks.....	102
Figure 53. Notes written by Professor M. Buhagiar 18 <sup>th</sup> April 1969, over one month after the site was discovered.....	104
Figure 54. Close up of crania; human remains found in the passageways of the Chapel of San Girgor.....	106
Figure 55. Close up of the inventorized human remains which were placed on wooden shelves in Passageway 3, Chapel of San Girgor .....	107
Figure 56. Evidence of baptism of two female adult ‘Black slaves’ in 1587 .....	111
Figure 57. Evidence of the baptism of a female ‘Black slave’ in 1587. ....	112
Figure 58. Evidence of the baptism of a female ‘Black slave’ in 1601. ....	113
Figure 59. Evidence of the baptism of a male and female adult ‘slave’ where affinity is not noted in 1588 .....	113

Figure 60. 1743 Map of West Africa .....	115
Figure 61. Evidence in the 1663 census of two female ‘Black slaves’ and one male ‘Black slave’, as well as a servant (affinity not identified) living within a household.....	117
Figure 62. (a) “Two Maltese noble women with their African slave”; (b) “Maltese noble woman with her African slave”. Painter Unknown. ....	118

## LIST OF TABLES

Table 1. Abbreviations used to log tool/cut marks on femurs. Raw data is available for reference in Appendix I.B. ....	57
Table 2. Siding of left (L) and right (R) os coxae for males and females. Raw data for analyses is available in Appendix I.C. ....	86
Table 3. Age Distribution of 64 male and female os coxae. ....	87
Table 4. Sex determination and distribution of 29 crania. Raw data for analyses is available in Appendix I.D. ....	89
Table 5. Age estimation and distribution based on 29 crania. Raw data for analyses is available in Appendix I.E. ....	89
Table 6. Age estimation and distribution based on 29 mandibles. ....	90
Table 7. Cranial Index (CI) statistical results. ....	91
Table 8. Upper Facial Index (UFI) statistical results. ....	92
Table 9. Nasal Index (NI) statistical results. ....	93
Table 10. Maxilloalveolar Index (MI) statistical results. ....	94
Table 11. Palatal Index (PI) statistical results. ....	94
Table 12. Descriptive Statistics: sex, age at death, & ancestry using 16 crania. Raw data for analyses is available in Appendix I.G. ....	96



## **CHAPTER 1. INTRODUCTION**

In 1969, commingled skeletal human remains were found in hidden passageways of the old parish of St Catherine's in Żejtun, Malta, now known as the Chapel of San Girgor. The discovery cultivated various beliefs for decades, about how the individuals came to rest in this location. Although the remains were analysed ten years after their initial discovery, questions remained unanswered regarding their location of origin, temporal period, and population affinity.

The aim of this dissertation is to utilise methods which were not pursued decades ago, in the context of recently obtained radiocarbon dating results, to provide further insight about the large assemblage of remains found in these passageways.

Researchers assessing skeletal remains are often required to analyse incomplete, fragmented, or commingled material of what may initially seem to be confusing assemblages. The fact that the commingled remains from the Chapel of San Girgor (from this point forward called San Girgor) is a very large assemblage makes the task significantly more complex and time consuming. Despite this, following standardised methods and practices in osteological analysis provides the foundation to sort through an assemblage, one bone at a time, and move towards a coherent understanding.

Ramaswamy and Pace (1979, 1980) first assessed the material from this assemblage in 1979, however, with limited archival information and no specific knowledge on the period to which these human remains belonged, gaps existed in their research reports.

This dissertation provides a unique opportunity to present the assessment of the skeletal elements found in the hidden passageways of San Girgor along with a comparative analysis of Ramaswamy and Pace's (1979, 1980) studies.

For the past 50 years, beliefs have circulated regarding the nature of these remains. This dissertation aims to clarify the origin of the remains and how they came to be

in the ‘secret passageways’ of San Girgor by assessing the actual skeletal evidence and by investigating taphonomic indicators, burial environment, and perimortem evidence versus postmortem alterations that have occurred due to disturbance that affected the skeletal remains.

This study begins with a literature review (Chapter 2) of the various methods used for osteological analysis of commingled remains including metric and non-metric traits. A review is given of a GIS-based approach (geographic information systems) and its applicability to the study of human skeletal remains, stemming from its use in zooarchaeology, encouraging a multidisciplinary approach. The various methods used to assess the skeletal remains are discussed thoroughly in Chapter 3, followed by a critical review of the methods and usefulness of assessing ancestry in order to determine population affinity. Naturally, the fundamental goal is to assess the skeletal evidence presented in Chapter 4 to understand who these individuals may be and to suggest how the human remains came to rest in the hidden rooftop passageways of a 700-year-old church. Finally, the intensive archival research coupled with recent radiocarbon dating results provides further insight into the origins of the commingled remains of San Girgor discussed in Chapter 5.

### *1.1 Importance of this study*

Bonnici (2019:448) notes that since their discovery in 1969, there were varying theories regarding the origins of the human remains found at San Girgor. Some believed that the remains belonged to those hiding from and later killed by the Turks in the Ottoman attack of 1614, or that they were left behind and starved to death (The Sunday Times 1969:55).

Over forty years ago in 1979, ten years after the initial discovery, the human remains of this commingled assemblage were the subject of a palaeopathological and anthropological analysis by Ramaswamy and Pace (1979, 1980). Their report provided a demographic profile of the remains with an assessment of the number of individuals, their sex, age, and pathologies, with the aim of ascertaining whether evidence existed to show prior burial under soil (Ramaswamy and Pace 1980:56). Based on their studies, Ramaswamy and Pace (1979:68) thought it was likely that

the remains could have come from burials around the area, removed when the church was being extended in the late 16<sup>th</sup> century or early 17<sup>th</sup> century and concluded that the passageways were probably used as an ossuary, therefore for secondary burial of the remains (Ramaswamy and Pace 1980:69).

Unfortunately, the raw data and bone inventory on which Ramaswamy and Pace's (1979, 1980) reports were based are no longer available and have possibly been lost. In addition, the reports do not suggest a date for the skeletal remains, or a date when the remains were placed within the passageways, nor does it suggest who these individuals might have been. The report does suggest the use of radiocarbon dating in the future to further clarify the origins of these remains.

The Superintendence of Cultural Heritage (SCH), in collaboration with Wirt iż-Żejtun and Heritage Malta, recognized the importance and the need for additional scientific analysis and research that could shed further light on this assemblage (Abela and Grima 2018, Heritage Malta & Wirt iż-Żejtun, Unpublished Report).

This was the springboard for the present study, which will focus on the nature and origins of the human remains found in the passageways of San Girgor. The results of demographic profiles, taphonomy, trauma and the ancestry analysis, as well as radiocarbon dating results and archival research are applied to justify conclusions made in this dissertation.

### *1.2 Aims and Objectives*

The aims and objectives of this dissertation are (1) to assess and extrapolate data from the commingled human remains, (2) to develop biological profiles, (3) to attempt the determination of ancestry of the individuals through osteological analysis, (4) to understand the trauma and taphonomic damage on bone elements, and finally (5) to show that the osteological analysis, in conjunction with extensive archival research and results of radiocarbon dating, can provide a historical link and context for the human remains found in the San Girgor passageways.

In order to carry out this study, an inventory of the skeletal material was necessary to account for each and every human bone, followed by the determination of the

sex, age, and ancestry of the individuals represented in the skeletal assemblage for the development of biological profiles. Antemortem, perimortem and postmortem trauma, pathologies and taphonomic damage were also assessed to check for any indications on the potential cause of death of the individuals. Perimortem evidence such as trauma resulting from violence could indicate the individuals had died at the site making this a primary burial. Antemortem trauma (for example healed fractures) or postmortem evidence (damage from tools on skeletal material after death) on the other hand could indicate the individuals had been moved from another area such as a cemetery, making this a secondary burial. A GIS-based approach to visually represent the spatial distribution and density of trauma and taphonomic damage will corroborate evidence of displacement and secondary burial and will show the applicability of this approach on skeletal material.

### *1.3 Historical Context*

To understand the presence of human remains in the passageways of the chapel and how this site became an element of fascination in the fabric of Maltese culture, one must understand the historical context of the old Parish of St Catherine's, now known as San Girgor.

Figure 1 shows a series of framed photographs, providing some of the first images from 1969 of the human remains exposed on the surface of the passageways made of fine sand. There are three passageways noted in this study referred to as Passageway 1, 2 and 3. The bones were subsequently stacked on shelving in Passageway 3, following studies in 1979 and 1980 (Ramaswamy and Pace 1979, 1980) to allow visitor access over the last 50 years. On completion of this present study, the inventoried and tagged remains were safely placed on wooden shelves again in Passageway 3, for continued visitor access (refer to Figure 2).



Figure 1. Framed pictures of the discovery from 12<sup>th</sup> March 1969 showing the sacristan next to the human remains found in Passageway 2 and 3. Courtesy of Wirt Iż-Żejtun. Pictures taken in April 1969.



Figure 2. Human remains inventoried and logged from the passageways at the Chapel of San Girgor, stacked on wooden shelving units in Passageway 3. Photograph by author, October 2020.

The area of Żejtun as it is known today, in which these remains were found, is located in the south eastern region of the Island of Malta (Figure 3). Until 1650, it was known as one of the *contrade* (districts) of the *Cappella Sancta Catherina*, which is the Parish of St Catherine's (Fiorini 2014:83), now known as San Girgor.

This parish, second in size to that of Mdina, was one of the twelve parishes (*cappellanie*) in Malta mentioned by Bishop de Mello in the Rollo (inventory) of 1436, providing evidence that parishes had already been well established (Ciappara 2008:675). Various districts and small hamlets made up the parish (Fiorini 2014:84) and by the early 17<sup>th</sup> century, the parishes of Żabbar and Għaxaq separated from San Ġirgor, becoming established in 1615 and 1626 respectively (Malta Parish Archives 2021).



Figure 3. Site Map showing the location of the old parish of St Catherine's, now known as the Chapel of San Ġirgor in Żejtun, circled in red. Taken from Geoserver 2021. Inset Map of Malta and Gozo. Żejtun area, circled in red. Google Maps 2021.

Although located in a very rural area, during the 15<sup>th</sup> and 16<sup>th</sup> centuries San Ġirgor was situated in the middle of its districts (Figure 4), making it easier for parishioners to attend, whilst being convenient for clergy to service the needs of their parishioners.



Figure 4. Old Parish of St Catherine circa 1940s, now known as San Ġirġor. Courtesy of Dr Ruben Abela. Taken from Fiorini (2014:85).

The area of Żejtun was known to be a major trading centre as well as a residential area for merchants making the sheltered harbours around Żejtun very strategic and attractive to the corsairs and enemies who regularly attacked Malta (Fiorini 2014:83). Located on one of the highest points in south-east Malta, at 60 metres above sea level, Żejtun and San Ġirġor for that matter, have excellent vantage points from where two significant harbours and ports could be seen including St Thomas Bay in the northwest, Marsaxlokk in the southeast and Marsascula Bay in between, to the east (refer to Figure 5).



Figure 5. Map of south eastern area of Malta showing San Ġirġor circled in red, and key surrounding bays. Taken from Google Maps 2021.

#### *1.4 Construction of the Chapel*

There is no known documentation providing a specific date for the establishment of the old parish church of St Catherine's and the burial grounds associated with it, however archival information does provide a frame of reference.

Buhagiar notes that the inscriptions within the church indicate that it was rebuilt and enlarged in 1492 from the original smaller, plain rectangular shaped structure. This would have been located where today we have the walls of the nave of the original chapel with the later additions extending beyond the footprint of the old chapel with transepts to the east-west (Buhagiar 1979:77). By the early 17<sup>th</sup> century, after several additions, the parish church would have looked very much like the present structure we see today, in the form of a cross (Figures 6 to 10 show the chapel and its walls).



Figure 6. Chapel of San Girgor, front facing entrance with cemeteries on the west and south sides. Photograph by author, October 2020.



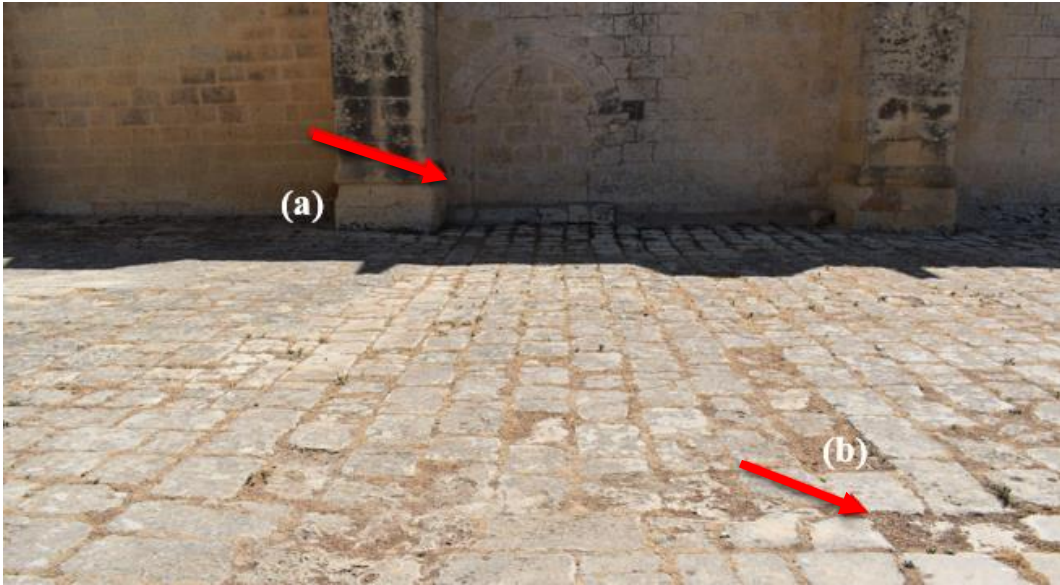


Figure 7. North side of the Chapel of San Girgor; (a) older entrance now blocked, most likely was an annex to a previously existing chapel;(b) foundations of a smaller chapel visible. Photograph by author, October 2020.

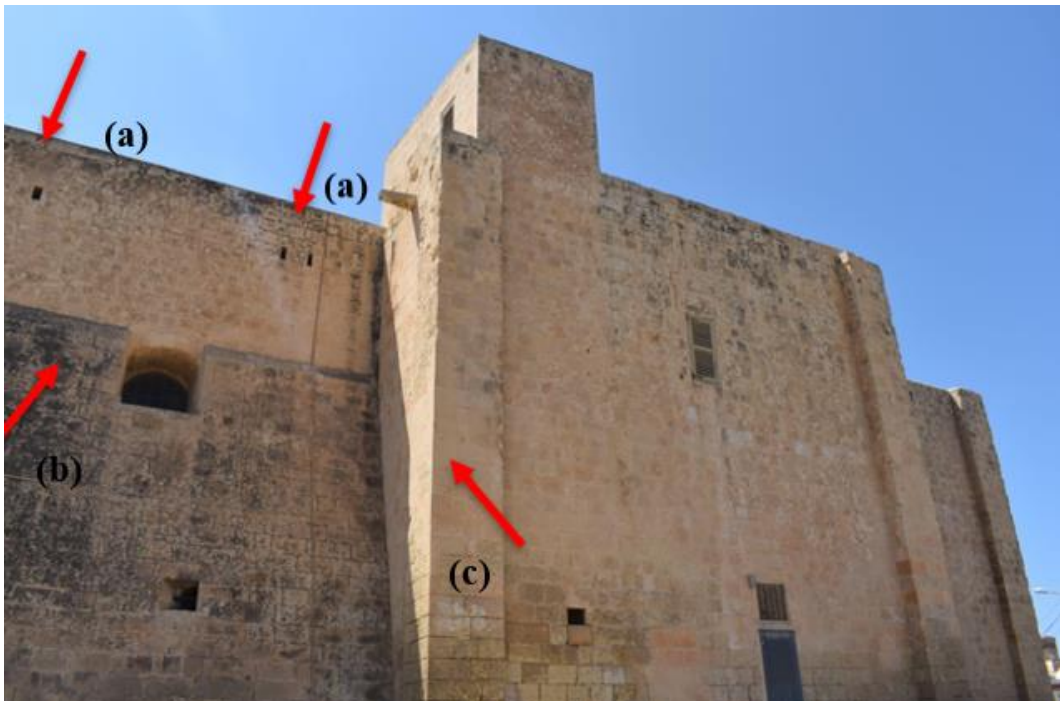


Figure 8. East side of Chapel of San Girgor: (a) lookout windows; (b) buttress; (c) a tower-like structure where the present-day spiral staircase is located. Photograph by author, October 2020.



Figure 9. South side of the Chapel of San Girgor. Arrows indicate lookout windows. Photograph by author, October 2020.



Figure 10. East side of Chapel of San Girgor showing buttress fortification on the south-east side. Photograph by author, October 2020.

Buhagiar (1990:146) points out that incisions can be seen in the roof area inside the church, showing dates of ‘1593’ in the south transept, ‘1603’ in the north, and ‘1606’ near the dome itself. Buhagiar notes the mention of the recent expansion of these two areas of the chapel in the episcopal visitation of 1615, providing further

evidence of the existence of the walls that make up these passageways. The design of the chapel utilised the advantage of its elevated physical position that provided direct views of the bays, and most would agree that its purpose extended to the defence of the region with lookout windows strategically positioned in the south and east walls (Buhagiar 1979:81; Fiorini 2014:87).

Within the chapel itself is a plaque commemorating the last attempt of the Ottomans to raid Malta in 1614. The Ottomans landed in St Thomas Bay as it was an unprotected area, and ravaged the village of Żejtun, including the chapel of San Ġirġor itself. Outnumbered by the Knights of St John and the Maltese, the Ottomans were forced to retreat within two days and instead moved to the north of Malta, instead of inwards towards Mdina. However, this devastation led to the recognition that, in addition to the lookout tower of St Lucian (erected in 1610) south of the chapel, further fortifications were needed in the northeast. In fact, following the attack of 1614, the lookout tower of St Thomas was built towards the east of the chapel for defensive purposes.

These attacks could have also led to the buttress being built on the east and south-east side of San Ġirġor, either just prior to or shortly after the attack of 1614. Whilst fortifying the area, the passageways provided full vantage points from the lookouts of the chapel towards the bays and the towers on either side of the parish. If in fact the passageways were built before the attack, they would have continued to be in use after 1614 as a lookout for possible future attacks. For this reason, it would be reasonable to assume the accessible passageways would not have been blocked off (or left with skeletal remains) following such an attack.

L'Abbé de Vertot (1989:60), who writes extensively about the history of the Knights of St John in Malta in his 1778 historical volumes, makes note of this attack but mentions 1615 as the date of the attack. He notes that although 60 Turkish galleys landed 5000 Turks, no locals were enslaved as they managed to retreat to the strongholds. This date might be a typographical error, but there is no mention of any Maltese militia being killed or individuals being confined in any areas.

It would be safe to assume that until this lookout was deemed no longer necessary, the passageways would have had to be accessible to allow those on watch to move about, certainly not with human remains scattered throughout.

### *1.5 Discovery of the Passageways and Contents*

While works were being done on the roof of San Girgor in 1969, the sacristan Gann Mari Debono, noticed an uneven patch on the roofing slabs and found what looked like a trap door. Refer to Figures 11 to 15 for views of the church from above and a layout plan.

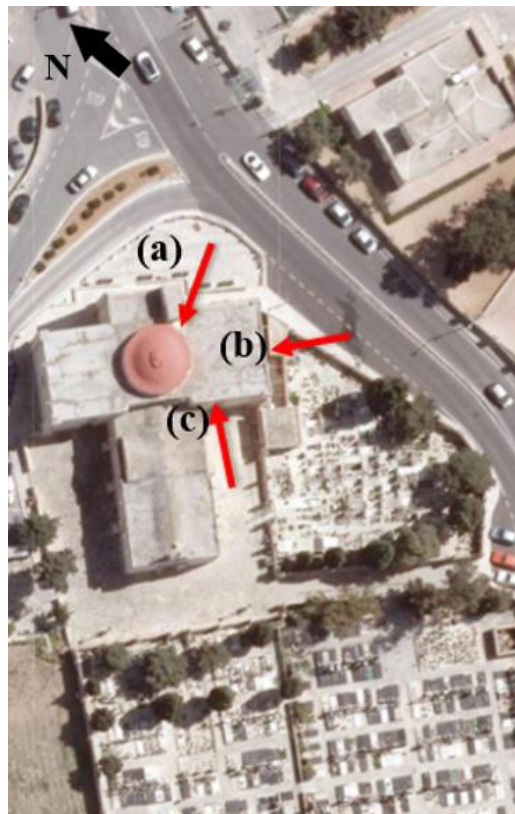


Figure 11. Close-up of San Girgor from above as it is situated today. Arrows show the location of three passageways; (a) Passageway 1; (b) Passageway 2; (c) Passageway 3. Taken from Geoserver 2021.

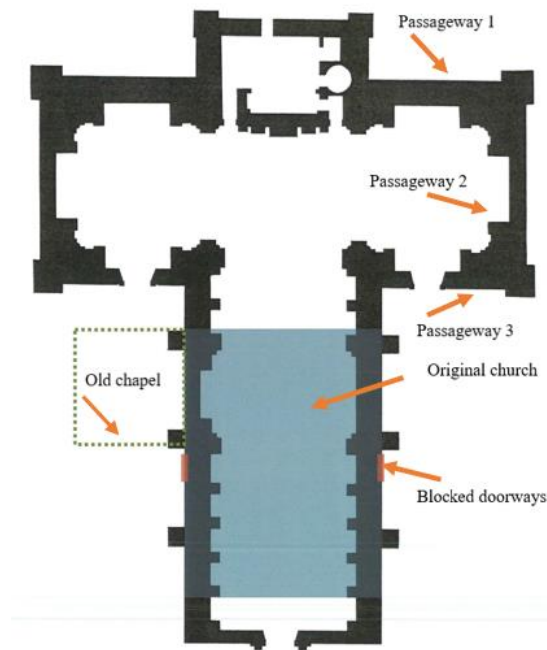


Figure 12. Architectural plan of San Girgor showing location of original 15<sup>th</sup>-century church (in blue), old chapel (dotted line), blocked doorways (in red) and the three hidden rooftop passageways (marked with red arrows). Plan adapted from Abela (2006) and Abela (2014).



Figure 13. Roof top of Chapel of San Girgor. Facing west. Malta in 360, <https://maltain360.com/page.aspx?ref=110023746>.

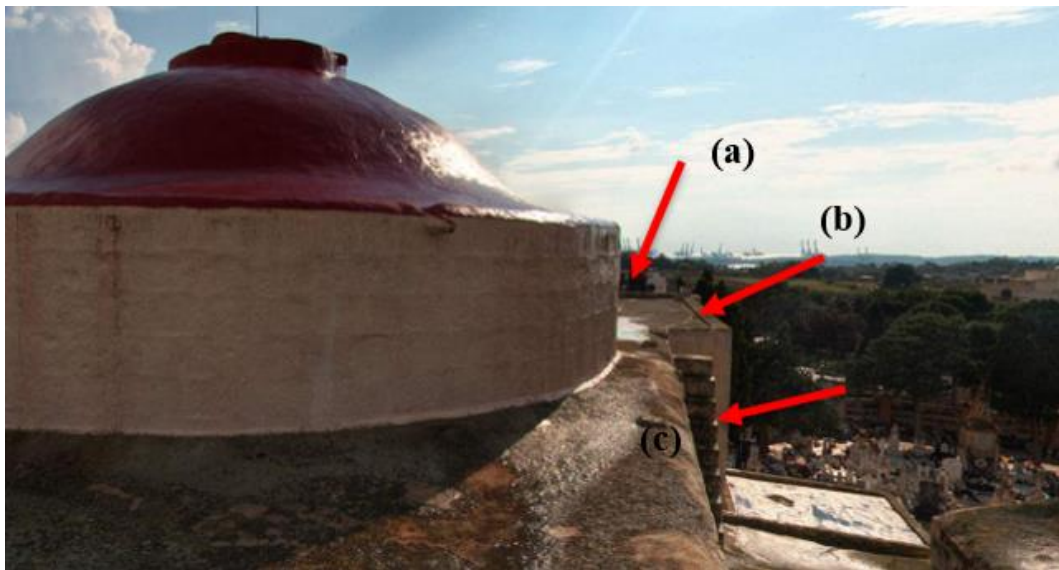


Figure 14. Dome on roof, Chapel of San Girgor. Facing south with views of Birżebbuġa. Arrows indicate: (a) Passageway 2; (b) Passageway 3; (c) external staircase. Malta in 360, <https://maltain360.com/page.aspx?ref=110023746>.



Figure 15. Roof of Chapel of San Girgor, facing northwest with views of St Thomas Bay, Malta in 360, <https://maltain360.com/page.aspx?ref=110023746>.

This original entrance to the passageways through the roof trap door is less than half a meter wide and one can barely squeeze through. The access to the roof and to this trap door must have been via the small external side staircase on the west side of the chapel (refer to Figure 16). Eventually following the discovery in 1969, a doorway was opened to connect to the internal spiral staircase (pers. comm. Ruben

Abela 12 December 2021) that led to the roof. The new modern entrance to the spiral staircase consists of a small doorway that has been cut into the wall allowing one to ascend a few large steps that have been created below the roof of the trap door (refer to Figure 17).



Figure 16. West facing, showing external staircase to roof, Chapel of San Girgor. Photograph by author, October 2020.

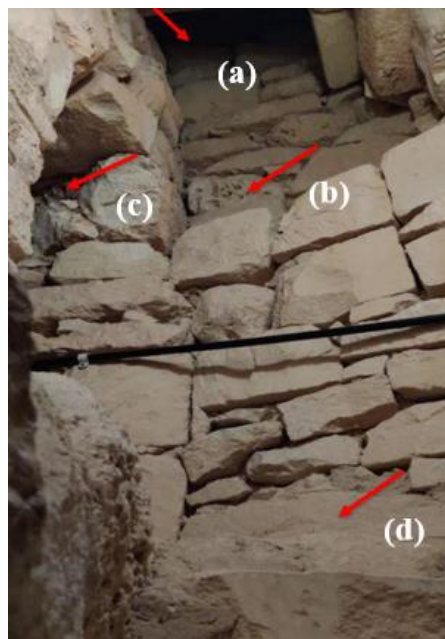


Figure 17. (a) Trap door to enter the hidden passageways from the roof of the Chapel of San Girgor; (b) ledge just below trap door; (c) entrance way to Passageway 1; (d) steps. Photograph by author, October 2020.

The first passageway (Passageway 1) measuring 1 metre (width) by 9 metres (length) and a height of 1.93 metres extends north to northeast (refer to Figure 18), narrowing slightly as one arrives at the corner of second passageway (Passageway 2), which measures the same in width and height, but measures 11 metres in length (refer to Figure 19).



Figure 18. Hidden Passageway 1. Photograph by author, October 2020.

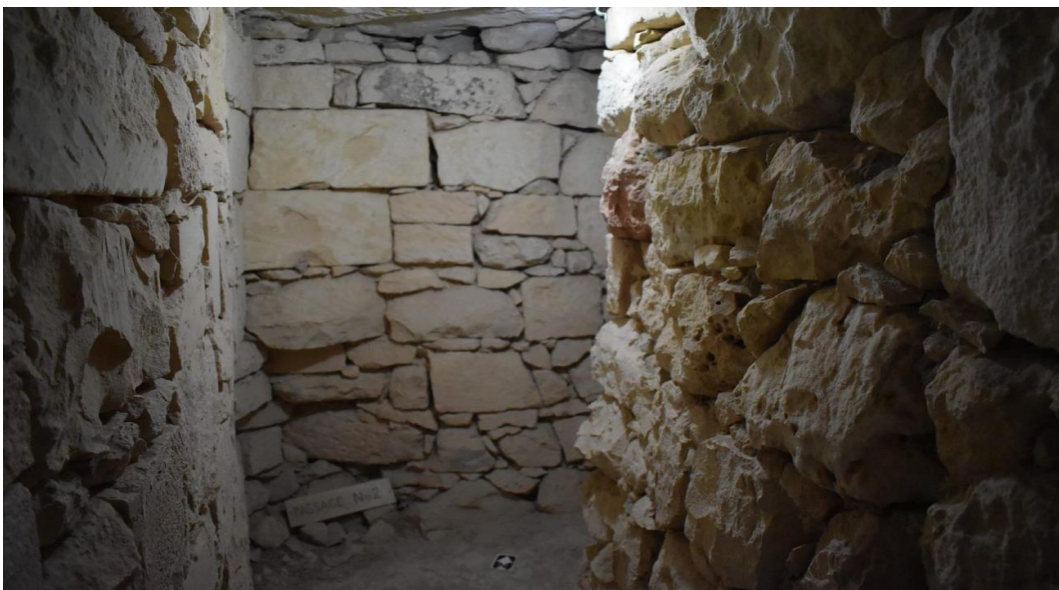


Figure 19. Hidden Passageway 2, Blind Corner, Chapel of San Girgor. Photograph by author, October 2020.



On the northeast side of the thick walls bordering the first passageway, there are three lookout windows. Two windows are situated very close to the entrance, and one is situated closer to the far end of the first passageway before turning a blind corner into the second passageway. There are two lookout windows located at either end of the second passageway facing east however, there are no windows in the third passageway. The latter, Passageway 3, faces south, and measures 1 metre (width) by 9.09 metres (length), and has a height of 1.93 metres. The windows in Passageways 1 and 2 differ slightly in size, approximately 0.26 metres in width and extending 0.75 metres outwards. They are approximately 210 metres above sea level, providing a clear view of the bays of St Thomas, Wied il-Għajn and Marsaxlokk. Figure 20 is an example of one of the windows.



Figure 20. Lookout window in Hidden Passageway 2, Chapel of San Ġirgor. Photograph by author, October 2020.

The ultimate purpose of these windows is thought to have been to view incoming ships entering the bays, and then warn others on the island of potential attacks (Fiorini 2014:88). The third passageway (refer to Figure 21) does not face any coastal bays and windows and therefore it would be understandable that there are no windows here if these served as lookouts to the bays.



Figure 21. Hidden Passageway 3, Chapel of San Girgor. Photograph by author, October 2020.

Interestingly, one can barely see the lookout windows from the external side of the chapel as they are constructed in such a way that makes the opening of the windows very small. The angle however from the interior side of the church allows for a wide view of the bays.

On the ceiling, along Passageway 1, a cross is found (Figure 22), etched on a boulder (date of incision is unknown), and on two other boulders on either side of the walls of the passage, two names are written in pencil in cursive script “Carmelo Zahra 1909” and “Giovanni Zahra 1909”. The latter date is not very clear, and could in fact be 1969 and not 1909, making one question if in fact these etchings were made in 1909 (Figures 23 and 24).



Figure 22. Cross incised into wall in Hidden Passageway 2, Chapel of San Girgor. Photograph by author, October 2020.



Figure 23. Inscription on wall above window in Passageway 2 ‘Carmelo Zahra 1909’, Chapel of San Girgor. Photograph by author, October 2020.



Figure 24. Inscription on wall in Passageway 2, 'Giovanni Zahra 1909' (or 1969?) opposite previous inscription, Chapel of San Girgor. Photograph by author, October 2020.

These were noted in April 1969 during an inspection by Buhagiar (2018:55), an employee (at the time) of the National Museums Department. However, his arrival on site was almost six weeks after the discovery, and others may have entered earlier. This does make one question when members of the public came to know of the hidden passageways and how this may have disturbed the context of the human remains in the passageways.

There is some disagreement with respect to the location and condition in which the bones were found and this further demonstrates the importance of standardized archaeological methods and practices that must be used to investigate and document a site to contextualise finds. In fact, Ramaswamy and Pace (1980:68) recognized the limitations of studying the human remains nine years after their initial discovery, finding the bones stacked on shelves at the back of Passageway 3 (not in their original location).

## CHAPTER 2. LITERATURE REVIEW

### *2.1 Commingled Remains*

Studies of large assemblages of commingled human remains have not often been conducted in Malta. Time constraints unfortunately restrict researchers from analysing hundreds if not thousands of bone elements required to obtain demographic statistics of populations or biological profiles of individuals. The aim of studying commingled remains is to attempt to understand, at the very least, when and how the human remains being investigated became commingled in the context in which they were found and, if possible, the population affinity of the individuals in a given assemblage (Buikstra and Ubelaker 1994; Osterholtz *et al.* 2014; Cunha and Ubelaker 2020).

Large assemblages of commingled human remains which have been found in unusual settings in the vicinity of churches or church grounds in Malta include those located in boxes in the basement of Casa Lanfreducci, as discussed by Cauchi (2019) in her master's thesis and, more recently, remains scattered across the garden grounds of the Chapel of Bir Miftuħ (Camilleri 2020). The remains from Casa Lanfreducci were found in what originally may have been an extension into a crypt of the adjacent church dedicated to Our Lady of Victory, in Valletta. The remains at Bir Miftuħ in Gudja on the other hand were found on the surface of gardens, most likely originating from the clearing of a nearby grave (Camilleri 2020). The remains were most likely thrown into a well and then inadvertently strewn across the gardens after the well was cleaned out in recent years. Preliminary studies to obtain an MNI along with demographic information and biological profiles were completed by this author on behalf of SCH (Camilleri 2020) and are documented in a report yet to be published. However, radiocarbon dating and ancestry determination have not yet been performed on the human remains from either of these sites. In the two cases noted above, the skeletal remains were not 'hidden' nor associated with particular historical incidents or folklore.

To study the complex nature of commingled remains and develop a biological and demographic profile, current literature and associated practices used to determine sex, age and ancestry are reviewed below. In some cases, methods used for decades were revised by researchers to increase efficiency without affecting accuracy and therefore the evolution of these methods is also discussed here.

Analysing origins of human remains from a context which has not been excavated utilizing standard archaeological practices can be challenging, and when remains are commingled the complex nature of the task is intensified. Disarticulated or commingled remains are defined by Ubelaker (2002:332), one of the leaders in the development of osteological assessment standards, as 'the mixing together of remains of different origins and usually of more than one individual'. The primary aims when studying commingled assemblages are to determine the nature of commingling and to understand depositional processes or burial practices, in addition to assessing the elements and the number of individuals represented. This must be done in a scientific manner using both quantitative and qualitative methods. The final objective is to develop biological profiles of the individuals and to understand the entire population.

Analysis of human remains, including those which are commingled, usually involves sexing, ageing, stature assessment and ancestry determination (Ubelaker & Buikstra 1994; White *et al.* 2012; Osterholtz *et al.* 2014). Márquez-Grant (2015) notes that in addition to the above analysis, several other factors must be considered when studying remains in order to develop biological profiles in both forensic and archaeological settings. These include determining whether the remains are human or faunal, assessing the number of persons in the assemblage, and understanding the events or context of the deposition. As many commingled assemblages may be affected by disturbance, remains can be fragmentary and should be reconstructed, factoring in the effects of taphonomic processes and the existence of any trauma which may have occurred before death (antemortem), around the time of death (perimortem) or after death (postmortem). Márquez-Grant goes further to include DNA analysis, radiocarbon dating or stable isotope analysis, and cranio-facial

reconstruction, when possible, to complete the biological profile of individuals (Márquez-Grant 2015:307).

Understanding the population itself and how the remains came to be at a particular site can also be complicated if clear documentation of the site is not available, if one is not involved in the extraction of the material, or if the context of the site is compromised in some way. The method of extraction and experience of the excavator at a site also heavily impact any future studies of what is extracted (post-excavation). Tuller (2008:7) comments that “care in exposing and removal of remains from a grave by an observant excavator, knowledgeable in human skeletal anatomy, is the single most important step limiting (and hopefully eliminating) further disarticulation during the recovery”. This cannot be emphasized enough in archaeological practice to facilitate the analysis of commingled remains. Although his reference is to forensic cases, Tuller argues that any recovery following a well-documented excavation led by archaeologists would prevent further commingling, and that set methods and practices would eliminate much confusion in understanding the context and the association of the material. This certainly applies to the remains at San Girgor, where the disturbance that occurred, along with the lack of proper documentation, compromised the context of the site and makes the analysis of the remains more complex.

Tuller (2008:8) also argues that spatial analysis utilizing three-dimensional distances and GIS software to determine the actual relationship between elements and creating mass grave mapping can provide an objective methodological approach to assist in reassociating skeletal material by comparing the locations of disarticulated elements. If the remains have not been documented accordingly based on depositional events, the context is lost and understanding the nature of the remains becomes difficult. Although using GIS with large assemblages of commingled remains, especially those which are fragmentary, could be time consuming, the benefits of the data obtained would prove to be extremely useful. Further discussion on utilizing GIS approaches is presented below in section 2.11.

After reviewing the numerous methods that exist to analyse human remains, it was evident in the literature that there is still a lack of standardized approaches and little

guidance on which methods one should utilize, particularly for commingled remains. The inconsistent scoring measures, varying terminology and definitions, and the broad result ranges with little statistical analysis to ensure accuracy, until recently, made the process of establishing a reliable biological profile difficult. As Palmiotto *et al.* (2019a:129) note, the inconsistent terminology and different methods used become an issue as assemblages are affected by various taphonomic conditions and are recovered from dissimilar contexts. Consistency and set standards are clearly needed for studies on commingled remains especially for future comparative analysis.

As is evidenced in manuals that guide osteological studies (Ubelaker 2008; Osterholtz *et al.* 2014) each assemblage varies according to the type of burial, context, and population, and therefore commingled remains require a tailored approach combining non-metric and metric methods of assessment. The various current practices and methods used for the assessment of sex, age, stature, and ancestry are reviewed and critiqued below.

One of the first steps in the osteological analysis of commingled remains is to sort through and identify the bone elements as noted by researchers (Buikstra and Ubelaker 1994; Outram *et al.* 2005; Osterholtz *et al.* 2014), in order to determine whether they are human or animal. Once this is established, bones are sided to establish a preliminary assessment of the minimum number of elements (MNE) and the minimum number of individuals (MNI) (Buikstra and Ubelaker 1994; Lyman 2008; Osterholtz *et al.* 2013). In many instances bone elements are fragmented in commingled assemblages, making the task of determining the MNE and MNI arduous and very time consuming, which possibly may not give a realistic result of the context. Essentially, commingled remains involve the analysis of skeletal elements not necessarily having *any* associated relationship, unlike that of articulated individuals on which so much of the research is based. The taphonomic processes often seen in fragmented remains, and the potential lack of associated material, complicates the assessment of the MNI and ultimately the understanding of the population overall.



In proceeding with the analysis, Atici (2013:213) stresses the need to use a multidisciplinary approach and to draw on the research of zooarchaeologists. These researchers often work with numerous fragmented or commingled faunal populations which are not always found in primary or undisturbed settings and as with commingled human populations, complete individuals are not necessarily “neatly entombed”.

## *2.2 Background of Osteological Analysis*

Most manuals used by osteologists, namely those of Buikstra and Ubelaker (1994), Bass (2005), and White (2005) amongst others, focus on analysing *articulated* skeletal material, and few studies dedicate pages, let alone a whole chapter to address commingled and fragmentary remains.

However, over the last few decades the need to identify commingled remains from mass graves or disasters for forensic purposes, plus the advancement of technology in a short span of time, has led to the emergence of significant research providing a solid foundation for forensic anthropology and in turn osteological analysis (Haglund 2001, 2002; Outram *et al.* 2005; Osterholtz *et al.* 2014).

Due to the often-fragmentary nature of bone elements found in commingled assemblages and time-consuming methods to determine the MNE and MNI, the common theme through much of the literature on assessing human remains stresses a multidisciplinary approach (Osterholz *et al.* 2014). The issue is frequently faced by zooarchaeologists who, as a result, were motivated to develop numerous standardized methods that offered time-efficient solutions with high levels of accuracy. This influenced the field of osteology and led the way for human osteologists to adopt methods used by zooarchaeologists as is discussed below.

The concept of the MNI was originally based on studies between the 1950s and 1970s on various Indigenous populations of North America, which involved some of the largest collections of commingled remains such as the Crow Creek massacre remains (Kendell and Willey 2014:88) and represented large communal deposits of individuals who were originally buried elsewhere (Ubelaker 2002:336). In fact, as Rose *et al.* (1996) show in their studies, this led to the establishment of the North

American Graves Protection and Repatriation Act (NAGPRA 1990) and from this *Guidelines and Standards for Recording Human Remains* by Buikstra & Ubelaker (1994) evolved in the 1990s. This manual provided comprehensive standards for sorting and assessing human remains (primarily articulated) and offered methods to determine size, sex, age, and health, used for decades by osteologists. Only in recent years, due to external pressures, have researchers slowly begun to integrate efficient techniques needed to record accurate and usable data for further comparative analysis, specifically designed for commingled remains (Knüsel and Outram 2004; Outram *et al.* 2005; Baustian *et al.* 2013; Byrd and Adams 2013; Fox and Marklein 2013; Osterholtz *et al.* 2013, 2014; Byrd and LeGarde 2014; Bertsatos and Chovalopoulou 2019).

Although established standards to study human remains in archaeological practice exist (Buikstra and Ubelaker 1994; Brickley and Mckinley 2004; Bass 2005; White 2005, 2012), this usually applies to complete skeletons found in specific contexts. By adopting zooarchaeological principles (such as landmark, and pairing and conjoining methods) for commingled assemblages, instead of traditional osteological methods (such as counting each element or fragment), to analyse thousands of commingled human remains, researchers were better able to understand taphonomic processes that may have caused severe fragmentation, and thus could efficiently calculate the MNI (Mack *et al.* 2016: 526).

Outram *et al.* (2005:1699) argue that human osteologists are often not equipped to deal with processes that are not associated with 'normal' inhumations and cremations, particularly in contexts which involve fragmented, disarticulated, and commingled deposits. Researchers stress that it would be of great benefit to those in osteology to use zooarchaeological quantitative approaches in conjunction with the standard methods that presently exist in osteology, as the methods have proven to be highly effective (Outram *et al.* 2005, Baustian *et al.* 2013:272).

### *2.3 Burial Settings & Cemeteries*

The type of burial and depositional context of remains is also a significant part of the process in understanding the nature of remains found. Two key types of burials

exist - primary and secondary, both of which could be disturbed. Pokines *et al.* (2014:11) note that primary burials usually have articulated skeletal elements which are characterized by soil staining, plant root damage and invasion, erosion (in acidic soil) of cortical surfaces, and a lack of weathering. A secondary burial on the other hand, they continue, could have these same characteristics, but with disarticulated elements. In the latter, there is less representation of smaller skeletal elements as well as more evidence of post-mortem breakage or ritual treatment due to transporting of material and/or reburial. The characteristics of secondary burials in archaeological settings where skeletal remains have been moved would therefore be commingling, as in the case of an ossuary or possibly a mass grave where individuals have been placed post primary burial.

Duday (2009:14) notes that a primary burial is where bodies are laid anatomically in a final resting state and where decomposition usually occurs as in the case of inhumations. Secondary burial usually takes place away from the area of decomposition and usually involves commingled dry bones. The reasons for the transfer of human remains to a secondary site could vary and the assessment of the context as well as the skeletal elements involved is important.

The criteria of a primary burial site can change over time. Mays (2010:31) notes that cultural rules regarding the orientation of a corpse, the location of the grave itself and inclusion of any grave goods govern the aspects of burials. Mays continues that the location of graves, particularly in cemeteries, is not random, and sex, age and any pathologies may dictate where burials are placed within cemeteries, which could change over time when a cemetery is in use. Mays (2010:32) warns that this would make the site difficult to assess archaeologically, potentially leading to a bias in the data obtained, rendering results which may not be representative of the community at large.

According to Parker Pearson (2001:14), European churchyards in medieval and post-medieval England usually were set up with hierarchical patterns, and therefore social status played a huge role in the geography of burials. Those with higher status such as lords and their families were usually buried within the church, while the rest of the affluent population would normally be buried on the sunnier south side of the

churchyard, just outside the entrance based. Those with lower status were buried on the north (darker) side of the churchyard, a result of the superstitious belief that the dark side was associated with evil. Parker Pearson continues that further evidence of segregation based on status is evident in seventeenth to eighteenth century burial grounds, for example in Virginia, where African American enslaved persons had a separate graveyard area since their burial in churchyards was forbidden. Therefore, in such instances of burial segregation as in the latter case, one may expect different population affinities amongst assemblages within the same cemetery and period of time. In both cases noted above, evidence of hard labour on skeletal material would probably be more prevalent on those buried outside the church. This means that one could hypothetically distinguish between individuals who are of lower status from those of higher status in commingled assemblages when found in cemeteries such as those described above.

#### *2.4 Decomposition and Positioning*

The physical condition and position of skeletal material can provide evidence on the original burial place and time lapse since the actual burial. Decomposition stages have been well studied (Duday & Guillon 2006). Roksandic (2002:101) argues that understanding the process of decomposition is extremely important, as differential preservation and decomposition are two key phenomena that could affect the interpretation of mortuary behaviour. One must therefore understand the consequences of decomposition, the sequence of disarticulation and the movement of remains. Roksandic (2002:103) cites Dirkmaat and Sienicki's chronological skeletonized sequence, showing that decomposition begins with the bones of the hands and wrists, the feet and ankles, the jaw and cranium, since these contain the least amount of flesh, followed by the pelvic bones, vertebrae, and long bones.

The skeletonization process varies according to the environment, and elements can be affected by other taphonomic factors (weathering, soil conditions, water, animal gnawing) wearing the surface of the bones away. Pinheiro (2006:111) explains that bodies decompose much faster in open air than in an enclosed environment. Citing various authors (Galloway 1989; Mann 1990; Knight 1996), Pinheiro notes that experimental research shows complete skeletonization could occur between one and

two weeks, with some exceptions, in a warm damp environment. However, in temperate climates, a period of 12–18 months is a normal period for skeletonization, with tendons, periosteum, and ligaments still present, and approximately three years for a skeleton to be considered “clean”. The ligaments and tendons are soft tissues that are most resistant and in some instances they may become “mummified”, leaving remains such as hands and feet partially skeletonized.

Mays (2010:237) notes that it is also important to assess the percentage of bones represented in the skeleton or the commingled assemblage. Secondary depositions of remains which are only partially decomposed and therefore somewhat articulated with connecting tissues still present would result in a high representation of bone elements (even small bones). On the other hand, fully skeletonized elements which have been moved (secondary burial) may show the absence of smaller elements. Bone representation is calculated when sorting the elements and determining the MNE and MNI (discussed further in section 2.5).

### *2.5 Determining Size of Population*

There is some disagreement in terms of the most accurate method that can determine the MNI within the commingled assemblage, as well as the most suitable approach to assess fragmented commingled remains.

Element counts can be complicated when determining the MNI in fragmented assemblages. One could assume fragments make up individual elements when in fact they may be associated parts of one element. Buikstra and Ubelaker (1994) developed osteological assessment standards that aim to eliminate this issue based on visually assessing any anatomically overlapping portions and noting percentages of each element present in a given assemblage. The cranium (which is the skull that does not include the mandible) and postcranial bones *not including* long bones are categorized as complete when at least 75% of the element is present; partially complete if between 25% and 75% is present; and poorly preserved when less than 25% of the element is present. For long bones, the process is slightly different. The proximal and distal epiphyses and three sections of the diaphyses (proximal,

midshaft and distal) are to be noted when assessing the degree of preservation (Ubelaker 2002: 232).

Texts which evolved as standards for osteological analysis decades ago, such as those by Krogman (1962), followed by Stewart (1979) and later Ubelaker (1994), dedicated little to the study of commingled remains and only offered a passing mention with little guidance. However, in his later work Ubelaker (2008:1) notes that determining the number of individuals represented in a group and the identification of single individuals within commingled remains, are key questions that need to be answered. He points out that increasingly, cases of commingled remains were being encountered, leading to new insights that deal with the challenges one faces with such remains. Interestingly Snow and Folk (1965) had presented material on statistical approaches to determine MNI much earlier, eliminating bias, yet this was not incorporated to any great extent in the related osteology literature noted above, until more recently.

Siding is one of the first processes used to sort and count individuals in an assemblage (Buikstra and Ubelaker 1994; Bass 2005; Brickley and McKinley 2004), however Palmiotto *et al.* (2019b: 61), note that the analysis of commingled human remains usually involves determining the MNI by considering other aspects from siding, such as articulation patterns, sex, and age where possible. Ubelaker (2008:3) adds that bone morphology and bone size should also be considered relevant. The process of determining the MNI with a high degree of accuracy is more complex than it seems, and with a large assemblage of commingled human remains this can prove to be very time consuming with methods (which will be discussed further in this dissertation) that do not always offer accuracy and reliability. These challenges were the impetus for research that led to the development of innovative practices and advanced software programs readily adopted by other disciplines. The process not only became more efficient but decidedly more accurate, propelling osteological analysis (following the field of zooarchaeology) into a new realm with a cross pollination between various disciplines that proved to be extremely useful in the study of commingled human remains. An example of this is the incorporation of Geographic Information

Systems (GIS) into taphonomic analysis and biological profile development (discussed in section 2.11).

### *2.5.1 Fragmentation*

Commingled remains are frequently fragmented and incomplete, creating various challenges to determine the MNI and the assessment of age, sex, pathology, and trauma. Baustian (2014:269) notes that commingled remains often become fragmented due to natural taphonomic processes and the degree of these processes will vary based on the length of time buried and the surrounding conditions. He adds that taphonomic factors could include disturbance or bone modification caused by humans or animals, environmental factors including soil or root erosion, as well as water damage, or climate conditions.

Osterholtz *et al.* (2014:37) state that “through careful sorting and a meticulous analytical technique for every fragment” one can obtain the base line data (including sex and age) along with the MNI. While Buikstra and Ubelaker’s (1994) work focused on standardized guidelines that count each identifiable element as one individual based on the percentage of the element present, Knüsel and Outram (2004) on the other hand use a zonation method. This latter method is carried out by separating bones into recognizable zones based on areas where bones have a natural tendency to break whilst acknowledging that human anatomical structures are not exactly the same. Using this method, Knüsel and Outram argue that MNI should be based on the highest count of individual features logged as present in particular defined zones, providing not only a more accurate calculation of MNI but also facilitating conjoining exercises (Outram *et al.* 2005:1702).

This latter technique, although time consuming, works well on assemblages that are extremely fragmented, and by incorporating GIS (discussed further below in section 2.11), which is the method often used by zooarchaeologists, this technique can be very applicable to human assemblages.

### 2.5.2 *Pair Matching*

To combat the issue posed by fragmentation whilst determining the MNI, some researchers have explored the idea of what Kerley (1972:355) calls “positive articulation” which assesses the number of individuals by matching up those elements which articulate and may belong to the same individual. Ubelaker (2002:333) however notes that the technique is limited by the skills of the examiner. This was later expanded into pair matching where the bones of the same element but of opposite sides are matched, for example a left femur with a right femur of similar morphology and age. The work of Byrd and Adams (2003) also shows that the method of pair-matching articulating bone segments and using bone measurements that represent the size and shape of the elements for quantitative and comparative analysis of paired bones, as well as other associated skeletal remains, could resolve issues that are associated with determining the number of individuals in commingled assemblages.

Following the field of zooarchaeology and the concept of pair matching, Adams and Konigsberg (2014) put forth the concept of determining the ‘Most Likely Number of Individuals’ (MLNI) as an alternative to determining the MNI following standards set by Buikstra and Ubelaker (1994). Le Garde (2019) validated Adams and Konigsberg’s (2014) assertion that pair-matching is an effective method to determine MLNI. By matching pairs first by size, then by robusticity and morphology, Le Garde (2019: 69) found the accuracy level to be between 84 - 99% and stressed that visual pair-matching should be one of the first methods of analysis.

However, there are limitations to this method. The process can be very time consuming for large assemblages of commingled remains and the lack of bone preservation can be problematic when trying to achieve a high degree of confidence in results.

Kendall and Willey (2014:100) argue that using the MNI method remains the best method for large, commingled assemblages, and as the mid-shafts of long bones are often the best preserved, the chances of representing the various age groups is increased, limiting the bias in population demographic analyses.



## 2.6 Sexing and Ageing

Estimating age and sex is fundamental in studying past population assemblages as is noted in major works by leading anthropologists (Krogman 1962; Buikstra and Ubelaker 1994; Bass 2005; Burns 2013; Osterholz *et al.* 2013) and the current related research is discussed and reviewed below.

Non-metric and metric approaches have been used to develop biological profiles, and in some instances a combined approach is taken. Although traditionally most sexing and ageing methods have focused on the os coxae and the cranium, research has surfaced on using other postcranial material as well, some of which has yet to be fully validated. What is evident in the literature is the debate on objectivity, standardization, quantification, and ease of methods. In addition, concerns exist about levels of accuracy, degree of confidence, issues with variations within and between populations, and whether one variable (for example sexing) is dependent on another variable (for example ageing or ancestry).

With the numerous non-metric and metric methods that exist and little guidance on which methods to use when working with commingled remains, the process can be challenging particularly if remains are of a fragmentary nature. Langley (2018:1) suggests that when skeletal material is fragmentary, non-metric traits are a useful alternative for sex estimation, adding that although the use of non-metric traits is criticized as being subjective, scoring systems, statistical analyses, precision of methods, along with interobserver agreement have made the approaches more reliable.

### 2.6.1 Sexing

Traditionally sex estimation is based on non-metric approaches complimented by metric analysis focusing on the cranium, mandible, os coxae, and sacrum primarily. Metric analysis is often thought to be more objective, however studies have shown (Hefner 2009) that using both methods within a statistical framework is best. Lewis and Garvin (2016:743) note that metric analysis is sometimes based on size which in turn could make this method somewhat subjective as well. Non-metric traits, on

the other hand, are not based on size, and are based instead on the degree of expression of sexually dimorphic, and often discrete traits.

According to Klales' work (2012, 2013, 2016, 2018, 2020) the os coxae is still considered the best indicator of sex estimation in adults. Klales (2012) provides a revised version of the Phenice (1969) method for sex estimation by expanding the original three Phenice traits - ventral arc, subpubic concavity (called subpubic contour by Klales), and medial aspect of the ischio pubic ramus - into five categories. This new method captures trait expression variability and probabilities with each sex classification.

Brůžek and Murail note various issues when determining sex including (1) the fact that sex determination for isolated bones is problematic; (2) reliable methods to sex non-adult skeletons have yet to be proposed and should be avoided (particularly because sexual dimorphism of the os coxae is not evident until segments are fully fused); (3) sexual dimorphism is population specific; and (4) determining ethnic origin is limited on skeletonized remains. In the end, as stated by Brůžek and Murail (2006:238), "one has to accept that the quest for reliability leads to unidentified individuals".

For sex estimation methods based on the cranium, Buikstra and Ubelaker (1994) developed "*Standards for Data Collection from Human Skeletal Remains*" from here on referred to as "Standards", still widely used today. In "Standards", Buikstra and Ubelaker (1994) provide descriptions by Broca (1875, as cited in Lesciotto and Doershuk 2018:151), with a scoring system by Acsádi & Nemeskéri (1970), later revised with population specific discriminant equations by Walker (2008). The sexually dimorphic nonmetric traits originally defined by Walker (2008; cited in Lewis and Garvin 2016:743) are the most often used traits in sex estimation known as the 'Walker method'. This involves four traits on the cranium (nuchal crest, mastoid process, orbital margin, and glabella/supraorbital ridge) and the fifth is the mental eminence, found on the mandible.

Recent studies by Lewis and Garvin (2016) and Spradley (2020) show that the mental eminence may not be as sexually dimorphic as originally asserted by Walker (2008). They all suggest not to include this trait in any analysis if other traits are

available when estimating sex, where trait variance due to age was evident and highest in African American males (Lesciotto and Doershuk 2018:154).

However, the recommendation to eliminate the use of the mental eminence is an issue when using the Walker method according to Langley (2018:4) as four of the six equations that were later incorporated by Walker utilize the mental eminence. He continues that the zygomatic extension, on the other hand, seems to be very helpful when added into the groupings. This trait provides high accuracy classification rates, as it seems to correlate with the development of the dimorphic temporalis muscle, where females exhibit gracile muscle attachments and no extension of the zygomatic root.

It is evident that there is a need for standardization in methods which provide clear descriptions, multiple photographs of trait variations for comparative analysis, and refined scoring categories.

Aside from interobserver error based on experience and lack of statistical analysis in the past, other key issues, consistently mentioned surrounding sex estimation, are the effects of age on non-metric cranial traits and the belief that female skulls tend to show ‘masculinization’ because of ageing, therefore resulting in errors in sex estimation (Buikstra & Ubelaker 1994; Moore 2013). However, studies (Perizonius 1979; Garvin 2014; Lesciotto and Doershuk 2018) have consistently disputed these observations. and the assertion that age or ancestry for that matter can affect sex determination is still debated.

Brůžek and Murail (2006:227) recommend using a sex estimation method which selects a series (but limited number) of traits with various combinations of measurements, along with descriptions of morphological traits, as no single trait or extreme values of such traits can provide reliable sex estimation.

### *2.6.2 Ageing*

There are several methods that can be used to estimate age, which includes the assessment of dentition, the ox coxae and the cranium, and their usefulness and limitations are discussed below. Age determination based on teeth in the calvarium,

the mandible and on loose teeth (the result of postmortem tooth loss) can be relatively precise (Alqahtani *et al.* 2014) particularly for subadults and individuals up to the age of 21 years. This method of age estimation that looks at deciduous and permanent teeth that have erupted, or are in the process of erupting, is based on known stages of development. However, beyond the age of maturity, it should be noted that the age categories become extremely broad. As very few teeth were found with the commingled remains of San Girgor, this established method was not utilized and is not discussed further.

Methods that seem to provide the highest degree of accuracy include the assessment of the metamorphosis of the pubic symphysis and the auricular surface on the ilium of the *os coxae*. Age estimation approaches based on the pubic symphysis have been used for decades, however originally the reference population was quite limiting as Todd (1920), followed by McKern and Stewart (1957), developed this method specifically using male samples. Female samples were later incorporated into the method by Gilbert and McKern (1973).

The Suchey-Brooks method (Brooks and Suchey 1990) evolved from these approaches with detailed descriptions, associated age ranges, and photographs that visually portray various categories for comparative analysis. However, as Bass (2005:200) notes, although this latter approach is more objective, the descriptions in the Suchey-Brooks method are complicated and not easy to apply against the photographs of samples. The use of the actual casts of *os coxae* (on which the photographs are based) would be of significant help to physically compare samples and attempt a more objective analysis. Nonetheless, with this method, the age ranges are quite broad and age estimation beyond the age of 50 years continues to be difficult to define. In fact, this issue of ageing beyond the age of 50 years could result in demographic population profiles that are not accurate, leading one to believe a population has a lower life expectancy.

The cranium is also another element that is utilized where the fusion of sutures is assessed with a scoring system. Unfortunately, the scoring can be somewhat subjective and the final composite scores are associated with extremely broad age ranges. Lovejoy *et al* (1985) developed a method based on ectocranial sutures,

whilst Acsádi and Nemeskéri (1970) used endocranial sutures; Perizonius (1984) used a combination of both methods, with the analysis of endocranial suture fusion specifically for younger individuals, and ectocranial suture closure specifically for older individuals. Several researchers, however, dispute the accuracy of age estimation based on cranial suture fusion. Hershkovitz *et al.* (1997) believe that sutures are independent of age and are sexually biased; Falys and Lewis (2011:12) suggest that researchers should utilize various ageing techniques and not rely on fusion of cranial sutures for age, since in their opinion, the technique lacks the standardization to provide a high level of accuracy.

As several bone elements display phases of development, age estimation on immature individuals can be easier and more precise. Methods to age immature skeletal elements can provide reliable age determination based on patterns of epiphyseal fusion and dentition development, processes which are delineated with little variation between the sexes as noted in the work of Scheuer and Black (2004). Such methods may not be suitable for adults where bone development is not taking place. Instead, useful ageing methods for adults are based on elements that provide evidence of morphological changes due to degeneration or obliteration.

Epiphyseal union on long bones is widely used as a criterion in age estimation for immature individuals (subadults) as fusion continues into the teenage years. The process is gradual with fusion occurring earlier in females. The sternal clavicle and sacrum fuse much later, when individuals are well into their mid-20s and early 30s as outlined in Buikstra and Ubelaker's (1994:43) comparative charts on fusion rates. As the time of epiphyseal union and the rate at which it occurs differs amongst the bones, Ubelaker (2002:332) cautions that this can result in ageing errors. For example, one element of an adolescent might fuse earlier than another element, creating confusion as to whether the person is mature or immature and whether they in fact belong to the same individual. This can be an issue when dealing with commingled remains. Therefore, although using several age estimation methods for commingled remains is imperative, one must keep in mind that elements which are not conjoined and aged differently can result in an assumption that the elements belong to two different individuals.

Lottering *et al.* (2015) provide another method used in conjunction with the above approaches to corroborate age determination and distinguish adults from immature individuals. This involves the status of the spheno-occipital synchondrosis (SOS) fusion - the last area of growth in the cranium. They note that earlier studies would suggest complete fusion of the SOS between the ages of 17 and 25 years in both sexes. However, their investigations on populations in Queensland (Australia) indicate otherwise, showing that sexual dimorphism and ossification both occur during adolescence, specifically by 13.8 years in females and 16.3 years in males with intrapopulation variation (Lottering *et al.* 2015:42).

Falys and Lewis (2011:704) argue that age categories and descriptions are not consistent, and no standardization exists amongst the various ageing methods used, particularly those that determine age of 'adulthood', and instead suggest the use of skeletal markers to identify adults. Beyond standardization, Cox (2000:63) warns that although ageing in living individuals causes degeneration of the joints and an increase in enamel wear, these processes might also be caused by the individual's lifestyle, the environment, or genetics, and hence these skeletal markers cannot be considered representative of actual age of an individual.

It is evident that using macroscopic techniques to estimate age can be very subjective, and unrefined age category descriptions, observer error, as well as insufficient population specific data for comparative assessment, could lead to errors. In addition, Cox (2000:62) states that inherent issues with ageing methods lie primarily with the samples themselves, some of which were based only on men (from deaths in wars) and later adjusted to include females.

To complicate matters, the sex of the individual has been found to be statistically significant when using the pubic symphysis in ageing approaches but not so when using the auricular surface (Brooks and Suchey 1990) which means that the ageing of skeletal remains is likely dependant on the sex of the individual. Therefore, determining the sex of the individual at the initial stage of analysis would be helpful before moving on to ageing skeletal remains. However, as sexing immature individuals is difficult (as discussed earlier), age estimation becomes complicated unless dental assessment can be performed.

Buckberry (2015:324) notes that issues with age estimation methods can create biased demographic results, either overestimating or underestimating ages. She acknowledges that ageing processes are variable, where biological age does not necessarily relate to chronological age due to environmental factors and genetics. Ubelaker (2002:333) however comments that ageing human remains even as adult or subadult (if not using defined age categories) can nonetheless provide a wealth of useful demographic information.

## *2.7 Ancestry*

The goal of ancestry determination in forensics is to obtain a positive identification of an individual, while in archaeology it is usually performed to understand population affinity. Historically, the process has been plagued by controversial methods which were based on lists of traits thought to be population specific and assigned to three-group models, namely 'Caucasoid', 'Negroid', and 'Mongoloid' as noted in Bass (2005:83), referring to White, Black, and Indigenous or Asian persons. This did not incorporate all populations let alone human variations within and amongst populations across the board. In addition, single use methods and lack of representative data and statistical models prevented the ability to validate assertions as shown in research by Dunn (2020), Hefner (2009), and Hefner and Ousley (2014). This section reviews the non-metric and metric approaches currently used to determine ancestry, the issues that permeate the approaches and the reliability of results.

### *2.7.1 Cranial Non-Metric and Metric Approaches in Ancestry Estimation*

Both non-metric and metric approaches have been used to determine likelihood of ancestry. Non-metric approaches using the cranium tend to focus on morphoscopic traits which assess the shape of features accompanied by extensive feature lists. Unfortunately, few standards exist on traits and related definitions that should be used when assessing ancestry. Specific discrete traits (asymptomatic) which are also utilized on the other hand, are believed to be generally population specific, however frequencies across populations have yet to be well documented (Cunha 2020:11). Hefner (2009) aimed to standardize the ancestry assessment method, consolidating

a list which focused on the facial features of the cranium. This was combined with the use of optimized summed scoring attributes (OSSA) designed to provide statistical analysis and quantified objectivity in conjunction with non-metric approaches, to determine the probability of population affinity. Hefner and Spradley (2016:6) later expanded on this process of standardization and performed experimental analyses to determine if they could correctly classify more than three population groups (African, European, Native American, Hispanic, or Asian) using non-metric cranial traits (often called macro morphoscopic traits or MMS traits) and compared these results to craniometric data. They argue that it is possible to differentiate various geographic groups including those with shared ancestry (for example Africans and Black Americans) and the estimation of geographic origin should be preferred over the previously used three-group model. Dunn (2020:2) notes that typological approaches traditionally used in the past are being discarded and advances in ancestry estimation have evolved with significant changes in methods, standardization, and statistical analyses improving classification accuracy. Recognizing the underlying issues with past methods and the refinement of approaches has led to a better understanding of the complex relationship between skeletal morphology, genetics, and geographic origin.

Researchers have begun to change the terminology associated with ancestry estimation, focusing on geographic regions (African, European, Asian), further defined by local terms (Cunha 2020:6) to take into consideration cultural and social constructs. However, Albanese and Saunders (2006:281) still question ancestry determination arguing that researchers are merely substituting one term for another without critically evaluating the existing basic assumptions regarding human variation. Unless these assumptions are acknowledged and addressed, ancestry estimation remains controversial. However, in archaeological assemblages one can obtain a wealth of information on the individuals within a population being studied, factoring in the context and temporal period, and keeping in mind that variation exists within, as well as amongst populations.

According to the Scientific Working Group for Forensic Anthropology (SWGANTH 2013:1), ancestry refers to the geographic region and the ancestral origin of a particular population group, which could affect other aspects of the



biological profile. Their guidelines note that modern human populations show more similarities than differences. Using genetic data or skeletal morphology, typically 85% of world-wide variation is found within populations, and 15% between populations (SWGANTH 2013:2). They caution that no single trait can determine ancestry, and that when performing assessment, appropriate reference groups and statistical methods of classification, in conjunction with clear morphological trait descriptions and measurement definitions, are needed to understand the between-group variations to aid determinations.

The importance of ancestry estimation needs to be considered on the basis of the purpose and value of proceeding with the determination of ancestry. In the case of this dissertation, the aim is to build biological profiles of a given assemblage and understand the context of the site being studied. By determining (1) the geographic origin and population affinity of the individuals in the San Girgor assemblage, (2) the context of the site, (3) the dating of the bone assemblage through radiocarbon dating, and then connecting all this to (4) the archival research, final conclusions could be substantiated.

The issue of subjectivity or standardization is an ever-present issue, and even more so in ancestry determination. To deal with this, Hefner (2009:987) presents refined and clear definitions along with numerous drawings that include the range of variability in skeletal populations. Traits may exist in any population, however frequencies and grade of occurrence may differ, where heritability and environmental influences must be considered (Cunha 2020:9). Hefner (2009:985) found that the range in variation of cranial non-metric traits exceeds what was previously asserted as 'extreme trait' expressions. Although single traits were thought to be diagnostic of ancestry to define a 'group', Hefner's (2009:994) work shows that accounting for the variation that appears within and across populations when using combinations of traits, highlights the errors of past approaches and that the trait list approach (indicating presence or absence) lacks scientific accountability (Hefner 2014:884). He also cautions that one cannot assume atypical traits can be assigned to admixture classifications unless all groups being studied had been "mixed" for some time, for example native Africans, pre-contact Indigenous populations of North America, or Europeans (Hefner 2009:991). Hefner

and Ousley (2014:887) in their later work, argue that as long as one is using a consistent scoring system with estimated error rates to capture the range in variation, non-metric cranial traits can be successfully used to assess ancestry instead of metric analysis, thus eliminating the need for instruments, aside from a contour gauge. They do however acknowledge that combining non-metric and metric assessments could reduce misclassification errors.

Metric approaches that are used in ancestry estimation have been evolving to provide statistical models that offer quantifiable levels of probability and uncertainty. Using these in conjunction with non-metric approaches appears to be surfacing as the preferable method. These methods are surfacing in the form of computer programs, facilitated by advances in technology such as those presented in works by Jantz and Ousley (2005), Spradley (2016), Urbanová and Ross (2016), and Klales (2020). Unfortunately, not all these programs are showing evidence of high levels of accuracy and so the debate rages on.

Metric assessment methods using the cranium were originally established near the end of the 19th century. Spradley (2016:1) notes that today the most used cranial measurements are found in the Buikstra and Ubelaker (1994) manual in 'Standards'.

Dunn (2020:3) notes that cranial landmarks from which cranial measurements (from here on called 'inter landmark distances' or 'ILDs') are taken, show significant heritability, and therefore are widely used for ancestry determination. To validate the metric approach, Giles and Elliot (1962) incorporated a statistical method by encompassing linear discriminant function analysis (LDFA), later refined by Gill (1984). Most of the reference data in the past, however, involved only North American populations, therefore posing limitations when assessing individuals outside of these populations if they did not include Africans or Europeans. Howell's work in the 1970s defined 61 measurements that capture the craniofacial morphology which many researchers today find useful. The definitions were modified into three-letter codes for efficiency (Howells 1973, as cited in Dunn 2020) however, the approach to obtain the ILDs and LDFA requires several types of instruments, includes numerous calculations, and requires a significant amount of time.

Advanced technology has encouraged researchers to adopt the most useful measurements and refine the method to increase accuracy, reliability, and efficiency, as well as recognize the need for new reference data that is more representative of worldwide populations. For example, the work of Urbanová and Ross (2016) presents a new 3D landmark database (3D-ID) using geometric morphometrics, focusing on the shape of cranium, incorporating populations from South America, Central, Southern and Southwestern Europe. However, although the focus has been on obtaining population-specific data, Spradley (2016:2) argues that more attention needs to be given to the use of *appropriate* data sets and method selection. Unfortunately, while some of the analytical software is free to access, others are costly, which can be prohibitive. Ultimately, as with all other analytical methods, one must assess which might be the most suitable based on the population being studied.

#### *2.7.2 Postcranial Non-Metric and Metric Approaches*

Postcranial non-metric and metric analysis is also emerging in several studies for ancestry estimation, such as the use of the femur (Meeusen *et al.* 2015) with limited success. The concept of analysing the curvature of the femur to estimate ancestry, originally proposed by Stewart (1962), was complex and did not involve statistical analysis to justify results. Dunn (2020:9) argues this method is not recommended for use as the data, methods, and results have not been standardized, replicated, or validated, and the accuracy levels are still quite low, thus potentially leading to classification errors. Advances in technology may very well change this, as it is evident in the current literature, that there are ongoing debates on the need for methods that provide high accuracy rates, reliable classification methods and efficient standardized techniques.

#### *2.8 Pathology*

Although pathology noted on skeletal elements of the San Girgor assemblage was logged, and only discussed when the pathology was unusual, detailed analysis with respect to prevalence of diseases is beyond the aim of this dissertation. Following Fox (2013:204), it is worthy to note that the overall analysis of the population may

be disputable when logging any pathological or non-pathological manifestations of commingled remains in the absence of associative elements. In addition, Fox (2013:204) notes that methods to quantify pathological lesions and non-pathological bony responses had not been standardized in the past, and that commingled remains often limit accurate diagnoses.

### *2.9 Taphonomy or Trauma?*

Assessing taphonomic factors carefully is part of the process to develop the story behind an assemblage, especially in an environment where disturbance has occurred and movement of material to a secondary burial has taken place. Baustian (2014:269) defines taphonomy as any process that affects the body of an individual upon death, and notes that the process may be intentional, natural, or accidental. Intentional processes could involve human modification prior to or at the time of death; processes that are natural could involve environmental factors; and accidental processes could involve trampling or bone modification when relocating human remains which could also be considered intentional.

In trying to assess bone, one must look at whether the process took place prior to death (antemortem), at death (perimortem) or following death (postmortem) and the results of this analysis become significant when trying to determine how commingled remains came to be, to rule out mass illness, disaster, or violence. In addition, Baustian *et al.* (2014:266) insist that, to understand why bones are commingled, contextual information must be assessed, along with the cultural significance of the actions that led to the commingling.

Although extensive research on assessing taphonomy has been performed more so with faunal remains than with human remains, Sorg (2019:10) states that taphonomic assessment standards have not yet been developed. Behrensmeyer's (1978) six progressive stages of weathering established effects of taphonomic variables on bone such as climate conditions, exposure to sun or soil versus animal gnawing, trampling, or water damage and can be assessed to determine sequence of postmortem events to rule out trauma. However, this too is subjective as it is based on photographs and descriptions, with no frame of reference or statistical grounds

to establish any determinations that could be considered ‘certain’. At this time, qualitative let alone quantitative statistical standardized methods for taphonomic analysis have yet to be presented to assist with systematic analysis of commingled remains. Incorporating other methods such as GIS, as will be discussed below in section 2.11, provides an opportunity for a more reliable approach.

Trying to determine whether taphonomy is in fact trauma becomes important when assessing commingled remains, as this could provide evidence of defensive wounds that could change the narrative of the assemblage. One must look at the environmental context and determine postmortem processes to discriminate between patterned injuries and any postmortem modifications. This in turn can provide some clarification of peri- and postmortem events.

Sorg (2019:1) explains that trauma itself would indicate an injury that occurred before or at the time of death (antemortem and peri-mortem respectively); taphonomic modifications on the other hand are ‘defects’ visible on remains and would have occurred postmortem where taphonomic changes evolve as do the environmental conditions surrounding the remains.

Pérez (2012:160), in his work on taphonomy and violence found on human skeletal remains, argues that one must not only note the presence of tool or cut marks, but also the location and appearance to determine the nature of the markings clarifying whether the marks are due to antemortem activity or perimortem injury. This would mean then, by eliminating antemortem or perimortem variables one can focus on postmortem causes of any taphonomy, such as burial disturbance and movement to a secondary burial site.

Unfortunately determining timing and cause of taphonomy on bone is not always so clear. Antemortem trauma can be identified by the evidence of healing or remodelling. However, Sorg (2019:2) citing Barbian and Sledzik (2008) points out that, in children the periosteal reactivity could be seen in as little as a few days on children, but only visible after one, two or more weeks in adults. In other words, there is a chance that if death occurred shortly after antemortem trauma, one might consider the trauma to be perimortem in adults. Perimortem evidence on skeletal remains would be related to an injury inflicted around the time of death, however,

this too could be impacted by environmental conditions leading one to assess otherwise.

Taphonomic breaks or defects that are dry or brittle would be considered postmortem, however, as some agents can affect bone in a similar manner, one must consider 'equifinality', where taphonomic modifications appear to be the same morphologically but are caused by different agents (Sorg 2019:3). As a result, problems with characteristics of taphonomic processes do exist and may not be so clearly delineated when assessing skeletal remains, particularly if the context of the assemblage is not known, and even more so when commingled.

Several factors can indicate taphonomy as opposed to trauma, displaying particular characteristics. These include staining, shape of cut marks (U or V shaped), desiccation cracks due to weathering, and loss of bone elasticity. For example, scavenger tooth marks, blood vessel channels, or marks created by plant roots that infiltrate bone, may sometimes be mistaken for cut marks made by a sharp tool which Sorg (2019:6) notes would reveal a V-shaped or square bottom groove, identified more clearly using magnification.

Modifications caused by carnivores also can be mistaken for blunt force trauma (Sorg 2019:7) and some clear indications of carnivore patterns include pits and punctures, long bone shafts missing proximal and distal ends (often on both right and left sides), and missing extremities. On the other hand, the removal or shortening of extremities (postmortem dismemberment) by sharp force trauma, will show evidence of tool marks indicative of humans as the taphonomic agents (Sorg 2019:9).

### *2.10 Trauma Analysis and Cut Marks*

The work of Rodríguez-Martín (2006) on *The Identification and Differential Diagnosis of Traumatic Lesions* on the skeleton clearly outlines the necessary steps to take to assess potential trauma and rule out any violence, particularly in a context that is unexplained. More recent work by Martin *et al.* (2014:130) discusses issues that arise when trying to study taphonomic processes and the potential origin of cut marks or what may seem to be cut marks. They point out (citing Marshal 1989:12)

various agents that may cause “groove-like cut marks or slice-like scratches”, including excavators, carnivore or rodent gnawing, or environmentally related agents such as rockfall, water transport and movement.

According to Martin *et al.* (2014:142) burials disturbed by carnivores or heavy equipment can show all the types of fractures along with spalling and flaking, cuts, splits, abrasions, scrape marks and peeling. She cites an example from the La Plata commingled assemblage studied in Mexico where a backhoe left the impression of a green (perimortem) fracture and peeling cranial and post cranial fragments, which usually would have been thought to be breaks noted on fresh bone. Moraitis and Spiliopoulou (2009:6) note that dry bone has a reduced collagen and moisture content, resulting in less elasticity. Fractures in such cases, are irregular and blunt where the breakage is usually at a right angle to the long axes with flat ends in postmortem situations. The edges would be lighter in colour as they would have been exposed to the environment at a later stage when compared to surrounding bone. Peri-mortem fractures on the other hand would have smooth edges and the surrounding bone would be of the same colour. In addition, long bones would display angled, jagged surfaces where the break has taken place (peri-mortem), and the bone tear near the break would seem as if it has been peeled.

While antemortem trauma would exhibit an osteogenic response, a sign of healing, this is absent in perimortem injuries and postmortem taphonomic processes, making the differentiation between peri and postmortem trauma more difficult. Experimental research performed by Moraitis (2009) on fracture patterns and the morphology of fractured edges can contribute to differentiating perimortem from postmortem trauma. In addition, hot and dry conditions versus wet environments, as well as acidic versus alkaline soils, could also affect the condition of the bone, making the differentiation between perimortem trauma and postmortem taphonomic analysis difficult, as discussed in works by Moraitis (2009) and Haglund (2014).

A study of trauma on skeletal material from a Benedictine Monastery in Croatia (Bedic *et al.* 2019), dating to the period of Late Medieval to Early Modern, provides some data for comparative analysis with the San Girgor assemblage. The results of

this study provide insight into distinguishing trauma that could have been inflicted, during this period when Ottoman raids were a constant threat, as they were in Malta. One would expect to see high levels of injuries in particular areas on the skeleton evidencing cases of interpersonal violence, and a higher incidence of males in the assemblage. Bedic *et al.* (2019) show that perimortem fractures, and a high frequency of trauma to the cranium in males, is characteristic of interpersonal violence, while the postcranial skeleton is more likely to show antemortem skeletal markers that result from non-lethal injuries which have healed. In addition, traumatic injuries such as fractures, projectile injuries and puncture wounds provide evidence of conflict that may lead to death particularly when one incorporates the sex distribution of the trauma. Finally, the location of the trauma is also important as evidence of perimortem trauma would be expected on the face, hands (defensive wounds), upper vertebrae (attempts at decapitation), cuts in the mastoid region (removal of ears), and on the scapula (attacked from behind); whereas one would expect markers on the ribs or on the os coxae when attacks occur directly from the front (Bedic *et al.* 2019:141). Identifying perimortem trauma versus taphonomic processes in commingled assemblages therefore becomes crucial to determine whether interpersonal violence may have taken place.

### 2.11 Geographic Information Systems (GIS)

As commingled remains pose a challenge in estimating the MNI, even more so if fragmented, methods encompassing technology to make the task less complicated and more efficient have been surfacing and again the approaches stem from the field of zooarchaeology. To deal with the mounds of fragmented remains, zooarchaeologists have turned to Geographic Information Systems (GIS). This has recently been applied by a few researchers to human remains, in an innovative manner to understand commingled remains in archaeological contexts, where human bone is the ‘geographic landscape’ (Marean *et al.* 2001; Abe *et al.* 2002; Stavrova *et al.* 2019).

Studies have emerged (Hermann and Devlin 2008; Ciesielski and Bohbot 2014) to provide some useful techniques particularly for the analysis of large assemblages. The method shows promise in providing an accurate estimate of the MNI, bone



survivorship, cut marks, and fracture densities when compared with traditional methods.

GIS efficiently manipulates and manages substantial amounts of information and creates visual representations of spatially referenced data. Features on maps in GIS (represented as points, lines, and polygons) are instead features of and on human bone (the elements themselves, cut marks, fractures, and modifications) where the bone becomes the base map.

Once again zooarchaeologists led the way in utilizing GIS. Marean *et al.* (2001) and Abe (2002) were the first to use this computer-based approach to deal with some of the issues researchers faced when trying to determine the MNE of large fragmentary assemblages. Using GIS software, identifiable elements were sided, visually recorded, and overlaid on a bone template of the given element, and then the MNE for each element in the assemblage was determined based on overlapping fragments.

Marean (2001:340) argues that GIS software has two characteristics that make it useful for this purpose. Firstly, GIS images have spatial coordinates which allow for copies to easily be made that accurately overlap and are highly effective when several specimens are involved. Additionally, a visual representation of the spatial distribution of, for example cut marks or taphonomic processes, can be created. Data is represented as features and grids where features are shapes represented by points, lines and or polygons; grids are represented by cells with numerical values; and the software calculates the MNE based on the overlap of features within the grids.

Essentially, Marean *et al.* (2001:345) note that this approach locks a fragment in space on a specific element and the overlapping features provide a visual representation of the material in an assemblage displayed using symbolism in various colours or classification themes. Other especially useful analyses, such as quantifying cut marks or showing the density of marks relative to bone survivorship, can be quickly calculated, and visualized. Few pursued this method until recently in zooarchaeology, let alone in bioarchaeology. In fact, little is available in the

current literature even though this software has proven to be extremely efficient and effective in providing data in visual form.

Abe (2002:660) argued that GIS has several strengths that other methods cannot offer in the analyses of bone when faced with the challenges of large assemblages and could be used not only to assess the MNI and MNE, but also to analyse density and distribution of cut marks by georeferencing data. Abe (2002:661) states that zooarchaeologists have been “attempting to describe bone fragments and their surface modifications as numbers on a database, when in reality the problem has always been one of image”.

Work on osteological remains in north-eastern Honduras is also insightful; here GIS software was used to obtain “rapid data” recovery of spatially referenced skeletal material, manipulated into visual representations (Herman 2002:21). Skeletal material left in situ was georeferenced on photographs, and then queried using GIS software to obtain the MNI and LI, which provided a visual perspective of deposition and burial practices. Although Herman (2002:22) acknowledges that the use of this approach is limited with highly fragmented assemblages and where material is unidentifiable or disturbed, but such methods provide the opportunity to leave material in situ where possible, whilst providing access to data during post-excavation.

Lyman (2008:276), in his work on quantitative analysis in paleozoology, states that GIS could be suitable for measuring the total surface area of taphonomy to assist with establishing the MNI and MNE, as well as patterns, however this is dependent on the accuracy of “mapping” the specimens and the associated taphonomy onto templates of skeletal elements.

Few studies followed suit until decades later when Parkinson (2018:32) used the GIS spatial analysis approach to assess patterns of bone modification and visualize patterns of bone fragmentation through the identification of tooth mark clusters and patterning of cut mark locations in a zooarchaeological study. Following Marean’s (2001) method, each element was treated as a map on which bone fragments and bone surface modifications were recorded and the visual representation of extensive data proved to be incredibly useful in providing behavioural analyses.

Stavrova *et al.* (2019) utilized GIS software to analyse the distribution of percussion marks on animal bone and found that digitization made the process of assessing the MNI of large assemblages more efficient, less time consuming and easier to perform comparative analysis. Their aim was to visually represent spatial links between non-geographic material, increase the efficiency of GIS as a tool, and develop a standardized process to deal with substantial amounts of data (Stavrova *et al.* 2019:25) - issues that deterred the adoption of GIS in the past.

Limitations with this approach were acknowledged by the researchers: (1) one must illustrate only the cortical surface of identifiable fragments by side and element, as elements that lost cortical surface but conserved the medullary area, due to taphonomic processes, would overlap causing biased results; (2) a georeferenced template of elements deforms metric measurements and does not provide exact replicas (therefore precise criteria must define the placement of points for cut marks or outlines of polygons for fragments); and (3) calculations must be expressed in frequency rates to provide statistically accurate data (Stavrova *et al.* 2019:25).

A review of the literature shows that the adoption of GIS methods in bioarchaeology appeared 10 years *after* zooarchaeologists were experimenting with the approach, and although the technology has advanced, few have embraced the method. In fact, Hermann (2014:365) commented that researchers were still not entirely convinced these approaches could be applicable to human remains.

Admittedly, the cost of GIS software can be prohibitive, and there is often resistance to using what may seem to be time consuming and complicated software, as with all new technology. However, this author believes that the studies discussed above (Hermann 2002; Hermann and Devlin 2008; Parkinson 2018; Stavrova *et al.* 2019) have demonstrated the potential of GIS as a useful tool to analyse commingled human remains and to provide clear visual representations that discern patterns, with relevant statistical data. The use of GIS software in this research to assist in determining the origins of the San Girgor remains is discussed below in Chapter 3.

## *2.12 Future of Studying Commingled Remains*

Baustian (2014:268), in looking at the challenges and future of studying commingled remains, notes that such assemblages often involve extensive data collection, and organizing the information gathered using innovative methods and technology is crucial to manage the mounds of material. Absorbing methods of other disciplines such as zooarchaeology and creatively using software such as GIS from the initial stages of archaeological analysis can only benefit the field of those studying the complex nature of commingled remains.

Fox and Marklein (2005:209) make a very valid point noting that the difficulties in assessing commingled remains had not led to much development of methodology or comparative analysis from bioarchaeologists in the past, and mounds of data from poorly excavated sites have resulted in a huge loss of potentially useful information. However, very recently, in addition to the work that stemmed from zooarchaeology as discussed above, forensic anthropologists became a driving force behind innovative methods, computer databases, and scientific literature. This was due to the inherent need to identify missing persons, prisoners of war and commingled human remains found in complex mass graves (Spradley 2016; Urbanová and Ross 2016; Klales 2018, 2020; Sorg 2019; Cunha and Ubelaker 2020).

In addition to the methods mentioned, osteological assessments and development of biological profiles for commingled remains will benefit from the increased access to radiocarbon dating and eventual affordability of DNA analysis. The costs involved at the present time did not allow for DNA analysis, however such analysis in the future, could prove to be of use to corroborate or dispute the results discussed in this study. Radiocarbon dating results (Molnár 2020) from tests on a selection of the San Girgor assemblage, however, were shared with this author, courtesy of Heritage Malta and Wirt iż-Żejtun, and this information guided and substantiated this dissertation as discussed further below.

The analysis of large, commingled assemblages clearly requires the use of a systematic approach which incorporates multiple methods simultaneously. The challenges and limitations of various methods, including time constraints, the complex and often fragmentary nature of commingled remains and the need to

provide a high level of accuracy and reliability, must continue to serve as the impetus for future development of innovative methods.

## **CHAPTER 3. METHODOLOGY**

The commingled human remains of San Girgor were inventoried in August of 2019 by staff (including this author) from the Superintendence of Cultural Heritage (SCH). The bone elements were originally stacked directly on wooden shelves, displayed for public viewing in Passageway 3, and these were removed one at a time and stored in crates for future studies. The site itself was given a site-code (SGR2019) and each element was issued an identification number - for example ID SGR2019/1 which referred to the site of San Girgor (SGR), the year of the inventory (2019) followed by the number ID. This information was logged into an Excel inventory database (Appendix I.A). The full inventory and associated raw data used for all analyses in this dissertation is available for reference via a link for Appendix I.A -I.G. A total of 40 crates were filled and the attempt was made to keep elements together based on bone type where possible. Any material that was fragmented or retained evidence of soft tissue that had not completely decomposed, was bagged to ensure its preservation, and provided an ID number. The crates were stored at San Girgor and later delivered to SCH labs to be analysed thoroughly for the purpose of this dissertation. Elements were checked to ensure the correct bone was listed, whilst any bones that were missed or did not have an ID were provided with one and added to the existing inventory.

Sorted elements were laid out on tables according to bone type and sided to determine which were left and right, where applicable. Once siding was determined, the completeness of the bone was logged to determine feasibility of further analysis (taphonomic processes, sexing, ageing, and ancestry where applicable). Following Buikstra and Ubelaker (1994:9), bone elements were rated for completeness as 1 = >75% present; 2 = 25% - 75% present; 3 = < 25% present. Those coded as “1” were considered good specimens that could provide useful diagnostic observations, “2” were considered fair, and those rated as “3” were considered poor specimens.

Photographs of elements that would highlight the results to be discussed were taken on a black cloth background to provide a contrast. A Nikon 7500 camera set at 8 (aperture)/160 (shutter speed)/100 (ISO), was attached to a stand to facilitate a view of the superior or inferior side of an element, and a tripod was utilized to obtain pictures for the frontal, posterior, lateral or medial view of elements.

Although most of the bones were in good condition, they had been handled and moved often. Pairing of different bone elements such as the long bones that articulate together or pairing left and right elements from the same individual could have assisted in refining the MNI, however given the large and commingled assemblage, the immense time required for this task, and the large workspace one would require, this method of assessment was deemed unfeasible to adopt for this study.

### *3.1 Establishing MNE and MNI*

The elements were counted to determine the MNE where each complete element was counted as one element. Any incomplete, but identifiable, elements were separated, and matching of the same bone element was attempted to reduce overestimation of elements. Therefore, for instance a proximal to mid-shaft tibia fragment pairing was attempted with other tibia fragments which consisted of the mid-shaft to distal aspect. Fragments which had maximum measurements of <20mm were listed as fragments of a particular element but not counted as an additional element when calculating the MNI, unless they could be considered as part of fragments which made up an additional element. Identifiable elements which were >20mm were included in the MNI if they were not considered part of other identifiable elements based on the zonation method provided by Knüsel and Outram (2004). The MNI for each element was then calculated based on the numbers of left and right elements where applicable (for example the femur) or based on each element (for example then cranium or the sacrum). The final MNI for the commingled assemblage was determined by taking the highest number of elements - in this case the humerus, which had a total of 92 left sided elements. Usually, complete crania would provide a good indication of the MNI however, for San Girgor

only 35 crania could be confirmed and thus, crania were not utilized to establish the MNI.

### *3.2 Assessment of Taphonomy and Trauma – GIS-based approach*

Assessment of taphonomy and trauma (antemortem, perimortem and postmortem) was made on all the skeletal material and was logged in the database (refer to the link provided in Appendix I for Appendix I.B.). The femur was one of the elements with a high BRI and had the most evidence of taphonomic processes or trauma. It was for this reason that this element was selected for the GIS-based approach to assess patterns and density distribution of taphonomic processes and trauma. The objective was to determine if these patterns could shed some light on the nature of the burial and provide evidence of secondary disturbance.

Data was collected for evidence of (1) antemortem trauma, such as healed fractures; (2) perimortem evidence, such as evidence of interpersonal violence including cut marks from weapons or unhealed fractures; (3) postmortem effects such as animal gnawing, environmental weathering, and tool/cut marks from undertakers' tools. Statistical information was obtained through comparative analysis to understand the extent of these processes (refer to the link provided in Appendix I for Appendix I.B.). The information collected which was based on the postmortem tool mark damage on the femurs, was quite extensive, and a GIS-based approach was deemed useful to manage all this data (Appendix I.B.) and visually represent the spatial distribution of these features. Following other similar methodologies (Marean *et al.* (2001) and Abe *et al.* (2002) on animal remains; Hermann (2002), Hermann and Devlin (2008), Ciesielski and Bohbot (2015) on human remains), this approach provided an opportunity to extrapolate a large amount of data that could be displayed in a clear and concise chart, the results of which are shown in Chapter 4.

Scans of a complete right and left femur were taken and converted into TIFF/PNG files which were used as the base maps for the tool/cut mark features. After digitizing the right and left femur, ArcGIS 10.6.1 was used to create a polygon shape file for each



view (anterior, posterior, lateral and medial) of both the right and left femur. All views were placed in the same layer respectively for the right and left side of the femur. Three sections (proximal, midshaft, distal) were created on each polygon of each view of the femur by splitting the polygon shapefile. A polyline shapefile was created on which tool/cut marks were drawn at the respective locations of the femur to populate the attribute table. Finally, the Kernel Density tool was utilized to create heat maps for each view which visually displayed ‘hotspots’ for the marks.

Each tool/cut mark was labelled based on the side of the femur, the view, and the location on the femur. For example, a tool/cut mark on the anterior side of the distal end of a right femur would be logged under RAD (Appendix I.B). The different abbreviations used during this exercise are listed below in Table 1.

RAPr	RAM	RAD	LAPr	LAM	LAD
RLaPr	RLaM	RLaD	LLaPr	LLaM	LLaD
RMePr	RMeM	RMeD	LMePr	LMeM	LMeD
RPPr	RPM	RPD	LPPr	LPM	LPD

Side: R = Right      L = Left

View: A = Anterior, La = Lateral, Me = Medial, P = Posterior

Location on Femur: Pr = Proximal, M = Midshaft, D = Distal

Table 1. Abbreviations used to log tool/cut marks on femurs. Raw data is available for reference in Appendix I.B.

### 3.3 Sexing

Research by Spradley and Jantz (2011) indicates that sex estimation via metric and non-metric multivariate analysis using the postcranial skeleton provides the most reliable results even with fragmented material. This varies from previous assertions that the best indicator of sex estimation is the os coxae and sacrum, followed by the cranium (Buikstra and Ubelaker 1994; Bass 2012). In fact, in the revised edition of his manual,

Bass (2012:151) does note that, based on studies by Spradley and Jantz (2011), postcranial skeletal material is proving to be a strong indicator of sex estimation.

Spradley and Jantz (2011:292) assert that the femoral epicondylar breadth, the tibial proximal epiphysial breadth and the scapula height individually provide more reliable sex estimation data than cranial metric and non-metric multivariate data. However, they do caution that the postcranial data should be compared to population specific data. Having commingled remains from San Girgor, meant that ancestry of postcranial elements could not be reliably ascertained, thus sex estimation was performed using the os coxae, cranium, and mandible.

The os coxae, crania and mandibles were analysed to estimate the distribution of sex in the San Girgor commingled assemblage following established and validated standards in osteology (Buikstra and Ubelaker 1994). Non-metric analysis was performed where elements were determined to be male (M), possibly male (M?), female (F), possibly female (F?), or indeterminate (?). The latter classification (indeterminate) was applied if taphonomic damage drastically modified the bone in areas being assessed, or where sexual dimorphism was not evident at all.

Researchers agree that relying on one single trait as opposed to multiple traits and methods when determining sex, does not provide a high degree of accuracy (Buikstra and Ubelaker 1994; Brůžek and Murail 2006; Burns 2016; Klales 2020). Sex determination in this study is based on the assessment of numerous traits regardless of element.

The traits utilized for each element along with the scoring process is provided below for the respective elements. Each trait was scored on each element before the next trait was assessed and an overall assessment was subsequently made based on all the trait scores. Alternatively, where applicable, a composite score was utilised to make the final determination.

### *3.3.1 Os Coxae: Non-Metric Analysis*

The os coxae were sorted by side, therefore left (L) or right (R), and each morphological trait was assessed on all ossa coxae before any other traits were assessed, in sequence. The aim here was to attempt to eliminate some of the bias that could have taken place if all traits were to be assessed at the same time on each individual element, before moving onto the next element. The approach also allowed for comparative analysis of the variation that existed amongst the elements for each trait being assessed.

As the material from San Girgor was commingled and not paired, the os coxae were assessed as single elements as opposed to an entire pelvis. In this study, 11 of the 17 morphological pelvic traits provided by Rogers and Saunders (1994:1051) were selected. For reference these are listed in Appendix III. The other traits were deemed inapplicable to this study of commingled remains.

Morphological traits 1, 2 and 3 listed in Appendix III were assessed using the Phenice method (Phenice 1969) by observing the presence or absence of three features: the ventral pubic arc, the subpubic concavity, and the ridge on the ischiopubic ramus. These features are generally present in females and absent in males and are presented in Figure 25.

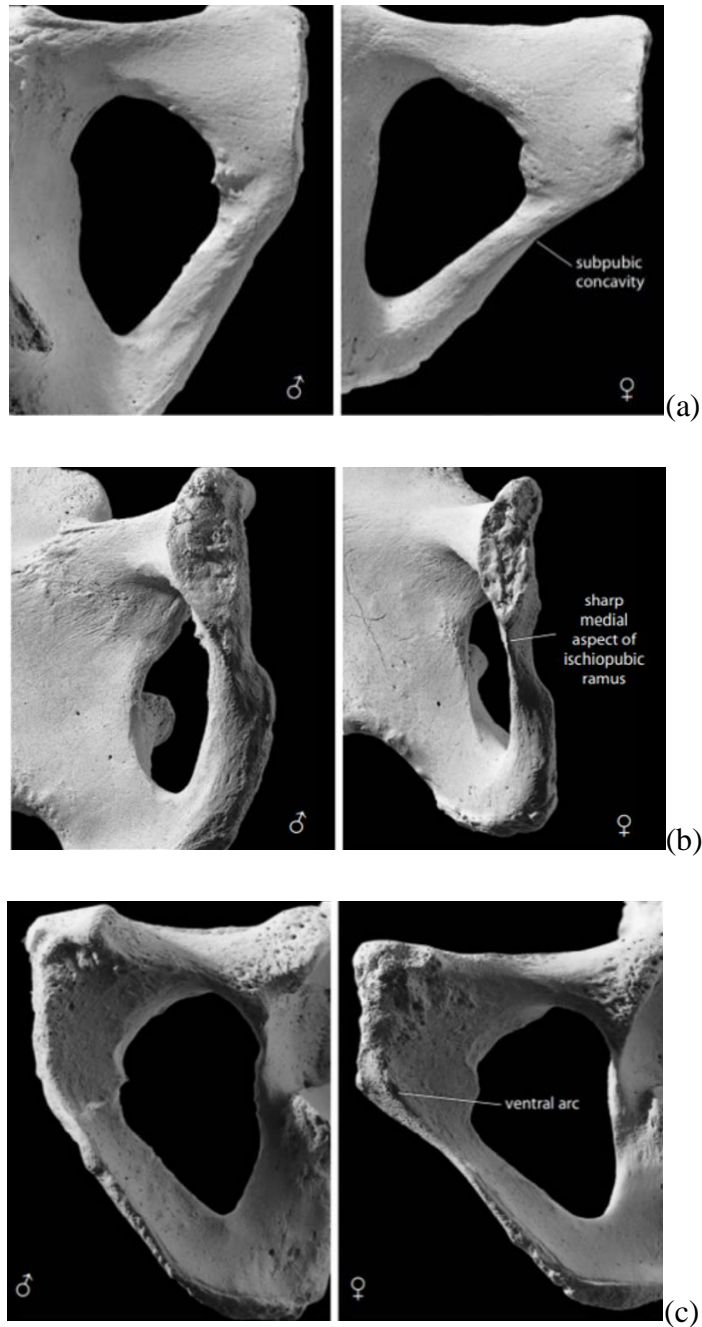


Figure 25. Sexual dimorphism in os coxae. Phenice method assessing 3 features on the pubis: (a) subpubic concavity (dorsal side), (b) medial aspect of ischiopubic ramus, and (c) ventral arc. After White et al. (2012:419).

♀ = female    ♂ = male

By observing the smooth dorsal convex surface, one would find a concave angle in females, which is minimally represented in males (refer to Figure 25a). Secondly, by

positioning the symphyseal surface face forward, one would observe a ridge just below the inferior edge of the pubic symphysis on the ischiopubic ramus in females, which is absent in males (refer to Figure 25b). Finally, when observing the rough ventral surface, in females one would usually see a ridge positioned inferiorly and laterally to the pubic symphysis that creates an elongated iliopubic ramus with a rectangular shape producing an arc. This is absent in males as presented in Figure 25c.

The greater sciatic notch (trait #5 in Appendix III), another feature used in sexing (White *et al.* 2012:417; Buikstra and Ubelaker 1994:18), is observed against a scoring chart as shown in Figure 26. The greater sciatic notch tends to be wider and shallower in females and would be issued a score of “1” or “2”, and narrower and deeper in males where the score given would be “4” or “5” when comparing against the chart in Figure 26. A score of “3” is used when the feature is questionable and is indeterminate. White *et al.* (2012:417) cautions that the reliability of using the sciatic notch to determine sex is low and should not be used as the sole determining factor. Instead, it should be used in conjunction with other morphological traits. In this study the analysis and scoring of the greater sciatic notch on the os coxae was used in conjunction with the other ten traits listed in Appendix III to determine sex.

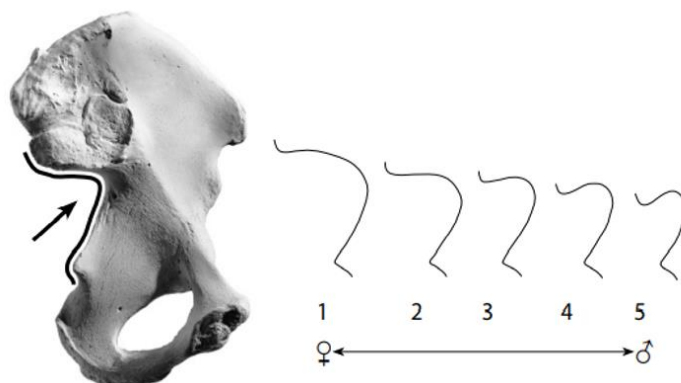


Figure 26. Sexual dimorphism in the greater sciatic notch; the arrow points to the angle of sciatic notch. After White *et al.* (2012:417) citing P. Walker in Buikstra and Ubelaker (1994).

Key: ♀ = female ♂ = male

1=hyperfeminine, 2=feminine, 3=indeterminate, 4=masculine, 5=hypermasculine.

When analysing traits #6 (auricular surface height) and #7 (preauricular sulcus) as noted in Table 1, all ossa coxae were laid out side by side with the dorsal side facing upwards for comparative analysis. Those with obviously raised auricular surfaces were noted as female, while those with flatter surfaces were noted as male, following Lovejoy *et al.* (1985).

The presence or absence of a preauricular sulcus (trait #7 in Appendix III), has often been considered a trait that is sexually dimorphic, it being present as evidence of the female sex (Buikstra and Ubelaker 1994:19, citing Walker 2008). However, Karsten (2018:605) notes that this trait is not one that should be used on its own for sex determination as variation does exist (both within and amongst populations), and the presence should not be considered absolute evidence of the female sex. Karsten's (2018:607) studies also indicate that the preauricular sulcus presence and morphology lack a statistically significant relationship to age and ancestry. The added assertion that parturition scars and pits are evidence of giving birth (and therefore making assumptions that the given element is that of a female) has not been fully substantiated (Cox 2000:135) and therefore in this dissertation, this method was used only for comparative purposes and not for sex determination.

Morphological pelvic traits #4 (shape of pubic bone), #8 (ilium shape), #9 (obturator foramen), #10 (acetabulum), and #11 (muscle markings) were assessed macroscopically and recorded accordingly based on female or male expression as per Appendix III.

### *3.3.2 Sexing Os Coxae: Metric Analysis*

To provide a comparative analysis and assist with sex determination, a metric method was also used to assess the ossa coxae. Only 45 of the 81 ossa coxae could be used in this method as features required for measurement assessment were absent in some cases.

Following Albanese (2003:266), the Ischium-Pubis Index (IPI) was calculated using the superior pubic ramus length (SPRL) and the acetabular ischium length (AIL). The original Washburn method cited in Bass (2012:196) and discussed at length in Drew (2013) is used to obtain measurements. As shown in Figure 27, point (A) is a notch on the anterior acetabular lunate surface, point (B) is the most proximal aspect of the symphyseal face, and point (C) is the ischial end point at the maximum expression of the ischial tuberosity. The length of the pubis (A to C) and the length of the ischium (A to B) were measured using sliding callipers with a digital gauge.

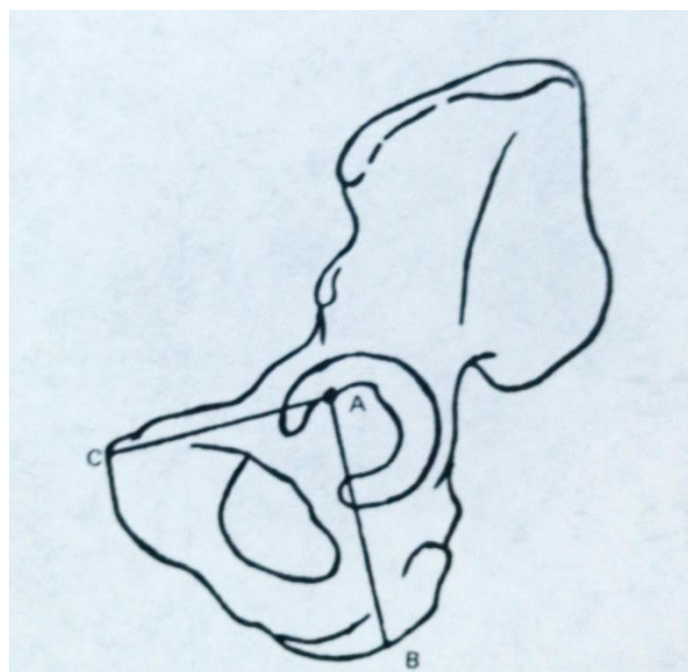


Figure 27. Landmarks for sexing the os coxae using Ischium-Pubis Index (IPI). After Bass (2012:200).

The index is calculated by dividing the length of the pubis (AC) by the length of the ischium (AB) and multiplying by 100 ( $IPI = AC/AB \times 100$ ), a method that can be useful in commingled assemblages, as it can be calculated from a single os coxae (Bass 2005:196).



Figure 28. (a) ID SGR2019/1750 right os coxae, older adult female; (b) ID SGR2019/1746 right os coxae, older adult male. Notice evidence of tool/cut-marks. Anterior view.

An example of a female and male os coxae in Figure 28 presents some of the visible morphological differences between both sexes. The female element (a) includes a wider but smaller body, a wider greater sciatic notch, a smaller obturator foramen, a raised auricular surface, a deeper preauricular sulcus, and a longer iliopubic rim.

### *3.4 Sexing: Metric and Non-Metric Analysis of the Crania*

To determine sex and distribution based on the crania, 11 traits were utilised following Walker (2008) and Klales (2018). The crania were laid out side by side on tables and each trait was assessed on each cranium for comparative analysis before the next trait was observed. As Bass (2012:81) notes, sex estimation of the crania is based on generalizations where the male is considered more robust and rugged due to muscle markings. Variations do exist and could be affected by population, lifestyle, and



environment however characteristics that are used to generally distinguish males from females are noted in Appendix IV.

The characteristics listed in Appendix IV are defined in the Glossary (Appendix II), and were assessed based on a scoring process, shown in Figure 29. Each cranium was placed against the drawings and compared to determine score and sex estimation.

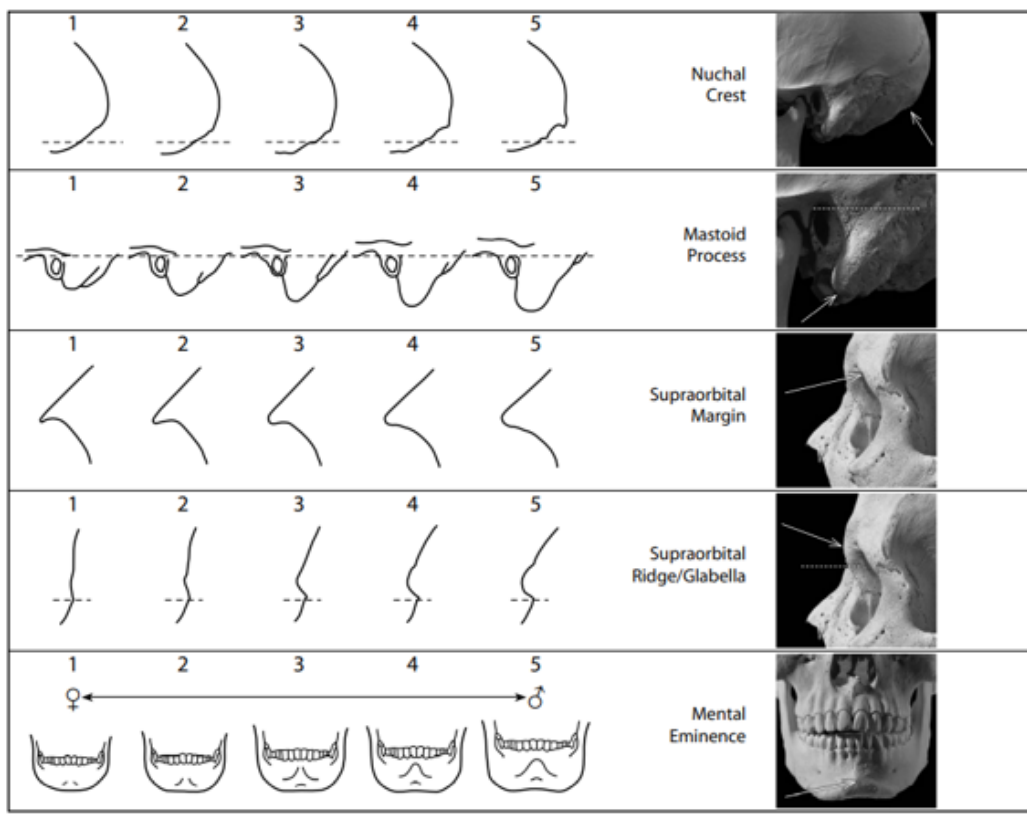


Figure 29. Sex determination using sexually dimorphic features of the cranium with a qualitative scoring system. From White et al. (2012:410) citing P. Walker in Buikstra and Ubelaker (1994).

♀ = female    ♂ = male

Key: 1 = hyperfeminine, 2 = feminine, 3 = indeterminate, 4 = masculine, 5 = hypermasculine.

The sex determination was then based on a review of all scores. As variation does occur, in some instances small gracile males could in fact be considered robust females and the opposite could be true as well where robust females might be considered gracile males. Metric analysis was also performed in the hopes that results could be

corroborated and considered more accurate. In instances where all characteristics were difficult to determine, an indeterminate score, noted as “?”, was given.

Figure 30 provides an example of comparative differences based on characteristics observed in males and females and Figure 31 shows an example of individuals of different sex, age, and ancestry.



Figure 30. (a) ID SGR2019/758 older adult male, European; (b) ID SGR2019/725 adult female, European.



Figure 31. (a) ID SGR2019/758 older adult male, European; (b) ID SGR2019/1740 adult female, European; (c) ID SGR2019/1785 sub-adult female, European (?).

As the San Girgor assemblage is commingled and definite pairing was not possible, the left and right sides of elements were assessed independently. However, both the left and right sides of each cranium and mandible were observed when compared to descriptions, drawn figures or actual photographs of bone samples, particularly those provided by Klales and Cole (2018) in their manual for the Morphopasse Database.

Klales and Cole (2018:15, citing Cole *et al.* 2017) caution that both left and right sides should be analysed (where applicable) as in asymmetric individuals, since it has been demonstrated that assessing the left side only seems to favour female classification, while the right side only often leads to male classification. Their detailed descriptions for each trait and related scores of 1 through to 5 and clear explanations on method of assessing the elements proved to be very helpful, over and above what was provided by White *et al.* (2012), Walker (2008) and Buikstra and Ubelaker (1994).

After all traits were analysed the overall rating of “M”, “M?”, “?”, “F”, “F?” was reviewed to make a final determination. If any of the traits were difficult to assess as specifically male or female, the trait was classified as “M?” or “F?” and the final overall assessment was listed as “M?” or “F?”. If the trait was impossible to score, it was assigned a “?” (undetermined). If 50% or more of the traits were difficult to assess and assigned “?”, the overall sex estimation for the cranium was listed as “?” (undetermined).

This non-metric analysis was later compared with craniometric analysis based on landmarks shown in Figure 32 and 33, and also defined in Appendix V. Indices (listed in Appendix VI) were calculated using the measurements obtained from these landmarks, providing data that further categorized the crania for comparative analysis, and determined if any discrepancies existed. Interestingly, the non-metric data that resulted in a questionable classification, for example, “M?”, resulted in a more definite estimation as “M” when metric analysis was performed. This would indicate the presence of gracile males and robust females highlighting the variation within

populations, as well as amongst populations. Crania that were not complete were assessed as undetermined (“?”) and no sex determination was logged.

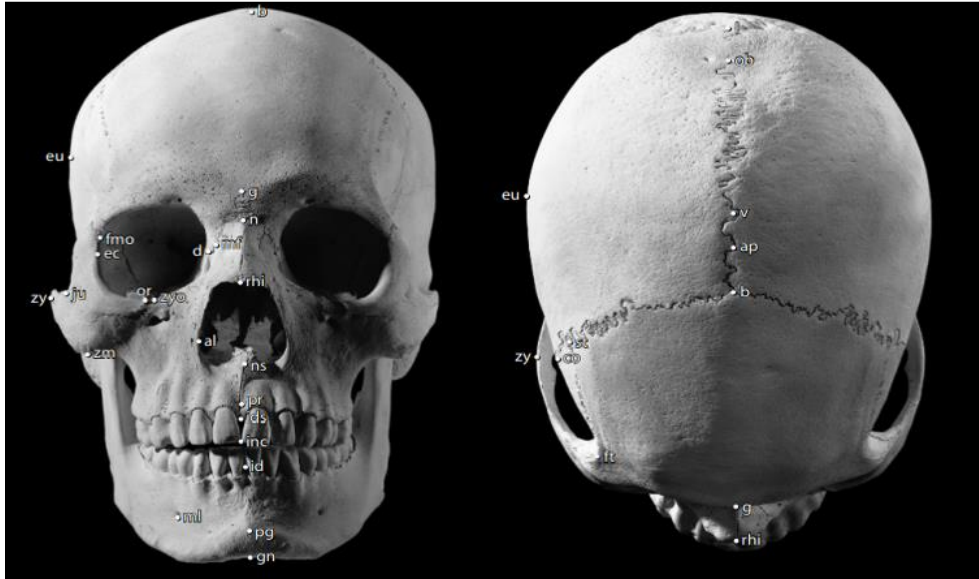


Figure 32. Craniometric landmark points (White et al. 2012:55). Descriptions are provided in Appendix V. Descriptions for points not used in this dissertation are not provided.



Figure 33. ID SGR2019/755 adult female, European (?), inferior view. Landmark points shown, used for craniometric analysis. Sphenoid-occipital synchondrosis used for ageing, indicated with red arrow.

### *3.5 Mandibles*

Sex determination of complete mandibles was performed by viewing the angle of the ramus and scoring the morphology of the mental eminence (or protuberance) along with the tubercles located lateral to the protuberance. The mental eminence was scored from 1 to 5 following Klales and Cole (2018:21) and as shown in Figure 29 (above) by assessing the shape of the mandible and the presence or absence of tubercles which they believe should be given most weight. A score of “1” (female) would be indicative of no tubercles and a more pointed or rounded mental eminence. A score of “5” (male) would indicate evidence of widely spaced tubercles and a square mental eminence. Scores “2” to “4” would be variations of these. The angle of the ramus was classified as ‘male’ if it was found to be flared, at a right angle, and had rough muscle markings, and considered ‘female’ if it was narrow, angled, and smooth. Both these traits were considered to then corroborate sex determination.

### *3.6 Ageing*

Researchers have for decades worked on validating, improving, and simplifying standard ageing methods used on the os coxae (Burns 2016:117). The broad categories for age groups associated with age estimation methods are an issue in that one cannot obtain specific ages, but rather wide age ranges. Age categories for the commingled remains in this study are outlined below and follow those provided in Buikstra and Ubelaker’s (1994:9) ‘Standards’.

F = Foetal = (< birth)

I = Infant (birth < 3 years)

C = Child (3-12 years)

AO = Adolescent (12-20 years)

YAd = Young Adult (20-35 years)

MAd = Middle Adult (35-50 years)

OAd = Old Adult (50 + years)

To clarify, if an element was aged 20+ years, the individual would fall into the young adult category (20-35 years old) and if the element was aged at 18 to 20 years, the individual would be placed in the adolescent category (12-20 years old). If age ranges determined included standard deviations, the average age would be used to categorize the age. Although age estimation based on the epiphyseal fusion rate of bones of younger individuals (20 years of age and under) discussed below, is very useful in determining age, very few elements in this assemblage were under the age of 20 years. Any individuals which did not show adult morphology and were estimated to have an age at death of <20 years of age using metric and non-metric analysis, were generally considered “subadult”, following Osterholtz (2014: 41).

### 3.6.1 Ageing: Non-Metric Analysis of the *Os Coxae*

The two key methods when ageing human remains involve the pubic symphysis and the auricular surface of the os coxae (Todd 1920; Brooks and Suchey 1990). Figure 34 presents the os coxae of an older adult female (a), and an adult male (b), with the areas used for age estimation noted.



Figure 34. (a) ID SGR2019/1614 left os coxae, older adult female; (b) ID SGR2019/1754 left os coxae, adult male. Anterior view. Top arrows indicate the auricular surface, and the lower arrows indicate the pubic symphysis.

The analysis of the pubic symphysis to estimate age was based on the Suchey-Brooks method (Brooks and Suchey 1990). The approach originally devised by Todd (1920) was revised to offer a simpler scoring process along with photographs to allow for comparative analysis. In addition, the reference data was obtained for both males and females, as previously female data was not incorporated. Figure 35 provides examples which are utilized for comparative purposes in trying to estimate age and detailed descriptions of the six pubic symphyseal phases (I-VI) and associated ages are listed in Appendix VII.A and VII.B.

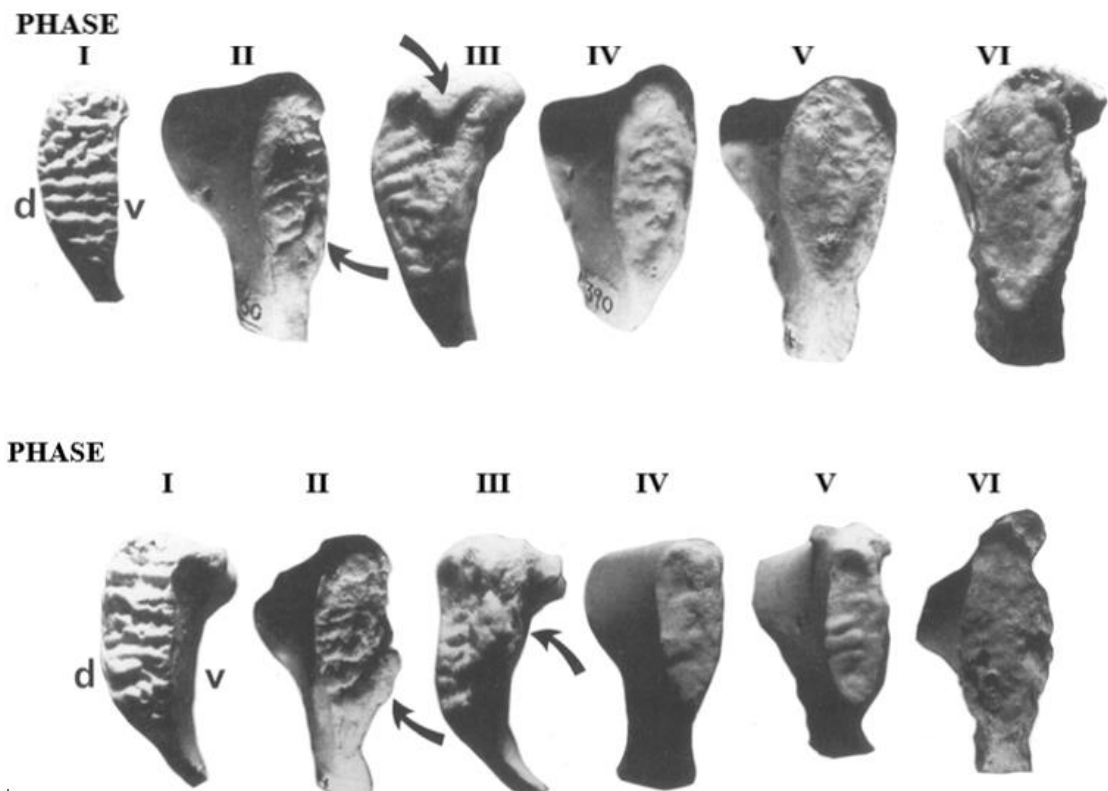


Figure 35. Age determination based on morphological changes of pubic symphysis - using Suchey-Brooks method. Above: Male pubic symphyses; Below: Female pubic symphyses; left side shown with d = dorsal side; v= ventral side; Arrows in males indicate ossific nodules in inferior and superior sections; Arrows in females indicate the ventral rampart being formed. Adapted from Brooks and Suchey (1990:230-231).

The 82 os coxae were laid on a table and separated according to left and right side, and then by sex. Each pubic symphysis was compared against the charts, photographs, and phase descriptions to determine the phase and age estimation. The process was time consuming and difficult at times as the comparison against the charts and photographs was not always clear. It was necessary and helpful to refer to other ossa coxae that were in the assemblage for comparative analysis. Physical cast examples of the pubic symphyseal phases would have facilitated the estimation, however online digital images provided clear visual representations for comparison (Klales and Cole 2018).

To strengthen the age estimated using the pubic symphysis, the next approach focused on the modification of morphological features that occur with age and are visible on the auricular surface of the ilium using the method by Lovejoy *et al.* (1985), with descriptions revised to a six-phase method by Osborne (2004). Increased age diminishes billowing and increases micro/macro porosity and degradation of the surfaces to varying degrees. Each os coxae was analysed by comparing the auricular surface features to photographs (Figure 36) and descriptions found in Appendix VIII.A, to obtain age estimation.

The age ranges are extremely broad when assessing an adult os coxae (for those over the age of 20 to 27 years) and specific age determination is not possible. Research by Mulhern and Jones (2005:63), shows that the Lovejoy *et al.* (1985) method is more accurate for individuals aged 20-49 years, whilst the revised method by Buckberry and Chamberlain (2002) is more suited to individuals aged 50-69 years. Reference to Buckberry and Chamberlain's (2002) method was therefore made to confirm age estimation for the those that seemed to fall into the older age categories, of which descriptions and scoring can be found in Appendix VIII.B.

The two age estimates obtained from the assessment of the morphological modifications of the pubic symphysis and auricular surface were compared and a mid-range was determined.



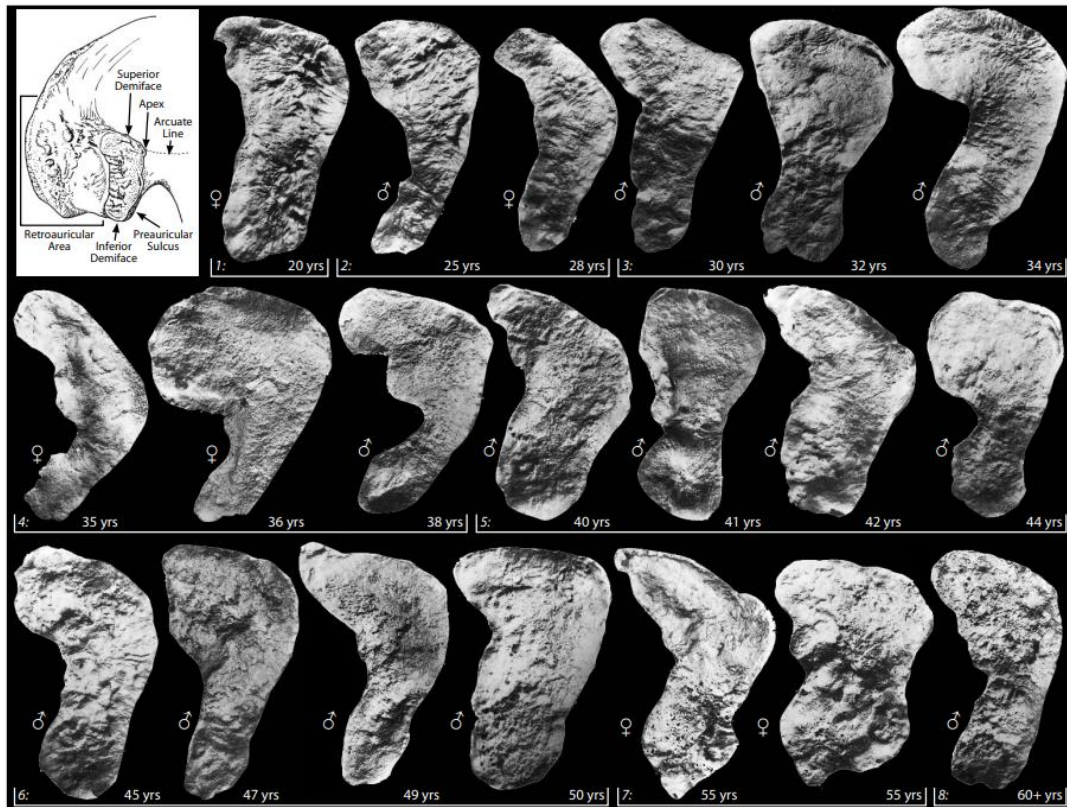


Figure 36. Age estimation based on morphological changes of the auricular surface in males and females. From White et al. (2012:402) citing P. Walker in Buikstra and Ubelaker (1994). ♀ = female ♂ = male

### 3.6.2 Ageing: Epiphyseal Fusion

The stage of epiphyseal fusion in various elements, as shown in Figure 37, is another excellent indicator of age (Brothwell 1981:66) particularly with sub-adults. This method was utilized on all applicable elements which were in good condition, particularly the long bones, scapulae, clavicles, vertebrae, ossa coxae, and sacra.

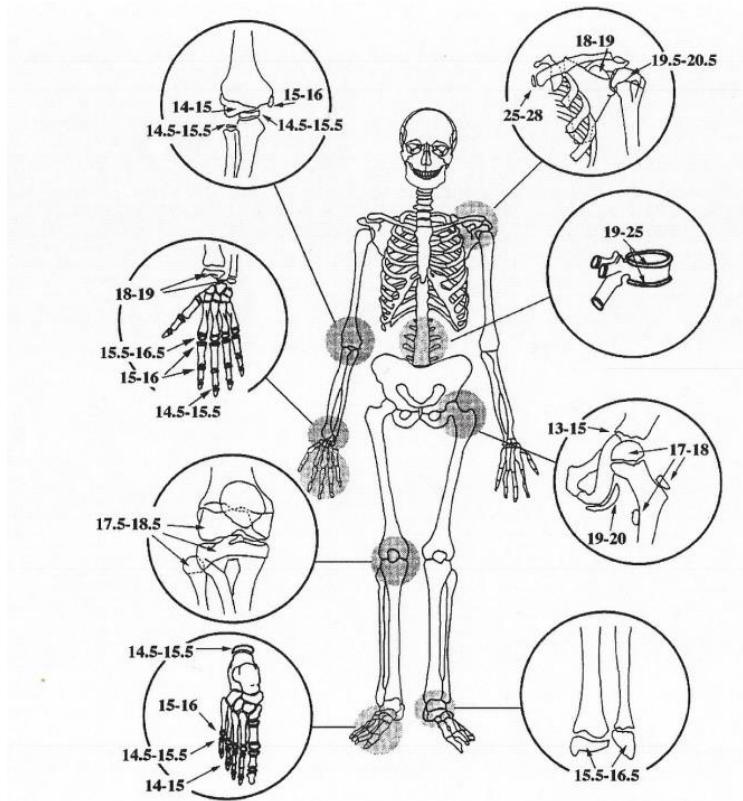


Figure 37. Age of epiphyseal fusion of various skeletal elements.  
 Taken from Brothwell (1981:66).

Following Webb and Suchey (1985:457), there are four key stages in the process of epiphyseal fusion: (1) non-union with no epiphyses, (2) non-union with separate epiphyses, (3) partial union, and (4) complete union. However, as the remains in this study were commingled, it was not possible to assess stage 2. The elements were classified in this dissertation as adult (complete union) or subadult (non-union with no epiphyses or partial union). Epiphyseal fusion rates are shown in Figure 37 and an example of a single os coxae found which belongs to that of a child, possibly male (a), and that of a subadult female (b) are shown in Figure 38.

An example of a right and left femur which may or may not be of the same individual shown in Figure 39 provides an example of a subadult where fusion of the epiphyses has not yet taken place in the long bones. Figure 40 shows an adult tibia (a) and a subadult tibia (c) with adult tibias (b) and (d) of varying sizes on either side of subadult

tibia for comparative purposes. The epiphyses on the distal and proximal ends of the subadult tibia (c) show incomplete fusion, allowing for age estimation.



Figure 38. (a) ID SGR2019/256 left os coxae, child, male (?), posterior view; (b) ID SGR2019/232 left os coxae, subadult, female, anterior view. In both cases the epiphyseal fusion is incomplete and age estimation is based on the data in Figure 37.



Figure 39. (a) ID SGR2019/100 right femur, subadult; (b) ID SGR2019/128 left femur, subadult. Anterior view.



Figure 40. (a) ID SGR2019/617 right tibia, adult, anterior view; (b) ID SGR2019/1580 left tibia, adult, medial view; (c) ID SGR2019/667 left tibia, subadult, medial view; (d) ID SGR2019/624 left tibia, adult, medial view.

### 3.6.3 Ageing: Cranial Sutures

Age estimation based on the fusion of cranial sutures which occur at different rates during the ageing process is not considered highly accurate. However, if other elements or characteristics are not available, this can be used if one acknowledges the broad age ranges associated with this method (Falys and Lewis 2011:12). The data could also be used for comparative analysis when other elements such as the maxilla, mandible or os coxae are available for age estimation analysis, ensuring more than one method is utilised to make a final estimation.

Meindl and Lovejoy's (1985:60) method shows that fusion starts with the sagittal suture, followed by the coronal and then lambdoidal suture, while the squamosal suture rarely fuses. Their scoring system to define age ranges, albeit broad, is the method used in this dissertation to quantify the progression of suture fusion and provide an estimation of age that could be used in conjunction with other methods noted above.

The process of identifying suture closures can be quite subjective. Comparing all the crania in the assemblage provided some clarification when obtaining a composite score of all areas of sutures assessed. Burns (2016: 51) notes that sutures may not always fuse even in older individuals and cites Todd and Lyon's (1924) classification of "lapsed unions" where the unfused sutures may bulge and become rounder with age, and therefore suggests classifying these as in fact closed. This important point was also taken into consideration as the other elements such as the ossa coxae suggest that the assemblage being assessed is that of middle adult (35-50 years) to older adult (50+ years) population.

Specific areas were assessed on 14 ectocranial sutures as defined in Appendix IX for each crania following the method by Meindl and Lovejoy (1985). The three endocranial sutures noted as #15, 16 and 17 in Figure 41 and listed in Appendix X were only used if the inner vault was fully visible. With this method, all sutures were scored at one time for each cranium, to minimize handling of the crania. Scores ranged from 0 to 3, where a score of "0" meant the suture was totally unfused (open), "1" meant minimal closure, "2" referred to significant closure, and "3" indicated total fusion of lapsed

union (complete obliteration). The composite scores as noted in Appendix X for the vault sutures (total scores of sutures 1 to 7) and for the lateral-anterior sutures (total score for sutures 6 to 10) provided the range for age estimation. Endocranial sutures were not assessed for this dissertation as they were difficult to see even with a flashlight, unless only the inner vault was present.

As the remains were commingled, the crania could not be associated with specific ossa coxae. However, age distribution in both elements could be used to corroborate population demographics established by the age estimation in both the crania and ossa coxae.

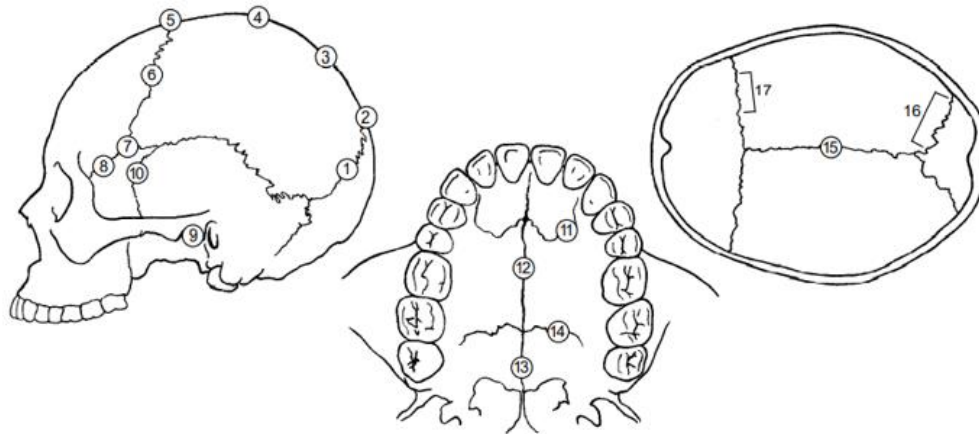


Figure 41. Age estimation using visual inspection of cranial suture closure based on distinct points (Meindl and Lovejoy 1985:60).

Definitions of sutures can be found in Appendix IX and location of suture sites 1 to 10 used in this dissertation are described in Appendix X.

#### 3.6.4 Ageing Based on Fusion of the Spheno-occipital synchondrosis

Located on the cranial base between the sphenoid bone and the occipital bone (refer to Figure 33 shown earlier), the spheno-occipital synchondrosis which is made up of cartilage, fuses by age 16 and becomes bone (Lottering *et al.* 2015:42). This was categorized as having no fusion (open), partial fusion, or complete fusion (closed)

based on macromorphological analysis. Although this feature was used to corroborate other data, it was limited to distinguishing between adult or subadult.

### 3.6.5 Ageing: Odontology

To assist with age determination, dentition present in maxillae and in mandibles was assessed using the London Atlas of human tooth development chart (Alqahtani *et al.* 2010:485; Alqahtani *et al.* 2014) provided in Appendix XI. The results from dentition in the maxillae which formed part of complete crania were used to corroborate other age estimation results obtained from the crania. Figure 42 shows the nomenclature for dentition of both permanent teeth found in adults and deciduous teeth found in children. The data obtained from the dentition of the 29 mandibles which were not associated with any crania due to the commingling of remains, were analysed to obtain age distribution data.

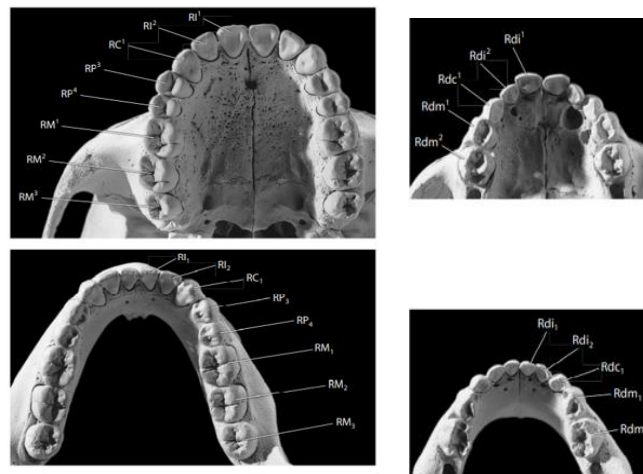


Figure 42. Maxillary (top) and mandibular (bottom) permanent and deciduous dentition, showing right side (R) marked; equivalent left side would be denoted as (L) (White *et al.* 2012:102).

Key: RI<sup>1</sup> = right permanent incisor, where superscript refers to upper (maxillary); RI<sub>1</sub> = right permanent incisor, where subscript refers to lower (mandibular); C = permanent canine; dc = deciduous canine; P = permanent premolar; m = deciduous molars (*replaced by permanent premolars, as permanent molars appear*); M = permanent molars.

### *3.7 Ancestry Determination*

To understand the origin of this assemblage, ancestry determination was attempted for this dissertation. Although this author acknowledges that DNA analysis would provide more conclusive evidence of ancestry and geographic origin, in the absence of the opportunity to perform such testing, metric and non-metric analysis was performed.

The fact that the commingled assemblage was found in passageways of this early medieval Catholic church, located in what was a remote and rural village on a small island in the Mediterranean, led this author to expect the remains would belong to locals, most likely of European ancestry. On visual inspection using characteristic traits noted in Appendix XII, it seemed that ancestry, other than that of a European ancestry, might in fact exist for a select number of the crania. This provided the motivation for assessing ancestry to understand the remains further. To do so, metric analysis was performed, and it was crucial to select a method where the reference population was representative of the assemblage being studied to obtain a high degree of accuracy in any demographics obtained.

The Giles and Elliot (1962, 1963) method using cranial measurements, discriminant function analysis and information forms devised by Gill (1984) was based on the Robert J. Terry Anatomical Skeletal Collection held at the Smithsonian Institute and the Hamann-Todd Osteological Collection housed at the Cleveland Museum of Natural History.

The Terry Collection includes a heterogenous population, both urban and rural, European and African males and females from the 19<sup>th</sup> century. Based on the time period, origin location (St Louis, Missouri, USA) and minimal migration of the individuals it is most likely that there was also very gradual gene flow and therefore slow changes to the gene pool as noted by İşcan (1992:39) when comparing reference databases for ancestry assessment. The mean age at death for males in this collection



is 54 years and for females 58 years, with age ranges from 20-81 years (Hunt and Albanese 2005:414).

The Hamann-Todd Collection was based on individuals from the early-mid 19<sup>th</sup> century from the Cleveland area (USA) and also included older males and females of European and African descent but of lower income status than those of the Terry Collection (İşcan 1992:39).

The biological profile results shown in Chapter 4 indicated that the human remains from San Girgor belonged to primarily older individuals, both male and female, from a rural area where many (but not all) most probably would have been of lower income status. This information required a method based on a reference collection that was comparable and therefore, the Giles and Elliot (1962, 1963) along with the Gill (1984) revisions, was deemed the most suitable method with the most relevant reference population data to assess the ancestry of the San Girgor commingled remains.

Appendix XIII provides an example of the worksheet (Giles and Elliot 1962) used with landmarks, measurements and calculations required to determine ancestry. As Snow *et al.* (1979:5) note in their tests which validated the use of the Giles and Elliot functions, the landmarks are well-defined and relatively easy to measure, with clear calculations outlined. In addition, Hunt and Albanese (2005:416) in their detailed discussion of the collection show that the data is based on meticulous processes to obtain complete and well-preserved specimens with accurate documentary data obtained in a consistent manner.

As Snow *et al.* (1979:2) explain, linear discriminant functions allow one to assess various metric characters, giving each a value which can then be classified into categories. In the case of the Giles and Elliot method, when the characters (eight linear measurements) are obtained from the unknown (unidentified cranium), the functions applied assign the cranium to one category or another (for example male/female, European/African).

Callipers were calibrated by closing the jaws and bring the scale back to zero to ensure accuracy. Sixteen of the 35 crania were selected for ancestry estimation, based on two criteria: (1) no pathology evident that could affect measurements, and (2) the presence of landmarks needed for measurements. Sliding digital callipers and spreading callipers were used to obtain measurements between the various landmarks, descriptions of which were mentioned earlier and provided in Appendix V.

Each cranium was placed on a table in a stable position with the anterior section of the skull facing front, and then measurements were taken and rechecked to ensure accuracy. For measurements of landmarks on the inferior section of the cranium and on the palate, the cranium was placed on a foam mat, with the inferior section facing upwards. This facilitated access to the landmarks and prevented damage to the crania.

The discriminant function for sex determination following Giles and Elliot (1962) was calculated using five measurements in millimetres along with the coefficients assigned (#1, 2, 5, 6 and 7 on the chart in Appendix XIII). The sectioning point provided is 891.12, to assign male or female determination. A score of  $> 891.12$  would place the cranium into the male category, while those with a score of  $< 891.12$  would be considered female. This determination was also compared with the non-metric sex determination data that had been completed earlier in the study.

The chart provided by Giles and Elliot (1962, 1963) along with revisions by Gill (1984) shown in Appendix XIII were then used to determine European/African ancestry. This author has replaced the use of terms 'White/Black' used by Giles and Elliot (1962, 1963) with 'European/African' to delineate the geographic origin. The five crania which were deemed to be of sub-Saharan ancestry based on this method are shown below in Figure 43, the data of which was used for further archival research to corroborate the findings. The measurements taken from the various landmarks, (listed and defined in Appendix V) to perform discriminant function analysis, were also used to develop indices (listed in Appendix VI). These indices provided morphometric data used for comparative analysis of all the crania.

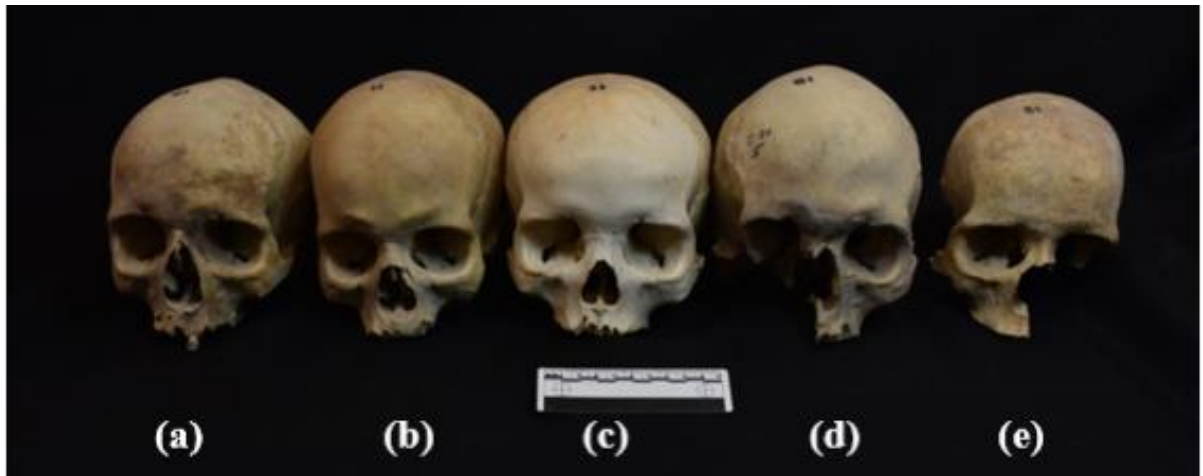


Figure 43. (a) ID SGR2019/713; (b) ID SGR2019/1730; (c) ID SGR2019/714; (d) ID SGR2019/754; (e) ID SGR2019/715. Adult sub-Saharan females, frontal view; (d) and (e) fall into older adult categories.

The data compiled on these five crania was compared with archival material retrieved from the San Gġrġor Parish for the periods discerned from radiocarbon testing results. It is important to mention that the initial results obtained to determine ancestry, which showed evidence of sub-Saharan individuals in the commingled remains from San Gġrġor, was compiled independently of the information which was later found in the archives. In fact, the ancestry results provided a springboard for the research that took place in the archives, thus allowing the author to substantiate the data.

The radiocarbon dating results (Molnár 2020) presented in Chapter 4, provided the period on which to focus within the Źejtun Parish Archives. The archival documents used for this dissertation ranged from 1580 to 1800 as no other documents prior to this period were available and they were not always legible or complete. Information from prior years was also found at the Mdina Cathedral Museum and through online databases on Maltese genealogy. The archival information was then extracted, compiled, and reviewed extensively with the intention of locating a connection to the remains being studied, particularly that which could substantiate the ancestry determination results to further understand the origin of the assemblage of San Gġrġor.

## CHAPTER 4. RESULTS

### *4.1 MNE/MNI*

The commingled assemblage from the chapel of San Girgor included 1857 bone elements most of which were in good condition. Evidence of taphonomic damage, much of which was due to disturbance, resulted in some unidentifiable fragmented bone elements which could not be included in the analysis. To develop a demographic biological profile, sexing, ageing, and ancestry were assessed, and trauma and taphonomic damage were analysed to further understand the origins of the remains from San Girgor. All elements are listed in Table 3 with the respective MNE and MNI. An MNI of 92 was established for the entire assemblage, based on the humerus which shows the highest number of MNI overall.

### *4.2 Bone Representation Index (BRI)*

Many of the bones are underrepresented based on expectations with an MNI of 92 (the results of the BRI are listed in Appendix XIV and graphically represented in Figure 44). This is particularly evident where the smaller bone elements are concerned, such as the carpals, metacarpals, tarsals, and metatarsals. Only 1% of the total hand bones and 4% of the total foot bones are represented. The BRI of long bones is substantially higher: humerus (96%), femur (78%), Fibula (89%), and Tibia (73%). The crania and os coxae which are crucial for sexing, ageing and ancestry assessment (Phenice 1969; Lovejoy *et al.* 1985; Buikstra and Ubelaker 1994; Hefner 2009; White *et al.* 2012; Spradley 2016; Klales 2020) resulted in a BRI of 38% and 44% respectively, providing the foundation for the demographic studies in this dissertation.

There is a slight discrepancy between the MNE calculated for elements in this study when compared to that of Ramaswamy and Pace (1980:57) as seen in Appendix XIV.

This could be inadvertently attributed to the disturbance of the material when it was transferred for analysis in 1979 and then again in 2019 and 2021 for this dissertation. For example, 73 vertebrae were found in the assemblage by this author as opposed to the 197 noted by earlier researchers; 176 humeri were found by this author versus the 160 noted earlier. It is not clear in Ramaswamy and Pace's (1979, 1980) reports how the MNE and MNI were established, or how fragments of bones were logged, apart from the crania. This information may have been included in Ramaswamy and Pace's raw data which unfortunately is no longer available for comparative analysis. The slight discrepancy does not affect or contradict the overall analysis presented in this dissertation. Fragments for this dissertation were assessed in detail, matched where possible to adjust the MNI and accounted for accordingly within the assemblage.

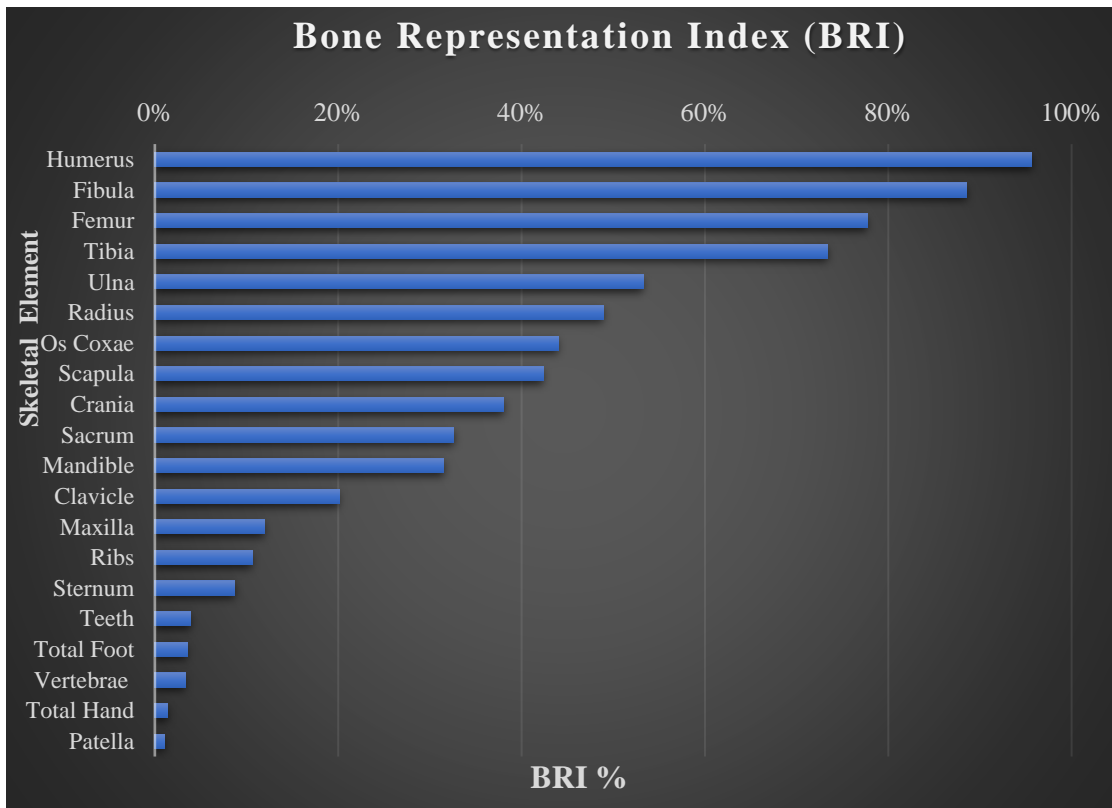


Figure 44. Percentage of bone elements represented, based on the MNI of 92.

### 4.3 Sexing, Siding and Ageing of the Os Coxae

Sex determination for this assemblage was based on the os coxae and crania. Of the 82 os coxae, 68 (83%) could be sexed; 25 (30%) were males or most likely males, and 43 (52%) were females or most likely females.

Siding of the os coxae was possible in 96% of these elements shown in Table 2. A total of 52% were left (L) os coxae and 41% were right (R). Males were represented by 31% (L) and 26% (R) os coxae, while females consisted of 44% (L) and 56% (R). Those which were questionable (? Male/? Female), or indeterminate (?) are also presented.

	45 Left Os Coxae					34 Right Os Coxae				
	Male	? Male	?	Female	? Female	Male	? Male	?	Female	? Female
n	14	1	7	20	3	9	1	4	19	1
%	31%	2%	16%	44%	7%	26%	3%	12%	56%	3%

Table 2. Siding of left (L) and right (R) os coxae for males and females. Raw data for analyses is available in Appendix I.C.

Siding of bone elements (where applicable and possible) is presented in Appendix XIV. Interestingly, the right side was represented most in the upper torso and arm bones (clavicle, scapula, radius), while the left side was represented more in the lower elements of the body (os coxae, femur, and fibula).

The bone elements mainly belong to those of young adults to older adults, with a small number that most likely belong to adolescents. Only one os coxae out of 81 identified belonged to a young child, approximately 8 years old. Of the os coxae, 79% could be aged and sexed, and the statistical distribution is presented in Table 3. Figure 45 highlights the evidence that the skeletal assemblage is representative of relatively older individuals, with 55% of the total population being over 50 years of age and 41% of these older individuals being females. The os coxae identified earlier relating to a child of about 8 years of age, is most likely male. However, changes in the os coxae during growth complicates sex determination of children

and cannot provide results with a high degree of certainty and therefore should be avoided (Brůžek and Murail 2006:238). Since only one os coxae under the age of 12 was present, this draws further the observation that the population in this assemblage falls into the adult to older adult age range.

The os coxae of the child whose sex could not be determined with confidence is noted in Table 3 to show age distribution. This was not included in the calculations to show age distribution between males and females (hence the total of 24 males versus 25 that could be both aged and sexed).

<b>Estimated Age Distribution Os Coxae</b>					
Age Range	Male		Female		n = 64*
	n	%	n	%	
<3 yrs	0	0%	0	0%	
3 – 12	1*	4%*	0	0%	
12 – 20	0	0%	0	0%	
20 – 35	6	25%	5	13%	
35 – 50	9	38%	9	23%	
50+	9	38%	26	65%	
<b>Total Male</b>	<b>24</b>	<b>38%</b>	<b>Total Female</b>	<b>40</b>	<b>63%</b>

Table 3. Age Distribution of 64 male and female os coxae.

\*The os coxae of the young child (<12 yrs of age) whose sex was not determined with certainty is not included in total counts.

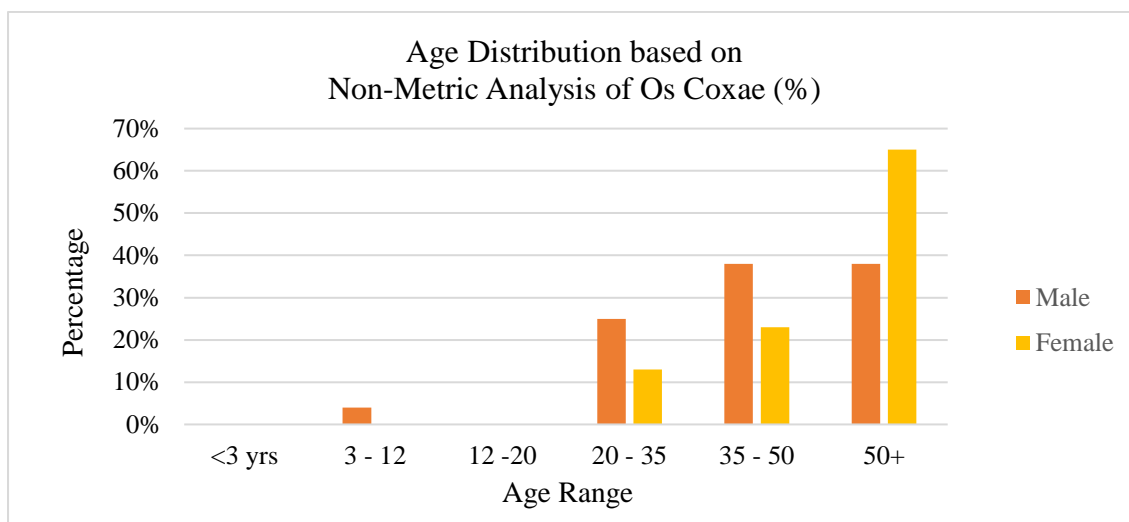


Figure 45. Graphic representation of age distribution based on os coxae.

#### 4.2 Dental Assessment

Loose teeth (teeth that have become dislodged from the mandible or maxilla at a postmortem stage) and teeth still in situ within the mandible or maxilla, all consisted of permanent teeth. These teeth resulted in a total BRI of 4% as noted in Appendix XIV. No deciduous teeth were found in the assemblage and as only one child was noted, this author expected few, if any, deciduous teeth. The teeth in the maxillae and mandibles were used for age determination. Observations were made to detect any anomalies, morphological variations, and the overall general health of the teeth. As only a small percentage of teeth were recovered, the siding, identification and study of the wear, abrasion and decay of loose teeth was not performed for this dissertation.

#### 4.4 Sexing and Ageing of Crania

There are 35 crania present in this assemblage with an MNI of 92, amounting to 32% of the expected crania. There are also 32 fragments which could not be attributed to these crania and were not suitable for sexing or ageing. Of these 35 crania, 29 were in the condition that would allow metric and non-metric geomorphological assessment to obtain sex determination and age determination with a high degree of confidence in the osteometric analysis of this commingled



assemblage (refer to Table 4). Female crania represent a higher percentage as the same is evident in the sex distribution of the os coxae discussed earlier.

<b>Sex Determination of Crania</b>					
	Male	? Male	?	Female	? Female
n	10	2	1	16	0
%	34%	7%	4%	55%	0%

Table 4. Sex determination and distribution of 29 crania. Raw data for analyses is available in Appendix I.D.

The analysis of the crania corroborates the fact that the population falls into the older age range. Overall, one individual lies in the 12-20 age category, and the majority of total males and females fall into the 35-50 age category (62%) and 50+ category (28%). The breakdown of age distribution for males and females based on cranial morphological and osteometric analysis is presented in Table 5 and graphically shown in Figure 46.

<b>Age Distribution of Crania</b>							
n = 29	Male		Female		Indeterminate		
Age Range	n	%	n	%	n	%	
< 3 yrs	0	0	0	0	0	0	
3 – 12	0	0%	0	0%	0	0	
12 – 20	0	0%	1	6%	0	0	
20 – 35	0	0%	2	12%	0	0	
35 – 50	7	58%	10	63%	1	100	
50+	5	42%	3	19%	0	0	
Total by Sex	12	41%	16	55%	1	4%	

Table 5. Age estimation and distribution based on 29 crania. Raw data for analyses is available in Appendix I.E.

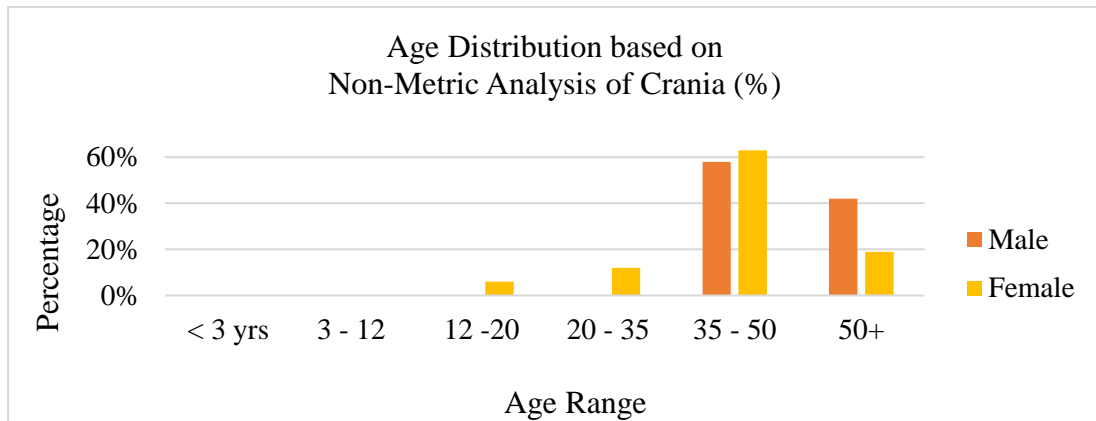


Figure 46. Graphic representation of age distribution based on 29 crania. The ‘Indeterminate’ cranium, 35-50 yrs of age, is not included in this chart.

In addition, speno-occipital synchondrosis was observed in the 29 crania that were used for sex and ageing estimation. All but one was fused confirming that the population included very few children or adolescents.

Although the total number of mandibles was less than the total number of crania and the MNI established for the assemblage, age estimation of 29 mandibles was performed using dentition. This information also corroborated the fact that there were very few children or adolescents represented and that the population fell into the older categories as can be seen in Table 6.

Age Distribution of Mandibles				
n = 29	Male		Female	
	n	%	n	%
<15 yrs	0	0%	0	0%
15.5 – 18.5 yrs	3	14%	0	0%
23.5+ yrs	18	86%	8	100%
Total Male	21	72%	Total Female	8 28%

Table 6. Age estimation and distribution based on 29 mandibles.

#### 4.6 Indices

Statistical data was derived from various indices to understand variation within the assemblage and not to determine ancestry. Tables 7 to 11 provide results of these indices outlining osteometric ranges. Twenty-eight crania that were utilized based on their condition of completeness could provide the required cranial measurements. These indices are presented to show the variation in the crania of this assemblage, expressed in numerical values or ranges in categories. Descriptions of the indices and their associated measurements used to derive each index are listed in Appendix VI and the raw data is available in Appendix I.F.

##### Cranial Module (CM)

The CM expresses a numerical value to compare the size of crania (Bass 2005:70) and it is used here to compare males to females in the entire population. The mean for the male crania in this assemblage is 151.39, while the mean for the female crania is 142.62. Generally, males tend to be larger than females (Krogman 1962:143) and although variation exists within all populations, the difference amongst populations is not significantly great (SWGANTH 2013:2).

##### Cranial Index (CI)

The CI index provides a ratio of the breadth to the length of the crania (Bass 2005:70) and is presented in Table 7. Most crania in this assemblage fall into the average/medium category (Mesocrany) with 50% of the males and 40% of the females falling in this category while 25% of the males and 33% of the females fall within the broad category (Brachycrany).

Category	Index	Male		Female		Total	
		n	%	n	%	n	%
Dolichocrany-narrow or long	X - 74.99	2	25	4	27	6	26
Mesocrany-average or medium	75.00 - 79.99	4	50	6	40	10	44
Brachycrany-broad or round	80.00- 84.99	2	25	5	33	7	30
Hyperbrachycrany-very broad	85.00 - X	0	0	0	0	0	0
Total		8	100	15	100	23	100

Table 7. Cranial Index (CI) statistical results.

### The Upper Facial Index (UFI)

The UFI is used in place of the Facial Index (FI) when the mandible is not present and expresses height to breadth of face (Bass 2005:76). Table 8 also shows that the average/medium (Meseny) category includes 50% of the males and 62% of the females; 23% of the females fall into the wide/broad category (Euryeny). Although 25% of the male crania fall into the very wide/broad face (Hypereuryeny) category, this only accounts for one male cranium that could be assessed.

Not as many of the males could be used for these measurements as not all crania were complete to allow for the required measurements. This must be taken into consideration as a higher incidence in particular categories will skew the demographic information of the population overall. It does not, however, affect the results of each cranium for comparative analysis.

UFI Category	Index	Male		Female		Total	
		n	%	n	%	n	%
Hypereuryeny – very wide or broad face	X - 44.99	1	25	0	0	1	5.9
Euryeny – wide or broad face	45.00 - 49.99	0	0	3	23	3	17.6
Meseny – average or medium	50.00 - 54.99	2	50	8	62	10	58.8
Lepteny – slender or narrow face	55.00 - 59.99	1	25	2	15	3	17.6
Hyperlepteny – very slender or narrow face	60.00 - X	0	0	0	0	0	0
Total		4	100	13	100	17	100

Table 8. Upper Facial Index (UFI) statistical results.

### Nasal Index (NI)

NI expresses the relation of the breadth to the height of the anterior nasal aperture (Bass 2005:76). Table 9 highlights the female crania that have broad nasal apertures (Platyrrhiny) with 27% of those analysed falling into this category. Overall, 53% of all males and females fall into the narrow category (Leptorrhiny). Male and female results are broken down and although the percentage of males that fall into the narrow aperture (Leptorrhiny) category is high at 75%, this is the result of a small sample of males that could be measured and may not be indicative of the population. However, as most of the population is deemed to be European, one would expect these results.

NI Category	Index	Male		Female		Total	
		n	%	n	%	n	%
Leptorrhiny-narrow nasal aperture	X to 47.99	3	75	7	47	10	53
Mesorrhiny-average to medium	48.00 - 52.99	1	25	4	27	5	26
Platyrrhiny-broad nasal aperture	53.00 - X	0	0	4	27	4	21
Total		4	100	15	100	19	100

Table 9. Nasal Index (NI) statistical results.

### Maxilloalveolar Index (MI)

MI represents the external measurements of the palate (Bass 2005:78). Table 10 shows consistent results with the previous indices when one looks at the distribution of males, females, and combined male and female percentages across the categories where the majority fall within the long and narrow palate range (Dolichurany) at 43%, and 33% fall within the broad category (Brachyurany).

MI Category	Index	Male		Female		Total	
		n	%	n	%	n	%
Dolichurany- long narrow palate	X - 109.99	2	33	7	47	9	43
Mesurany - average	110.00 -114.99	2	33	3	20	5	24
Brachyurany - broad	115.00 – X	2	33	5	33	7	33
Total		6	100	15	100	21	100

Table 10. Maxilloalveolar Index (MI) statistical results.

### Palatal Index (PI)

PI represents the internal measurements of the palate (Bass 2005:79). Table 11 provides details on the width of the palate and 42% overall are narrow (Leptostaphyline) while 42% fall into the broad category (Brachystaphyline). Again, the high percentages that result for males when compared to females is skewed as a small number of male crania were in a condition to allow for this index assessment. The results would not mean that more males than females, for example, tend to fall into the Leptostaphyline (narrow palate) category, but rather, that of the males that could be studied in this assemblage, 50% fell into Leptostaphyline category.

PI Category	Index	Males		Females		Total	
		n	%	n	%	n	%
Leptostaphyline- narrow palate	X - 79.99	2	50	6	40	8	42
Mesostaphyline- average or medium	80.00 - 84.99	0	0	3	20	3	16
Brachystaphyline- broad palate	85.00 - X	2	50	6	40	8	42
Total		4	100	15	100	19	100

Table 11. Palatal Index (PI) statistical results.

Figure 47 provides a clearer picture of the variation within the entire population in the assemblage. The results indicate that the majority of the population has an average/medium CI, UFI with narrow NI, MI, and PI.

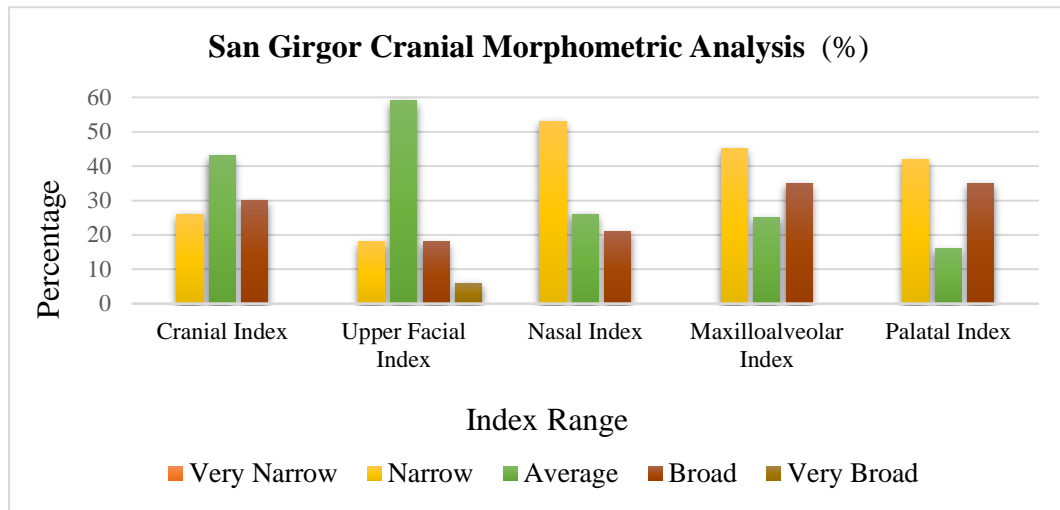


Figure 47. Morphometric Analysis based on Indices. Percentages are based on combined data for males and females.

#### 4.5 Ancestry Determination using Crania

Although sex and age determination could be established for 29 of 35 crania, only 16 (55%) were suitable to attempt ancestry determination. This amounts to 17% of the MNI (92) which may skew the percentage of Europeans versus non-Europeans, as the total established population is not fully represented by the crania in this assemblage. Table 12 provides the details of the sex and age estimation along with ancestry determination to clarify the distribution of the 16 crania utilized.

The purpose of performing ancestry determination was to understand the population affinity of the assemblage and the variations that exist within and amongst the populations. The crania that could be assessed included two males and 14 females and of these, two males and nine females were considered most likely to be of European ancestry. Five females (31% of the crania being utilized for ancestry determination) were considered most likely to be of sub-Saharan ancestry.

Crania n = 16	Age Range					Ancestry		
	Juvenile (0-11)	Adolescent (12-19)	Young Adult (20-35)	Middle Adult (36-50)	Older Adult (50+)	Total	European	Sub- Saharan
Sex								
Male	--	--	--	1	1	2	2	0
Probable Male	--	--	--	--	--	--	--	--
Indeterminate	--	--	--	--	--	--	--	--
Probable Female	--	--	--	--	--	--	--	--
Female	--	1	--	7	6	14	9	5
Total in Age Range	0	1	0	8	7	16	11	5

Table 12. Descriptive Statistics: sex, age at death, & ancestry using 16 crania. Raw data for analyses is available in Appendix I.G.

As noted in the methodology, for the temporal period discussed in this dissertation, European ancestry would include North African ancestry, while any other African ancestry would include sub-Saharan ancestry for the purpose of this dissertation. Figure 43 (presented earlier) shows the five crania that were deemed to be of sub-Saharan ancestry using multivariate statistical analysis and discriminant function analysis.

The information derived from indices shown in Appendix XV and represented in Figure 48 expresses the variation within the population, and highlights preliminary non-metric morphological characteristics assessed independently, that corroborate the population affinity. If no representation within a given range exists in the assemblage, that particular range is not shown on the graph.



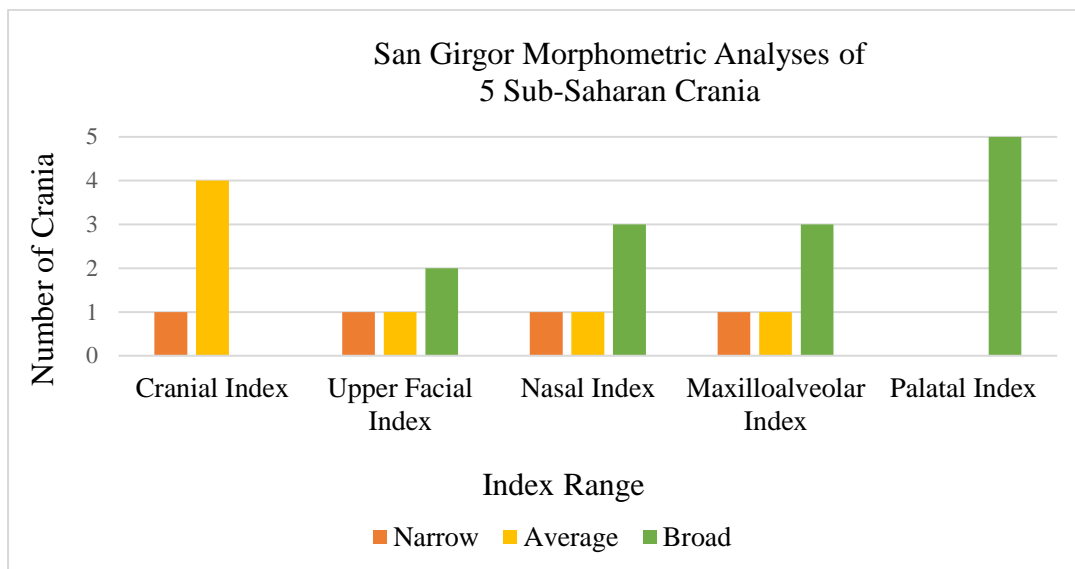


Figure 48. Index analysis of five female sub-Saharan crania.

#### 4.7 Comparative Analysis

Four of the five crania deemed to be of sub-Saharan ancestry were considered to have an average or medium size crania (Mesocrany) with one that was classified as narrow (Dolichocrany) based on the CI.

Upper facial measurements could be obtained from four of the five crania, and of these, two were found to be wide (broad), one slender (narrow), and one average based on the UFI.

The NI showed that three of the five had broad nasal apertures (Platyrrhiny), while one was categorized as narrow (Leptorrhiny) and one as average (Mesorrhiny). Three of the five were categorized as having a broad upper palate (Brachyurany), one as average (Mesurany) and one long/narrow (Dolichurany) based on the MI; while all five were categorized with a broad lower palate (Brachystaphyline) for the PI.

These results stress that variation exists within groups as well as amongst groups, and therefore ancestry could not be based on these indices alone. Each index result on its own or macroscopic analysis on morphological features alone could not accurately determine ancestry with a high degree of certainty. Performing multivariate statistical analysis and discriminant linear analysis (DLA) increases the degree of confidence.

#### 4.8 Radiocarbon Dating Results

Radiocarbon dating was completed at the request of Wirt iż-Żejtun and Heritage Malta prior to the research and analysis that was performed for this dissertation. The full report (shared with the author courtesy of Matthew Grima from Heritage Malta and Ruben Abela from Wirt iż-Żejtun) is presented in Appendix XVI. The results provided the frame of reference for archival research shedding light on evidence of the origins of the assemblage.

Seven samples which included permanent teeth extracted from crania were provided for testing. These were selected based on their level of preservation by the Senior Osteologist, Bernardette Mercieca-Spiteri, at the Superintendence of Cultural Heritage (SCH). When comparing the crania, this author noticed that the samples were taken from crania which coincidentally varied in terms of bone discoloration. This variation is most likely the result of the skeletal material being buried at different times, as is evidenced by the radiocarbon dating and timeline, as well as perhaps buried in different environments. When comparing the biological profiles performed *after* the radiocarbon dating results were issued, it was noted that six of the seven samples were female, and one was male. The sample derived from element ID SGR2019/714 is based on one of the five crania deemed to be of sub-Saharan ancestry.

The sample distribution, although not known at the time when collected, were representative of the population overall where the majority are European, female and fall into the older age category and where a small percentage of the assemblage are of sub-Saharan origin, but also female and older.

It is important to note that although the samples came from crania which were primarily female, the biological profiles of the 29 crania and 64 os coxae that could be analysed showed females comprised 55% and 63% respectively of the population. As there is an established MNI of 92, the biological profiles may not be fully representative of the entire assemblage in terms of sex distribution.

The report on radiocarbon dates for this assemblage (refer to Appendix XVI) indicates that at least one sample (SGR2019/756) is dated from AD 1440 – 1660, another (SGR2019/757) is dated at AD 1520 to 1660 and the other 5 samples are

dated from 1640 to 1950. The dates beyond 1750s are somewhat misleading and may be a discrepancy due to increased carbon from the industrial revolution to the present time which affects carbon dating (pers. comm. Matthew Grima, Heritage Malta 13 April 2022)

The data is plotted and represented in Figure 49 showing the overlap that exists. Although one cannot rule out that many of the individuals could have died at or around the same period of time, some of the samples do show that some of the deaths did occur earlier in the date range. This would indicate that the individuals are from different periods and did not in fact all die inside the hidden passageways at one point in time. A few points are worth mentioning: (1) the samples used for dating only make up 8% of the MNI (92) and other future samples could skew the results; (2) no deaths are indicated in a time period before 1440, which coincides with the views that the church was established around this period of time; (3) SGR2019/714 (the sample deemed sub-Saharan) falls in the period that coincides with the archival information found (Żejtun Parish Archives 1580-1750, Malta Parish Archives, Geneanu.com), as compiled in Appendix XVII and is discussed further in Chapter 5.

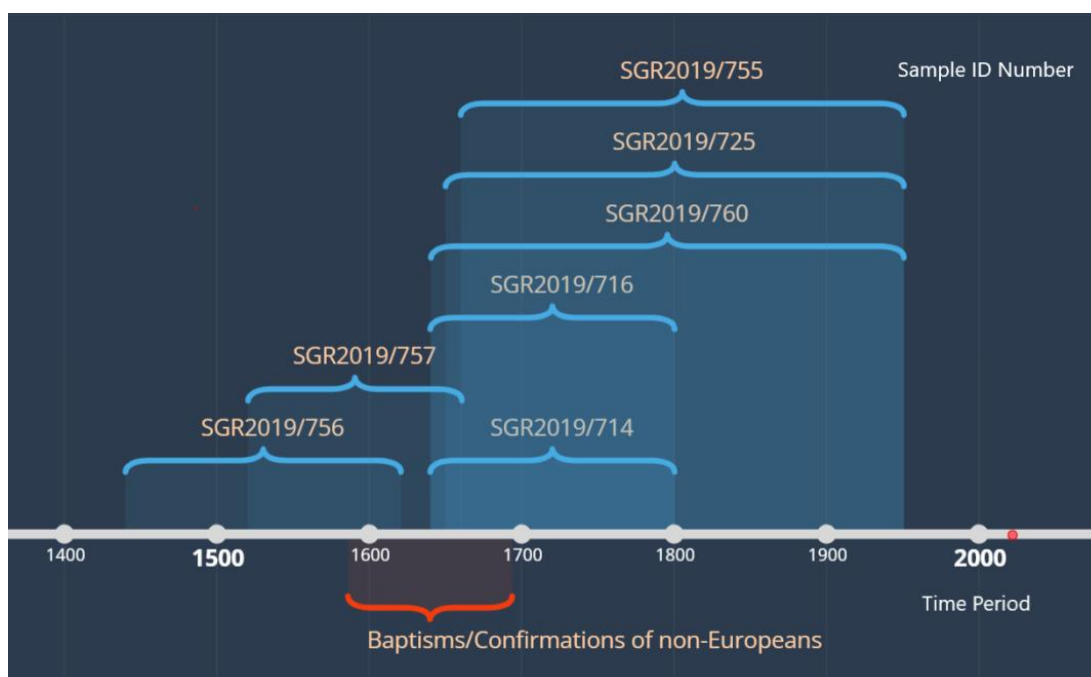


Figure 49. Timeline chart of radiocarbon dating results for samples from San Girgor assemblage. Red dot notes present date. Results utilized are courtesy of Matthew Grima, Heritage Malta and Ruben Abela, Wirt iż-Żejtun.

#### 4.9 Taphonomy and GIS

As no significant trauma is visible on the skeletal remains, there is no evidence to show that those found in the passageways died at the same time and in the same location. The taphonomic evidence clearly indicates disturbance and secondary burial and is visually presented using a GIS-based approach which highlights the taphonomic characteristics on which this assertion is based. The left and right femurs used as a base map for the data is represented as a polygon shapefile with four views (refer to Figure 50). The extent and layout of tool marks/cut marks observed was captured using a polyline vector layer. The latter was plotted on each view in each section of the respective femurs proximal, midshaft and distal (refer to Figure 51).

The value selected for the population field was 'None', as each feature (polyline) was to be counted once, and the geographic coordinate system utilized was 'Web Mercator'. A magnitude-per unit area from the polyline features is calculated using the kernel function which determines the density of features in a neighbourhood around those features (ArcGIS 2022). This shows the concentration in any given area.

'Hotspots' (dark red shading) are evident on the heat maps which represents the highest density of tool/cut marks in each section on each view (refer to Figure 52). Areas where very few or no tool/cut marks existed are represented by the very light pink shading. The distal ends of the of both femurs in all views seem to have the highest density, with the highest located on the anterior side of both the left and right femurs as well as medial sides. Based on this author's assessment of the taphonomic processes versus potential trauma using studies by Ubelaker and Adams (1995), Moraitis and Spiliopoulou (2006, 2009), and Sorg (2019), the tool/cut marks could be an indication of an undertaker's tool used to rake the skeletal material from left to right (affecting the distal ends of left femur and medial of the right) or right to left (affecting the distal ends of the right femur and medial ends of the left). As soft tissue was evident on the skeletal material, much of which was located in the distal ends, increased force may have been required in these areas. One cannot rule out that the tool/cut marks may have occurred while in the passageways if the skeletal material was moved from one passageway to another.

However, with the limited width of the passageways, one would expect to find the same damage on *all* skeletal material, yet this was not observed.

While assessing the postmortem tool/cut marks it is worth noting that out of the 127 femurs (53% left and 47% right), 32% had soft tissue; 9% had healed fractures with 58% of fractures located on the midshaft; none of the tool/cut marks appeared to be due to interpersonal violence.

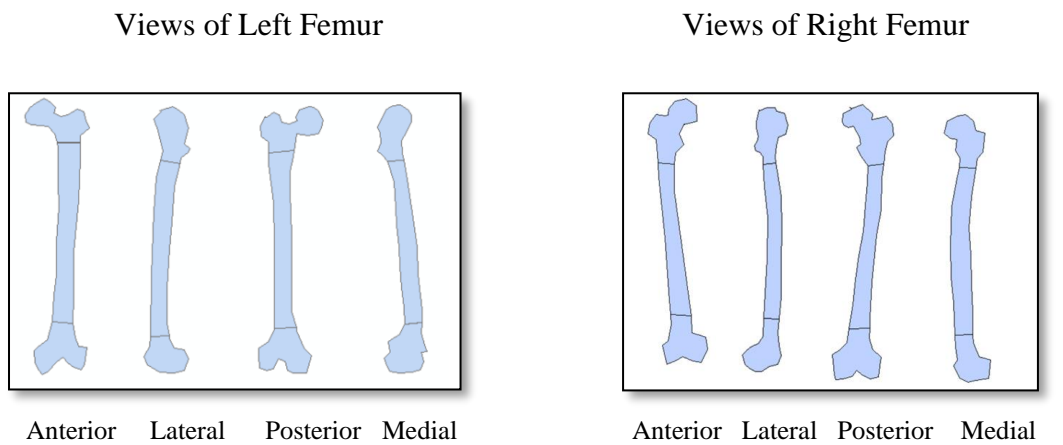


Figure 50. Polygons of four views of left and right femur, with proximal, mid-shaft and distal ends presented in separate polygons.

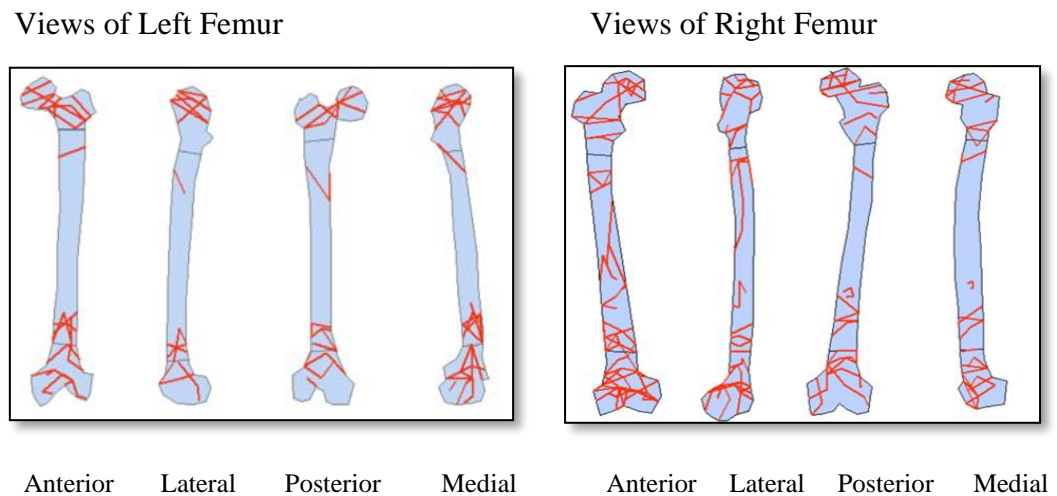


Figure 51. Polylines representing tool/cut marks on left and right femurs.

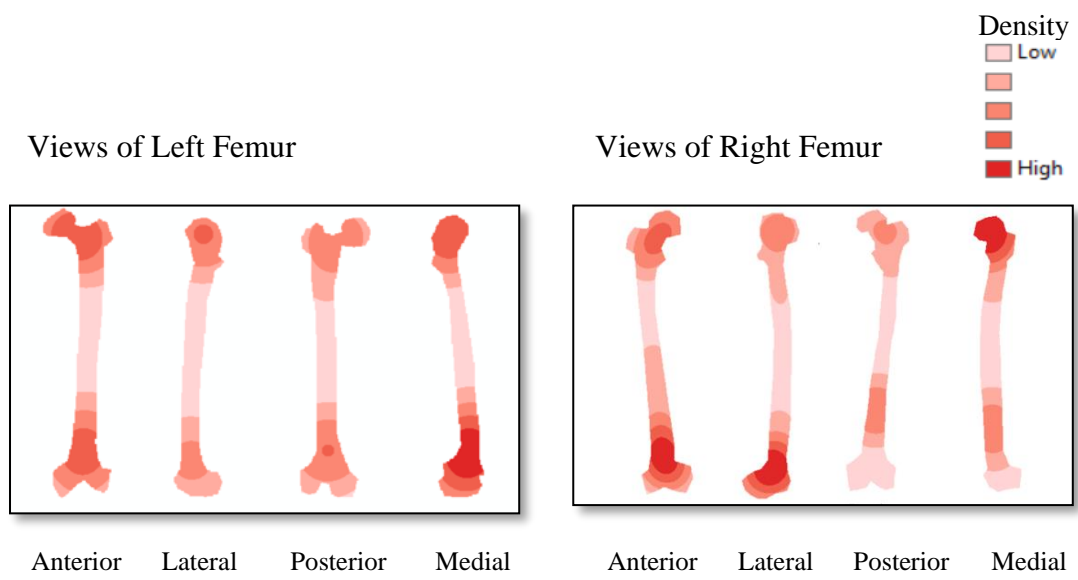


Figure 52. Heat map showing 'hot spots' of tool/cut marks. Darker red zones indicate high density and lighter coloured zones represent lower densities.

## CHAPTER 5. DISCUSSION

The demographic profiles and ancestry determination through osteological analysis performed in this study, in conjunction with the radiocarbon dating results provide a context for the human remains from San Ġirgor, the general period of their existence and probable cause of death. In addition, linking these results with extensive archival research provides insight into the ancestry of the population in this study.

The condition of the remains and the area of discovery impacts the overall assessment and this is discussed further in section 5.1 of this chapter. This is connected to the examination of antemortem and perimortem injuries, as well possible postmortem disturbance, and is significant in determining the cause of death and obtaining evidence of primary or secondary burial. The compilation of information on trauma and taphonomic characteristics resulted in a vast amount of data which was managed by using a GIS-based approach. This method visually demonstrated evidence of the secondary burial, confirming that these individuals could not have perished within the passageways of San Ġirgor.

This is followed by a discussion in section 5.2 on burial practices in relation to social structures in Malta from the 16<sup>th</sup> century to the present, to understand where individuals would have been buried based on status and religion within the community, to further explain the use of the hidden passageways in San Ġirgor.

Finally, the discussion in section 5.3 on populations and enslaved persons in Malta from the 16<sup>th</sup> to 17<sup>th</sup> century provides insight into the connection between the results of the demographic analysis of the human remains found in the passageways of San Ġirgor and the archival data extracted from the Żejtun Parish.

### 5.1 Hidden Passageways and Skeletal Remains

Officially discovered on 12<sup>th</sup> March 1969, the hidden passageways of San Girgor were not made public until 15<sup>th</sup> April 1969 (The Sunday Times 1969). The site was investigated three days later, on 18<sup>th</sup> April, by an employee (at the time) of the National Museums Department, now Professor Buhagiar. According to his notes (Figure 53), no bones were found in Passageway 1, some scattered bones were found in Passageway 2, and a wall blocked the entrance to Passageway 3. This wall was made of boulders and packed with earth and seemed to indicate it was recently constructed (Buhagiar 2018).

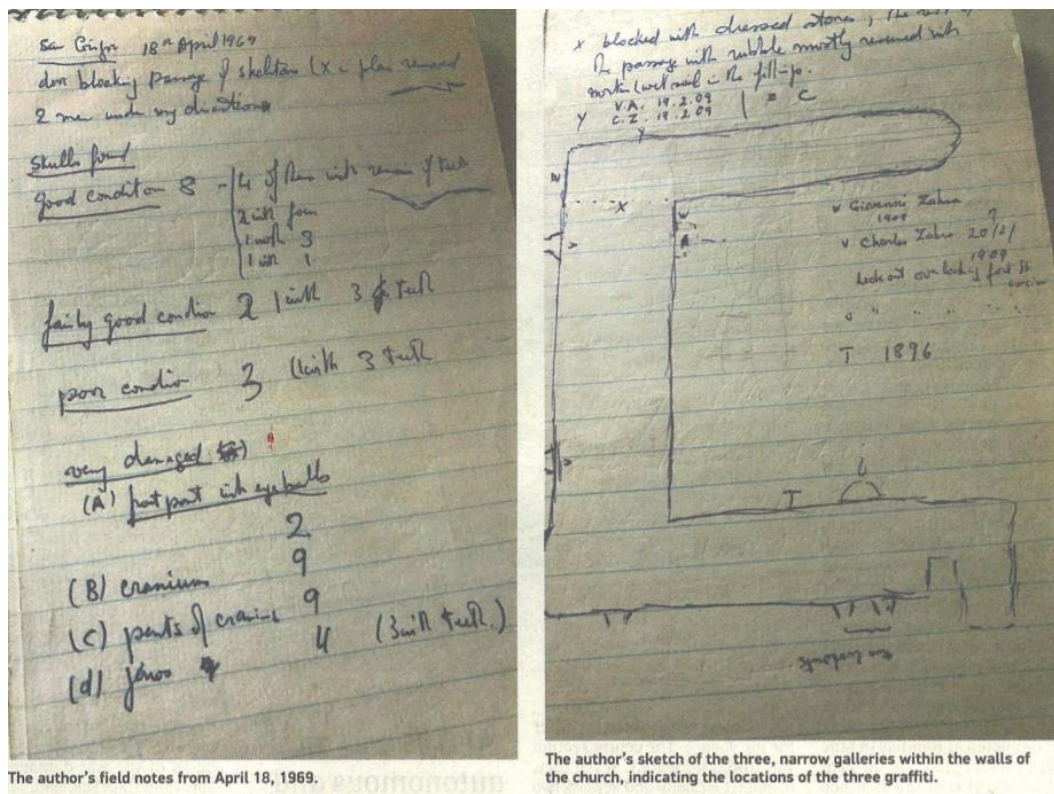


Figure 53. Notes written by Professor M. Buhagiar 18<sup>th</sup> April 1969, over one month after the site was discovered (Buhagiar 2018).

Interestingly, the pictures presented earlier in Figure 1 of the sacristan standing with bones located in the passageways in March of 1969 do not show this wall, leading one to believe that the wall may have been built just after their discovery in March of 1969 and before April of 1969 when the inspection was carried out by Buhagiar



on behalf of the National Museums Department. It seems that these bones were originally scattered throughout most of the passageways, then after their discovery they were collected and moved behind the newly constructed wall into Passageway 3. This is corroborated by an interview with the sacristan's son Charles Debono (Vella 2018) where he states that his father moved the bones into the third corridor since he wanted to ensure they would not be 'trodden upon'.

Aside from the human remains, other materials were found and documented in the report by Buhagiar (2018:55). These finds included a wooden women's shoe, a gilt cross of Byzantine features, three coins (two of which were bronze showing the Order of St John's cross and one gold coin), pottery fragments, a few wooden buttons with the remains of cloth coverings, the skin of a pomegranate and a few chestnut shells (Buhagiar 2018:55). In addition, what seems to be a piece of a chain mail armour vest and some pieces of gilt wood were found that Buhagiar did not note in his report but were noted in an article written by Vella (2014). In 2019 the finds were taken to Heritage Malta for conservation and further assessment. Unfortunately, the coins were not in a state of preservation that could provide a precise date and context (pers. comm. Dr Ruben Abela, *Wirt iż-Żejtun* 12 December 2021).

During the analysis of the human remains in this most recent investigation by this author, a small piece of textile was found attached to a bone, and a 5 mills Maltese coin was found in the sediment with the bones, the latter clearly a modern remnant as this type of coin was issued in 1972.

There is no official documentation outlining the original spatial distribution of the human remains in relation to the passageways and other bone elements in the form of a plan, aside from what is visible in the photographs taken in 1969 (as shown earlier in Figure 1). However, in an interview with Charles Debono, whose father made the initial discovery in 1969, he states he was taken to see the human remains and found they were spread across the three corridors, laid next to one another as if they had been arranged in this way and covered in about 3 cm of dust (Vella 2018).

Without contextual information, the relationship of the commingled human remains is difficult to understand. In addition, no documentation is available that outlines how the bones were preserved after the discovery, which could have been helpful when assessing perimortem versus postmortem damage in this dissertation.

The data collected on antemortem, perimortem and postmortem characteristics (refer to Appendix I.B) show little if any evidence of perimortem trauma corroborating the findings that the death of the individuals was most likely due to natural causes. The tool/cutmarks and taphonomic characteristics indicate postmortem disturbance, a result of the movement of the human remains from another burial area. Some of the disturbance may also have been caused if and when the human remains were being moved around in the passageways or during transport for analysis after the discovery in 1969.

The human remains now have been placed back on secured wooden shelving units to ensure their conservation and protection and for the public to view but not handle. The long bones are now located on bottom shelves; other elements are located to the back; and the crania are located on the top shelves as can be seen in Figures 54 and 55. The passageways today are lit up with electricity as very little light enters through the windows, but otherwise they have not been altered in any way.



Figure 54. Close up of crania; human remains found in the passageways of the Chapel of San Girgor. Photograph by author, October 2020.



Figure 55. Close up of the inventorized human remains which were placed on wooden shelves in Passageway 3, Chapel of San Ġirġor. Photograph by author, October 2020.

## 5.2 *Burials in Malta*

Social structures with respect to status and burial location existed in Malta and examples of this particularly for Żejtun are noted below. Wettinger's (1990:39) work presents evidence that private ownership of graves in Maltese churches may have started in the early 15<sup>th</sup> century, but officially most likely started after 1575 based on detailed reports written by Pietro Dusina, the Apostolic Visitor to the Maltese Diocese following his visit to Malta. The evidence that Żejtun burials were taking place within the church of San Ġirġor or elsewhere around the period of 1436 to 1580 does not exist in the parish archives housed in the Mdina Cathedral Archives or Żejtun Parish. Births, baptisms, deaths, and marriage information for Żejtun only surfaces in the archives from 1580 onwards, following Dusina's 1575 visit.

However, notarial archives show that for example, a family grave in the Mdina Cathedral was purchased in 1419 by nobleman Antonius de Vagnolo and his wife Ismiralda from Żejtun, after making an endowment of two *tenimenta terrarum* (parcels of land) in the district of "Żeytuni called Rachal Bayada (Ħal Bajda)" and

retaining the right to select a priest to take charge of the altar (Wettinger 1990:40). Parishioners were very proud and protective of their parish as discussed by Ciappara (2008:688) and surely if the chapel was an established parish and being used for burials in 1419, they would have wished to be buried in their home village of Żejtun as did so many noble families documented almost a century later. This purchase of a grave in Mdina by a noble family from Żejtun in 1419 provides additional evidence that the original small rectangular chapel was most likely not a parish until after 1419 but would have certainly been well established by 1436.

In 1502, for example, the vice-parish priest Antonius de Nicholachi of St Catherine of Żejtun granted Antonius Randuni a grave within the chapel of San Girgor as compensation for a field in Tal-Ġwiedi that was donated to the church. This land was sold on the same day to another person in Żejtun to help pay for future work on the church, showing that by this time, the Chapel of San Girgor was in full use and graves were granted within the church, well before the arrival of Dusina in 1575.

Buhagiar (1979:77) refers to a 16<sup>th</sup>-century chapel of Saints Mark and James which belonged to the Giulinus Bonnici family that annexed the chapel of San Girgor on the northwest side. This may have had burials located below but no documentation of this has been found. Bonnici (2019:477) notes that according to Dusina's reports in 1575, the southside of the area around the San Girgor chapel was surrounded by a wall that enclosed a cemetery and the chapel of St James also owned by the Bonnici family, which was not being used. Dusina mentions that burials were inappropriately taking place in the loose earth of the church instead of proper tombs and to rectify the situation instructed the removal of a 'cataletto' (stretcher on wheels which carried the dead) and the construction of at least two graves (Visitato Dusina 1575, as referenced by Buhagiar 1979:78). Although still a small population, this direction by Dusina is evidence of the need for graves, perhaps due to an increase in the population in the area, and that proper burials for all had to be placed within church grounds.

Dusina's request may make one assume that graves within churches were being granted only after 1575, however Wettinger's (1990) research shows that there is

evidence of privately owned family graves within churches being purchased by nobles in the early 15<sup>th</sup> century, a century and half before Dusina's arrival. In addition, he also cites examples from the Notarial Archives of Valletta (Malta) of local craftsmen and villagers and their heirs being given graves within the church as payment for work done over 150 years before Dusina's arrival, noting that the interpretation of when graves were being granted within churches may need to be revisited (Wettinger 1990:41).

Where people were buried and when these areas were assigned as burial spaces and more importantly, no longer used becomes very significant in this dissertation. Interestingly, Parker Pearson (2001:18) argues that archaeologists often concentrate on when a cemetery was in use and less on when it was set up or abandoned. He suggests that it is important to assess the founding and abandonment of cemeteries as this knowledge could provide information about social changes within the community or society. This information clearly could assist with understanding the population being studied from San Girgor in terms of the origin of human remains and potential evidence of secondary burials.

### *5.3 Population*

The San Girgor parish archive registries of marriages, births, baptisms, deaths, and the status animarum (census) are available from 1580 onwards and provide insight into the population during these periods. Abela (2006: 41) notes that as the chapel of San Girgor was ravaged in the attack of 1614, baptisms, masses, and sacraments were not held here again until 1634. Interestingly, a gap in archival information at the Parish of Żejtun does exist, however this extends over the periods of 1634 to 1663 and the material seems to be lost or has gone missing.

According to Abela (2006:58) archival research shows the population of San Girgor during the arrival of the Knights in Malta in 1530 was approximately 1000 inhabitants, and barely exceeded 2000 individuals until after the 1700s. This would amount to 5% of the entire Maltese population at the time based on studies of the Maltese population (Wettinger 1969:83). Based on statistics presented in research by Brogini (2004) one can determine that the enslaved population, primarily

acquired by the Knights, was between 2% to 5% in Malta for most of the 16<sup>th</sup> and 17<sup>th</sup> century, peaking to just under 9% in 1599. The number of private enslaved persons was considerably lower in the parish of San Ġirġor, at least based on those documented in baptismal records (refer to Appendix XVII). This corroborates the percentage of those deemed to be sub-Saharan in this assemblage.

The Status Animarum of the Żejtun Parish Archives provides a census of existing family households with names, ages, and enslaved persons who lived with them. The ages listed are of interest as it offers a demographic profile of the parish in the 16<sup>th</sup> and 17<sup>th</sup> century. Overall, marriages and the birth of children occurred at a young age where in some cases mothers were 13 to 15 years of age but often under 20 years of age; the number of births, noted by baptisms, amounts to an average of 68 per year for example between 1679 and 1688 and continues to increase (for the most part) every decade (Żejtun Parish Archives 1601-1700). Infant mortality (before the age of one) is not significantly high and adult deaths must have occurred generally early in life as most listed are not beyond the age of 55 to 60 years of age.

Information regarding enslaved persons (refer to Appendix XVII) is primarily gathered from baptismal archives (Żejtun Parish Archives 1580-1606; 1606-1766) as these individuals are not usually listed as 'slaves' in marriage or death registries. The data collected and listed in sequence by year from 1586 to 1693 (Appendix XVII) does not include enslaved persons who were not baptised. As the focus here is on the human remains found within the passageways of the church, one can theorize that these individuals would have been patrons of the parish, baptised and listed in these registries. A link can be made between the individuals from the passageways and the individuals listed in Żejtun Parish Archives (1580-1606, 1606-1766) based on the percentage of enslaved persons as listed in Appendix XVII, and the demographic analysis of the human remains demonstrating the presence of a comparable number of non-Europeans in the assemblage. However, as the human remains are commingled, they cannot be associated specifically with particular individuals who are listed in Appendix XVII.

Reviewing the archival information highlights established noble families, living in the area who were key benefactors of the parish, were well respected and were often

listed as godparents in baptismal archives (Žejtun Parish Archives 1580 -1750). The fact that they were noble, and wealthy can also be attributed to the fact that they are listed as ‘slave’ owners in various archives (Žejtun Parish Archives 1580-1750).

Most of the enslaved persons would have been captured from Ottoman attacks or corsair raids along the Barbary coast (North Africa) and would have been primarily non-Christian individuals from the Ottoman empire in the eastern Mediterranean or the northern parts of Africa as discussed in studies on slavery by Wettinger (2002, 2006) and Manning (2017).

Black African enslaved persons, although few in number, were specifically noted as ‘negro’ or ‘negra’ (black in Italian) in the archival baptismal registry, differentiating them from other ‘slaves’ (Figures 56 to 59).

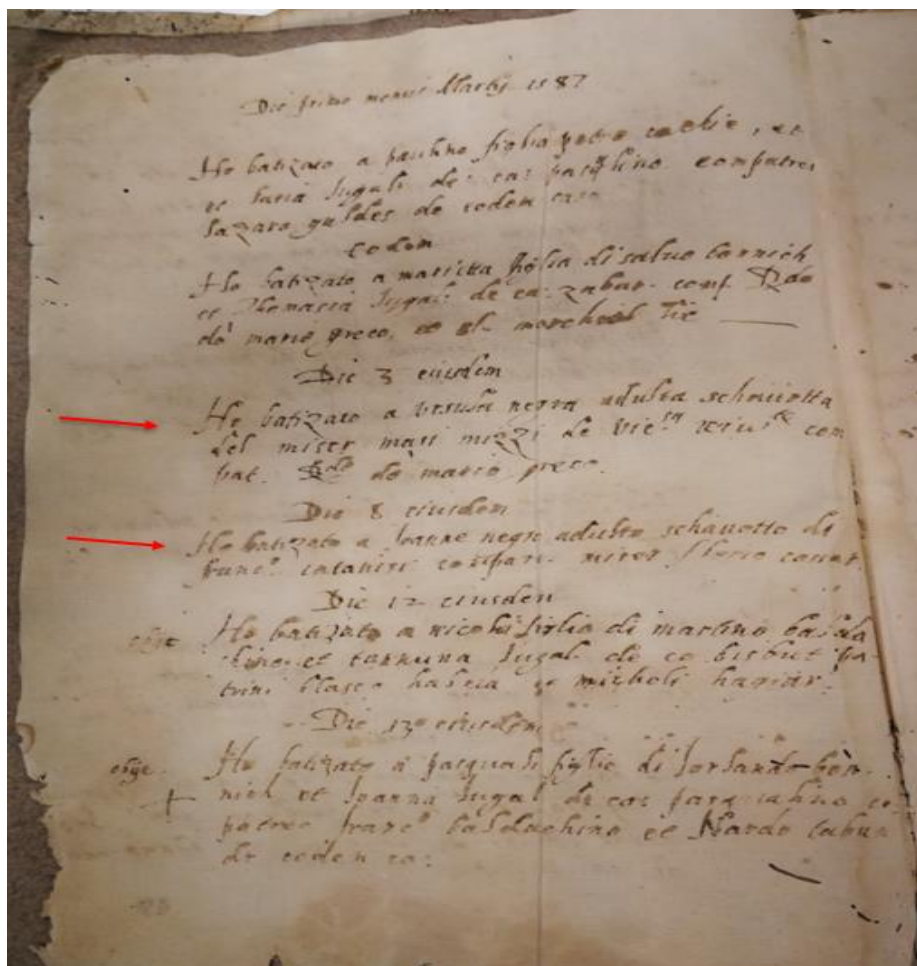


Figure 56. Evidence of baptism of two female adult ‘Black slaves’ in 1587. Žejtun Parish Archives, 1580-1606.

Codem  
 Ho batizato a Isidora negra schiava di b'ascoq  
 habola di ca. parquahia patino L. do  
 Angelo nallia.

Codem  
 obyt Ho batizato a Joa Leonardo figlio di Vincenzo  
 caruana et. Agostina legal. de ca. Gabar  
 babia et. meschior he et L. do mario  
 greco.  
 Die 16 eundem

Ho batizato a vittoria figlia di petronio Bernich  
 et imperia legal. de ca. Gabar compatre marie  
 ta moglie di navi he he et castro castar.

Die 26 eundem  
 obyt He batizato a gergio figlio di mariano vella  
 de ca. axae et gioaella legal. compatre  
 chorari vella de ca. car. et nario ta  
 luni de ca. bibul.

Die 27 eundem  
 Ho batizato a ventura figlio di bastiano  
 parde et francio legal. de ca. Gabar, pa  
 rino hironimo bernich de eodem cas.

Die 28 eundem  
 Ho batizato a domico figlio di Joanni sar  
 ruge et barthelema legal. de ca. parq<sup>a</sup> hia  
 patrin pasqueli casta de eode ca.

Figure 57. Evidence of the baptism of a female 'Black slave' in 1587. Żejtun Parish Archives, 1580 -1606.



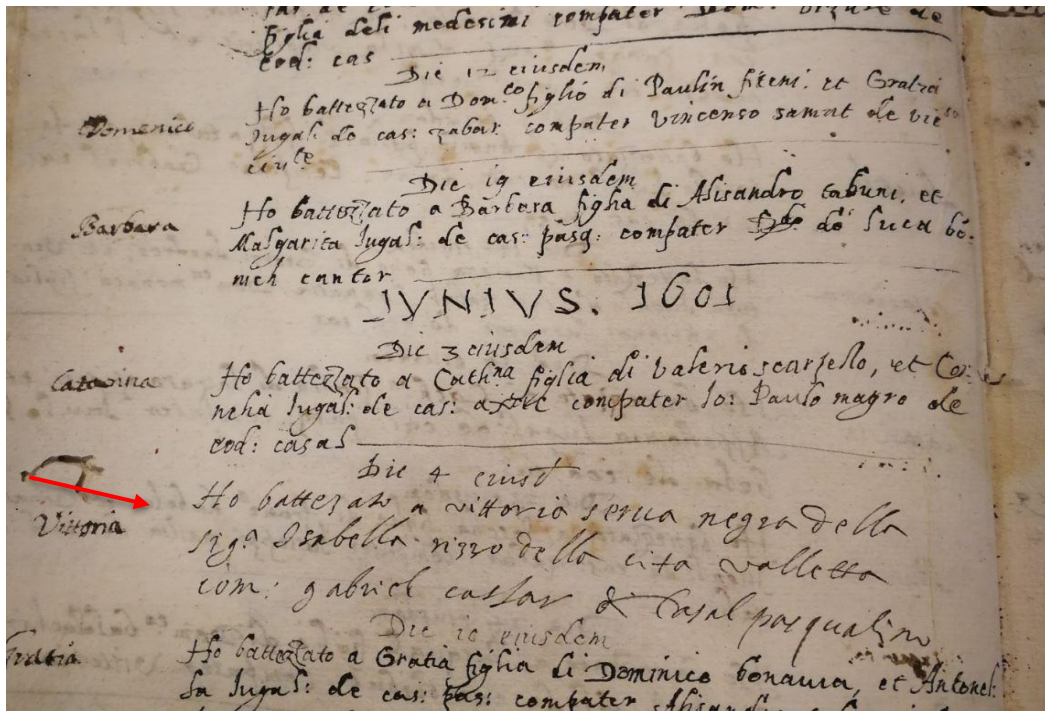


Figure 58. Evidence of the baptism of a female 'Black slave' in 1601. Żejtun Parish Archives, 1580-1606.

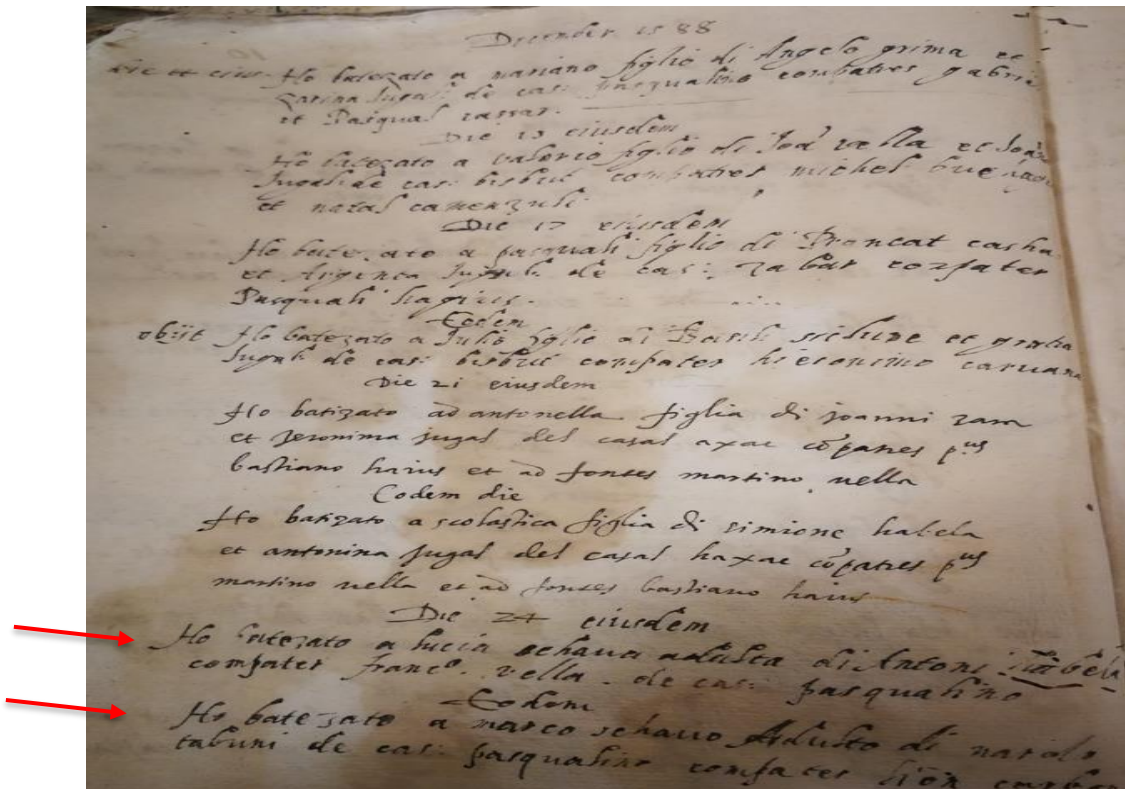


Figure 59. Evidence of the baptism of a male and female adult 'slave' where affinity is not noted in 1588. Żejtun Parish Archives, 1580-1606.

These slaves most likely originated from the slave trade that emanated from and along West Africa in the 15<sup>th</sup> century and through the southern borders of North African countries (Manning 2017:102).

Although the slave trade flourished in the mid-16<sup>th</sup> century with the arrival of the Knights of St John from 1530 onwards (Wettinger 2006:68), there is reference to Black African enslaved persons on the island in notarial archives as early as the 15<sup>th</sup> century. For example, on 6<sup>th</sup> March 1488, Notary Giacomo Zabbara files a legal contract (in Latin) showing a dowry issued by a family in the Żejtun area which includes ‘servam unam Ethiopem eligendam’ – ‘a choice of one Ethiopian (Black) slave’ (Fiorini 1996: 334).

Wettinger (2006:65) notes the repeated preference of Black African enslaved persons for private ownership documented in sales transactions in notarial archives and the increasing number between the 16<sup>th</sup> and 18<sup>th</sup> century is also corroborated by baptismal archives (Żejtun Parish Archives, 1580-1700).

The nobles who were private wealthy citizens could purchase individuals from the market that was stationed at St George’s square in Valletta (Malta) and those from Africa are often noted as originating from the Kingdom of Bornu or ‘Aethiopia’ (Wettinger 2006:66). Up until the early 18<sup>th</sup> century West Africa was in fact called ‘Aethiopia and as can be seen in Figure 60, the Kingdom of Bornu is situated in the area where today we have West African countries bordering North African countries under the Ottoman Empire. Several references are made to this region when referencing enslaved persons to distinguish the enslaved persons of other regions. Hence those from Africa were described as ‘Etiopico’ or ‘di Etiopia’ before the arrival of the Order in Malta and later noted as ‘negro’ or ‘negra’ (black) in archival material such as that found in the Żejtun Parish Archives (refer to Appendix XVII).



Figure 60. 1743 Map of West Africa. Note the area named Aethiopia, south of the North African area controlled by the Ottoman Empire. Homann Heirs map of West Africa or Guinea. <https://www.geographicus.com/P/AntiqueMap/africapropria-homannheirs-1743>.

This not to say that Black Africans may not have originated from North Africa as admixture certainly could have taken place. However, during the 16<sup>th</sup> century when the ‘slave trade’ was focused on West Africa, the point of origin of Black African enslaved persons was most likely not North Africa, although they may have been sold here, nor would their origin have been from East Africa as the reference to ‘Aethiopia’ would lead one to believe.

As with all enslaved persons, if they converted to Christianity, wilfully or not, they would have been given Christian names and taken on their owner’s surnames as is evident in the baptismal archives (Žejtun Parish Archives, 1580-1606). For example, Andreanna, noted on the compiled list in Appendix XVII, as the first enslaved person documented in the Žejtun Parish Archives (1580-1606), would have been known as Andreanna de Tabuni, ‘slave’ of Leonardo Tabuni di Casal Pasqualino (Leonardo Tabuni of Žejtun, as it is known today). This would change

if enslaved persons were sold or given away as gifts and was applied to the children of enslaved persons as well. For example, in reference to Appendix XVII, Martino, baptised on 1<sup>st</sup> June 1621, the enslaved person of Alessandro Tabuni, later received his confirmation as the enslaved person of Alessandro Habela; marriage archives show Martino married Barbara an enslaved person of Alessandro Habela, and then had a child named Domenica who was confirmed in 1686, also listed as a ‘slave’ of Alessandro Habela (Żejtun Parish Archives, 1600 -1700).

In some cases, the enslaved person’s owner was in fact the father of the enslaved person’s child. Although not mentioned in all cases, fathering children with enslaved persons likely occurred more often than is noted in the archives as is evident in various wills to show distribution of inheritance to enslaved persons and their children or their emancipation. An example of this would be Antonius Cumbo, from Raħal Bisqallin, who emancipated his two legitimate daughters Agnesia and Dulcia in 1487 (Fiorini 1996:130). This in essence is an example of the attempt to integrate enslaved persons within aspects of community life, even though one cannot deny that ‘segregation’ is evident in the archives.

Most enslaved persons stemming from North Africa, or the Eastern Mediterranean were used in the galleys of ships, having had experience on the high seas, however Black African enslaved persons were considered better suited for construction or domestic work and the few female Black African enslaved persons who arrived in Malta were purchased to work within noble households (Wettinger 2006:69). Cassar (1968:271) notes that the number of female enslaved persons was not high, where in the year 1632 there were 649 privately owned enslaved persons and 1284 ‘galley-slaves’. Approximately only 100 of these privately owned enslaved persons were female, based on a survey conducted by the Special Commission of Knights in 1645.

Cassar (1968:273) also notes that decrees set by the Grand Masters of Malta show enslaved persons were cared for when ill at the old infirmary in Birgu, later replaced by the Holy Infirmary in Valletta, and the infirmary at the ‘Slave Prison’ in Valletta located on St Christopher and St Ursula streets. In addition, an enslaved persons’ cemetery existed, as enslaved persons were given a plot of ground at the ‘Marsa’ at





Figure 62. (a) “Two Maltese noble women with their African slave”; (b) “Maltese noble woman with her African slave”. Painter Unknown. Wettinger (2002:386-387).

The fact that domestic enslaved persons were baptised and became Christians provides further evidence that those working in noble households most likely would have been buried in the same manner as other Christians. There is no documentation that this author could find that would indicate exact burial locations and whether household enslaved persons’ burials would have been segregated. Ciappara (2008:673) argues that most people were buried in common graves, while the clergy and nobles had their own burial sites or chapels. However, Bonnici (2019:480) makes note of the parish archives indicating that Grigor Bonnici in 1687 made arrangements for his servant Katerina who died at the age of 40 to be buried in the Chapel of St Angelu in Żejtun. Later Grigor Bonnici, as well as his family were also buried in the same chapel, further evidence that servants were in fact buried within the same areas.

Bonnici (2019:485) notes that the origins of the Santa Roccu cemetery built next to the chapel of San Girgor dates to around the period of the plague of 1675-1676. Ninety-two people living in Żejtun and who died during this time were buried in this cemetery, followed by those who died in the plague of 1813. Although the number of individuals (92) is similar to the number of individuals found in the

assemblage of San Girgor, and the dates of cemetery use falls within the range noted by the radiocarbon dating results, the San Girgor skeletal evidence would indicate that the individuals were not all deceased at the same time and would not necessarily have made up this population. This is not to negate the possibility that some of the individuals may have come from this area.

Radiocarbon dating results (Molnár 2020:1) of the human remains in this study, place the material in the period of 1450-1650 which would predate the remains at the Santa Roccu cemetery. However, as only a very small sample of the human remains was tested, the possibility could exist that some of the remains in the passageway were placed later than others. Without testing all material and without having archaeological planning and mapping of the human remains in context, one cannot be certain of the relationship among the bone elements or that all the material predates 1650.

Dun Abela had completed a significant amount of archival research on the baptismal records of Żejtun, including the listing of some of the enslaved persons noted in the archives (Abela 2003, 2009). Following Abela (2009), for this dissertation, this author developed a detailed list (refer to Appendix XVII) using the Żejtun Parish Archives (1580-1750) and information found in archives online (Geneanum, accessed December 2021) that most likely relate to some of the human remains found in the passageways of San Girgor based on the information established by the radiocarbon dating results.

The importance of the reference to Black African enslaved persons becomes apparent when viewing the results of the biological profiles, as ancestry determination and population affinity analysis links several of the individuals found in the passageways of San Girgor to individuals noted in the 16<sup>th</sup> and 17<sup>th</sup> century baptismal records, some of which include Black African enslaved persons.

## CONCLUSION

The aim of this study is to extrapolate data from the commingled remains found in San Girgor, using various osteological morphometric methods of analysis to develop biological profiles, including ancestry determination. In addition, an assessment of the presence of trauma or taphonomic processes on the bone elements is imperative to understand the possible cause of death and burial settings. Using both quantitative and qualitative methods, this study aims to show that the osteological analysis, in conjunction with a GIS-based approach to manage large amounts of taphonomic data, extensive archival research and the results of radiocarbon dating, provide a historical link and context for the human remains found in the passageways of San Girgor.

Although anthropological and palaeopathological studies had been completed by Ramaswamy and Pace in 1979 and 1980, questions remained about the dating, origins, and population affinity of the assemblage. In addition, the full inventory and raw data had been lost, without which the biological profiles could not have been developed to meet the objectives of this study and achieve the aims noted above.

The osteological analysis shows that the assemblage was comprised of at least 92 individuals, primarily older adults, with a higher percentage of females, very few juveniles and no infants. Dark brown soil (not present in the passageways) was present on many of the skeletal elements which had colorations that varied, and postmortem tool/cut marks were also evident. Heat maps created using a GIS-approach provided a clear visual representation of the tool/cut mark densities and locations which provided further evidence of a secondary burial. These factors together lead one to conclude that these individuals most likely did come from a cemetery and were transported to the 'hidden passageways', perhaps to make space for the expansion of the Chapel of San Girgor in the late 16<sup>th</sup> century. Ancestry determination showed that the individuals were mainly European but at least five



of the group seem to be sub-Saharan African. Radiocarbon dates provided a framework which corroborated the extensive archival research. The results show that some of the deaths would have taken place as early as 1440 while the majority (based on the samples taken) would have occurred approximately between 1600 and 1750. Some of the radiocarbon dates overlap, and therefore it is possible that some deaths took place at the same time. However, the archival material pertaining to the sub-Saharan population seems to indicate deaths may have taken place generations apart assuming of course the individuals in the assemblage are in fact those noted in the archives. The same hypothesis could be applied to the Europeans in the assemblage, however further radiocarbon dating would have to be performed on additional samples to obtain a clearer picture.

The ancestry determination, radiocarbon dating results and extensive archival information provide an important connection between the non-European skeletal material in this commingled assemblage and those individuals listed in the archives.

The evidence shows that sub-Saharan individuals were part of the community in Żejtun, being baptized, most likely living in local households, and also being buried in the same areas around the church as other members of this assemblage and community. This provides a glimpse into the social context of Żejtun from the early 15<sup>th</sup> century to the late 18<sup>th</sup> century and deserves further study beyond the region of Żejtun, which could potentially provide a significant source of historical information about rural life in Malta.

As with most studies, questions can be answered, or may create further uncertainty leading to additional research questions. In this dissertation, the archival research in conjunction with the use of new technology has provided insight into who these individuals may be and has corroborated earlier studies within the framework of a designated period. One may never know for certain how the skeletal remains were transported to the passageways however, excavations in and around the church may lead to an understanding of the graves that may have been disturbed during the expansion of San Ġirgor. Soil analysis could prove to be quite useful in determining origin and could be compared if excavations were to take place. In addition, with further radiocarbon dating of other samples combined with DNA analysis,

information can be obtained on relationships of the individuals in the assemblage and the periods of burial. This could add to the insights into how this skeletal assemblage came to be in the hidden passageways of San Girgor.

## REFERENCES

- ABE, Y., C.W. MAREAN, P.J. NILSSEN, Z. ASSEFA, & E.C. STONE 2002. The analysis of cutmarks on archaeofauna: a review and critique of quantification procedures, and a new image-analysis GIS approach, *American Antiquity* 67(4): 643-663.
- ABELA, J.D. 2003. L-importanza kbira tal-familja Tabone iż-Żejtun 400 sena ilu. *Għaqda Muzikali Beland, Żejtun:25 Sena Planċier*: 63-67.
- ABELA, J.D. 2006. *The Parish of Żejtun through the ages*. Malta: Midsea Books.
- ABELA, J.D. 2009. Ilsiera ma' familji Żwieten fl-imghoddi, *Għaqda Muzikali Beland, Żejtun* 28: 5-59.
- ABELA, K. 2014. The old parish church of Żejtun: a structural analysis. Unpublished Bachelor of Engineering and Architecture dissertation, University of Malta.
- ABELA, R. 2021. Personal Communication, 12<sup>th</sup> December 2021.
- ABELA, R. & M. GRIMA 2018. Request for permission to study the Żejtun St Gregory Church bone collection by way of an osteological and C14 Dating study. Unpublished report, DOC N094/18, Heritage Malta Diagnostic Science Laboratories and Wirt Iż- Żejtun.
- ACSÁDI, G. & J. NEMESKÉRI 1970. *History of human life span and mortality*. Budapest: Akad. Kiadó.
- ADAMS, B.J. & J.E. BYRD 2008. *Recovery, analysis, and identification of commingled human remains*. Totowa, NJ: Humana Press.
- ADAMS, B.J. & L.W. KONIGSBERG 2008. How many people? Determining the number of individuals represented by commingled human remains, in B.J. ADAMS, and J.E. BYRD (eds) *Recovery, analysis, and identification of commingled human remains*: 241- 255. Totowa, NJ: Humana Press.
- ALBANESE, J. & S.R SAUNDERS 2006. Is it possible to escape racial typology in forensic identification?, in A. SCHMIDT, E. CUNHA, & J. PINHEIRO (eds) *Forensic anthropology and medicine: complementary sciences from recovery to cause of death*: 281-316. Totowa, NJ: Humana Press.
- ALQAHTANI, S. J., M.P. HECTOR & H.M. LIVERSIDGE 2010. Brief communication: Atlas of tooth development and eruption, *American Journal of Physical Anthropology* 142:481–490.

ALQAHTANI, S.J., M.P. HECTOR & H.M. LIVERSIDGE 2014. Accuracy of dental age estimation charts: Schour and Massler, Ubelaker and the London Atlas, *American Journal of Physical Anthropology* 154 (1):70–78.

ArcGIS Desktop. Available at:

<https://desktop.arcgis.com/en/arcmap/latest/tools/spatial-analyst-toolbox/kernel-density.htm> (accessed on 20<sup>th</sup> June 2022).

ATICI, L. 2013. Commingled bone assemblages: insights from zooarchaeology and taphonomy of a bone bed at Karain B Cave, SW Turkey, in A.J. OSTERHOLTZ, K.M. BAUSTIAN & D.L. MARTIN (eds) *Commingled and disarticulated human remains: working toward improved theory, method, and data*: 213-253. New York, NY: Springer New York.

BASS, W.M., 2005. *Human osteology, a laboratory and field manual*, 5th ed., Columbia: Missouri Archaeological Society.

BAUSTIAN, K.M., A.J OSTERHOLTZ & D.C. COOK 2013. Taking analyses of commingled remains into the future: challenges and prospects, in A.J. OSTERHOLTZ, K.M. BAUSTIAN & D.L. MARTIN (eds) *Commingled and disarticulated human remains: working toward improved theory, method, and data*: 265-274. New York, NY: Springer New York.

BEDIĆ, Ž, A. JANEŠ, A. & M. ŠLAUS 2019. *Anthropological analysis of trauma frequencies and distribution in the skeletal series from the Benedictine Monastery of St Margaret in Bijela, Croatia*. Hrvatsko Antropološko Društvo.

BEHRENSMEYER, A.K. 1978. Taphonomic and ecological information from bone weathering, *Paleontological Society* 4(2): 150-162.

BERTSATOS, A. and M. CHOVALOPOULOU 2019. Validation study of osteometric techniques for sorting commingled human skeletal remains in archaeological samples, *International Journal of Osteoarchaeology* 29(2): 253-259.

BLAU, S. & D.H. UBELAKER 2016. *Handbook of forensic anthropology and archaeology*, 2nd ed., London: Routledge, Taylor & Francis Group.

BONNICI, E. 2019. *Id-dfin f' Malta*. Malta: Horizons.

BOSCHIN, F. & J. CREZZINI 2012. Morphometrical analysis on cut marks using a 3D digital microscope, *International Journal of Osteoarchaeology* 22(5): 549-562.

BEHRENSMEYER, A.K. 1978. Taphonomic and ecologic information from bone weathering, *Paleobiology* 4(2):150-162.

BRICKLEY, M. & J.I. MCKINLEY 2004. Guidelines to the standards for recording human remains, IFA Paper No.7, Southampton, UK: British Association of Biological Anthropology and Osteoarchaeology.

BROGINI, A. 2004. La population de Malte au Evie siècle, reflet d'une modernité, *Cahiers de la Méditerranée* 68:1-15.

- BROOKS, S. & J.M. SUCHEY 1990. Skeletal age determination based on the os pubis: a comparison of the Acsádi-Nemeskéri and Suchey-Brooks methods, *Human Evolution* 5(3): 227-238.
- BROTHWELL, D.R. 1981. *Digging up bones*. 3rd ed., Ithaca, N.Y: Cornell University Press.
- BRŮŽEK, J. & P. MURAIL 2006. Methodology and reliability of sex determination from the skeleton, in A. SCHMITT, E. CUNHA & J. PINHEIRO (eds) *Forensic anthropology and medicine: complementary sciences from recovery to cause of death: 225-242*. Totowa, NJ: Humana Press.
- BUCKBERRY, J.L. & A.T. CHAMBERLAIN 2002. Age estimation from the auricular surface of the ilium: a revised method, *American Journal of Physical Anthropology* 119(3):231-239.
- BUCKBERRY, J., 2015. The (mis)use of adult age estimates in osteology, *Annals of Human Biology* 42(4): 323-331.
- BUHAGIAR, M. 1979. *St Catherine of Alexandria: her churches, paintings and statues in the Maltese Islands*. Malta: St Catherine Musical Society.
- BUHAGIAR, M. 1990. The date of the skeletal remains at Żejtun, In T. F. C. Blagg, A. Bonanno, & A. T. Luttrell, *Excavations at Ħal Millieri, Malta: a report on the 1977 campaign conducted on behalf of the National Museum of Malta and the University of Malta*: 146. Msida: Malta University Press.
- BUHAGIAR, M. 2018. The secret passages of Żejtun's old parish church, *The Sunday Times of Malta*, 29 April 2018, p.55.
- BUIKSTRA, J.E. & D.H. UBELAKER 1994. *Standards for data collection from human skeletal remains*, Proceedings of a Seminar at the Field Museum of Natural History Organized by J. Hass: Report No. 44. Fayetteville, AR: Arkansas Archaeological Survey Research Report.
- BURNS, K.R. 2016. *Forensic anthropology training manual*. New York, NY: Routledge, Taylor, and Francis.
- BYRD, J.E. & B.J. ADAMS 2003. Osteometric sorting of commingled human remains, *Journal of Forensic Sciences* 48(4): 1-8.
- BYRD, J.E. & C.B. LEGARDE 2014. Osteometric sorting, in B.J. ADAMS & J.E. BYRD (eds) *Commingled human remains: methods in recovery, analysis, and identification*:167-191. Amsterdam, NL: Elsevier Academic Press.
- CAMILLERI, D. 2020. Report on the investigation of skeletal remains found at Kappella ta' Santa Marija, Bir Miftuħ, Gudja (FTH 2020). Unpublished report, Superintendence of Cultural Heritage.
- CANNON, M.D. 2013. NISP, Bone fragmentation, and the measurement of taxonomic abundance, *Journal of Archaeological Method and Theory* 20(3): 397-419.

- CAPPELLA, A., A. AMADASI, E. CASTOLDI, D. MAZZARELLI, D. GAUDIO & C. CATTANEO 2014. The difficult task of assessing perimortem and postmortem fractures on the skeleton: a blind text on 210 fractures of known origin, *Journal of Forensic Sciences* 59(6): 1598-1601.
- CASSAR, P. 1968. A medical service for slaves in Malta during the rule of the order of St John of Jerusalem, *Medical History* 12(3): 270-277.
- CAUCHI, T. 2019. The Casa Lanfreducci bone assemblage from Valetta, Malta: a human remains assessment and study of the historical context. Unpublished Master's thesis, University of Malta.
- CIAPPARA, F. 2008. The parish community in eighteenth-century Malta, *The Catholic Historical Review* 94(4): 671-694.
- CIESIELSKI, E., & H. BOHBOT 2015. Analysis of bone modifications on human remains: A GIS approach, in F. GILIGNY, F. DJINDJIAN, L. COSTA, P. MOSCATI & S. ROBERT (eds) *CAA 2014 21<sup>st</sup> century archaeology: Proceedings of the 42<sup>nd</sup> annual conference on computer applications and quantitative methods in archaeology*: 423-430. Oxford, UK: Archaeopress.
- COX, M. 2000. Ageing adults from the skeleton, in M. COX and S. Mays (eds) *Human osteology in archaeology and forensic science*: 61-81. London, UK: Cambridge University Press, Greenwich Medical Media Ltd.
- CUNHA, E. & D.H. UBELAKER 2020. Evaluation of ancestry from human skeletal remains: a concise review, *Forensic Sciences Research* 5(2): 89-97.
- DOMÍNGUEZ-RODRIGO, M. 2012. Critical review of the MNI (minimum number of individuals) as a zooarchaeological unit of quantification, *Archaeological and Anthropological Sciences* 4(1): 47-59.
- DREW, R. 2013. A review of the ischium-pubis index: accuracy, reliability, and common errors, *Human Biology* 85(4): 579-596.
- DUDAY, H. 2009. *The archaeology of the dead*. Oxford, UK: Oxbow Books.
- DUDAY, H. & M. GUILLON 2006. Understanding the circumstances of decomposition when a skeleton is skeletonized, in A. SCHMITT, E. CUNHA & J. PINHEIRO (eds) *Forensic anthropology and medicine: complementary sciences from recovery to cause of death*: 117-157. Totowa, NJ: Humana Press Inc.
- DUNN, R.R., M.C. SPIROS, K.R. KAMNIKAR, A.M. PLEMONS & J.T. HEFNER 2020. Ancestry estimation in forensic anthropology: a review, *WIREs Forensic Science*, 2(4):1-26.
- FALYS, C.G. & M.E. LEWIS 2011. Proposing a way forward: a review of standardisation in the use of age categories and ageing techniques in osteological analysis (2004-2009), *International Journal of Osteoarchaeology* 21(6): 704-716.
- FIORINI, S. 1996. *Documentary sources of Maltese history: part 1 notarial documents, notary Giacomo Zabbara R494/1(I): 1486-1488*. University of Malta.

FIORINI, S. 2014. The south east of Malta and its defence up to 1614, in R. Abela (ed.) *The Turkish raid of 1614*: 82-93. Malta: Wirt iż-Żejtun.

FOX, S.C. & K. MARKLEIN 2013. Primary and Secondary burials with commingled remains from archaeological contexts in Cyprus, Greece, and Turkey, in A.J. OSTERHOLTZ, K.M. BAUSTIAN & D.L. MARTIN (eds) *Commingled and disarticulated human remains: working toward improved theory, method, and data*: 193-211. New York, NY: Springer New York

GARVIN, H.M., S.B. SHOLTS & L.A. MOSCA 2014. Sexual dimorphism in human cranial trait scores: Effects of population, age, and body size, *American Journal of Physical Anthropology* 154(2): 259-269.

GENEANUM.com. Available at:

<https://en.geneanum.com/malta/databases/baptisMshtml/> (accessed on 1<sup>st</sup> December 2021).

GILBERT, B.M. & T.W. MCKERN 1973. A method for aging the female Os pubis. *American Journal of Physical Anthropology* 38:31-38.

GILES, E. & O. ELLIOT 1962. Race identification from cranial measurements, *Journal of Forensic Sciences* 7:147-157.

GILES, E. & O. ELLIOT 1963. Sex determination by discriminant function analysis of crania, *American Journal of Physical Anthropology* 21:53-68.

GILL, G.W. 1984. A forensic test case for a new method of geographical race determination, in T.A. Rathburn & J.E. Buikstra (eds) *Human Identification: Case studies in Forensic Anthropology*: 329-339. Springfield, IL: Charles C Thomas Publisher Ltd.

HAGLUND, W. 2001. Archaeology and forensic death investigations, *Historical Archaeology* 35(1): 26-34.

HAGLUND, W.D. & M.H. SORG (eds) 2002. *Advances in forensic taphonomy (method, theory, and archaeological perspectives)*. Boca Raton, Florida: CRC Press LLC.

HEFNER, J.T. 2009. Cranial nonmetric variation and estimating ancestry, *Journal of Forensic Sciences* 54(5): 985-995.

HEFNER, J.T. & S.D. OUSLEY 2014. Statistical classification methods for estimating ancestry using morphoscopic traits, *Journal of Forensic Sciences* 59(4): 883-890.

HEFNER, J.T., M.K. SPRADLEY & B. ANDERSON 2014. Ancestry assessment using random forest modelling, *Journal of Forensic Sciences* 59(3): 583-589.

HERMANN, N.P. 2002. GIS applied to bioarchaeology: an example from the Rio Talgua Caves in Northeast Honduras, *Journal of Cave and Karst Studies* 64(1): 17-22.

HERMANN, N.P. & J.B. DEVLIN 2008. Assessment of commingled human remains using a GIS-based approach in B.J. ADAMS, & J.E. BYRD (eds) *Recovery, analysis, and identification of commingled human remains: 257-269*. Totowa, NJ: Humana Press.

HERSHKOVITZ, I., B. LATIMER, O. DUTOUR, L.M. JELLEMA, S. WISH-BARATZ, C. ROTHSCHILD & B.M. ROTHSCHILD 1997. Why do we fail in aging the skull from the sagittal suture?, *American Journal of Physical Anthropology* 103(3): 393-399.

HOMANN HEIRS 2021. Map of Africa or Guinea, *Geographicus*. Available at: [https://www.geographicus.com/P/ctgy&Category\\_Code=homannheirs](https://www.geographicus.com/P/ctgy&Category_Code=homannheirs) (accessed on 12<sup>th</sup> December 2021).

HUNT, D.R. & J. ALBANESE 2005. History and demographic composition of the Robert J. Terry Anatomical Collection, *American Journal of Physical Anthropology* 127:406 – 417.

İŞCAN, M.S. 1992. A comparison of the Hamann–Todd and Terry collections, *Anthropologie* 30(1): 35-40.

JANTZ, R. L. & S.D. OUSLEY 2005. *FORDISC*, version 3.0. Knoxville, TN: University of Tennessee.

KARSTEN, J.K. 2018. A test of the preauricular sulcus as an indicator of sex, *American Journal of Physical Anthropology* 165:604-608.

KENDELL, A. & P. WILLEY 2014. Crow Creek bone bed commingling: relationship between bone mineral density and minimum number of individuals and its effect on paleodemographic analyses, in A.J. OSTERHOLTZ, K.M. BAUSTIAN & D.L. MARTIN (eds) *Commingled and disarticulated human remains: working toward improved theory, method, and data: 85-104*. New York, NY: Springer New York

KERLEY, E.R. 1972. Special observations in skeletal identification, *Journal of Forensic Sciences* 17(3): 349-357.

KHANDARE, S.V., S. BHISE & A.B. SHINDE 2015. Age estimation from cranial sutures – a postmortem study, *International Journal of Healthcare and Biomedical Research* 3(3): 192-202.

KLALES, A.R., S.D OUSLEY & J.M. VOLLNER 2012. A Revised Method of Sexing the Human Innominate Using Phenice’s Nonmetric Traits and Statistical Methods, *American Journal of Physical Anthropology* 149(1): 104-14.

KLALES, A.R. 2013. Current practices in physical anthropology for sex estimation in unidentified adult individuals. *Proceedings of the 82nd Annual Meeting of the American Association of Physical Anthropologists*. Knoxville, TN.

KLALES, A.R. 2018. MorphoPASSE: the morphological pelvis and skull sex estimation database. Topeka, KS: Washburn, University.



- KLALES, A.R. 2020. Examining the reliability of morphological traits for sex estimation, *Forensic Anthropology* 3(3): 139-150.
- KLALES, A.R., M. KENYHERCZ, K. STULL, K. MCCORMICK & S. CALL 2016. Worldwide population variation in pelvic sexual dimorphism: forensic applications of human skeletal biology and variation. *Presented at the 2016 Annual Meeting of the American Association of Physical Anthropologists: 5-6. Atlanta, GA.*
- KNÜSEL, C.J. & A.K. OUTRAM 2004. Fragmentation: the zonation method applied to fragmented human remains from archaeological and forensic contexts, *Environmental Archaeology: The Journal of Human Palaeoecology* 9(1): 85-98.
- KROGMAN, W.M. 1962. *The human skeleton in forensic medicine*. Springfield, Ill: Charles C Thomas Publisher Ltd.
- LANGLEY, N.R., L.M. JANTZ, S.D. OUSLEY, R.L. JANTZ, G. MILNER 2016. *Data collection procedures for forensic skeletal material 2.0*. Knoxville, TN: University of Tennessee Forensic Anthropology Center.
- LANGLEY, N.R., B. DUDZIK & A. CLOUTIER 2018. A decision tree for nonmetric sex assessment from the skull, *Journal of Forensic Sciences* 63(1): 31-37.
- LEGARDE, C.B. 2019. Preliminary findings from a visual pair-matching study in a large commingled assemblage, *Forensic Anthropology* 2(2):65–71.
- LESCIOTTO, K. & L. DOERSHUK 2018. Effect of age on nonmetric cranial traits for sex estimation in adults, *Forensic Anthropology* 1(3): 150-159.
- LEWIS, C.J. & H.M. GARVIN 2016. Reliability of the Walker cranial nonmetric method and implications for sex estimation, *Journal of Forensic Sciences* 61(3): 743-751.
- LONG, H. & A.R. KLALES 2020. Application of the Optimized summed score attributes method for sex estimation, *Forensic Anthropology* 3(4): 224–233.
- LOTTERING, N., D.M. MACGREGOR, C.L. ALSTON & L.S. GREGORY 2015. Ontogeny of the sphenoid-occipital synchondrosis in a modern Queensland, Australian population using computed tomography, *American Journal of Physical Anthropology* 157(1): 42-57.
- LOVEJOY, C.O., R.S. MEINDL, T.R. PRYZBECK, R.P. MENSFORTH 1985. Chronological metamorphosis of the auricular surface of the ilium: a new method for the determination of adult skeletal age at death, *American Journal of Physical Anthropology* 68: 15-28.
- LYMAN, R.L. 2008. *Quantitative paleozoology*. New York, NY: Cambridge University Press.
- MACK, J.E., A.J. WATERMAN, A. RACILA, J.A. ARTZ & K.T. LILLIOS 2016. Applying zooarchaeological methods to interpret mortuary behaviour and taphonomy in commingled burials: the case study of the late neolithic site of Bolores, Portugal, *International Journal of Osteoarchaeology* 26(3): 524-536.

Malta in 360. Available at:  
<https://maltain360.com/page.aspx?ref=110023746> (accessed on 1<sup>st</sup> December 2021).

Malta Independent. Isn't it time to solve some of St Gregory's mysteries? 24 August 2014. Available at:  
<https://www.independent.com.mt/articles/2014-07-16/news/isnt-it-time-to-solve-some-of-st-gregorys-mysteries-5818056708> (accessed 1<sup>st</sup> March 2021).

Malta Parish Archives. Available at:  
<https://www.maltaparisharchives.org/> (accessed on 1<sup>st</sup> December 2021).

MANNING, P. 2017. Slavery & slave trade in West Africa 1450-1930, in E.K. Akyeampong (ed.) *Themes in West Africa's history*: 99-117. Available at:  
<https://www.cambridge.org/core/books/abs/themes-in-west-africas-history/slavery-slave-trade-in-west-africa-4501930/0FC9D05AA24662CD804226EFD05C13EC> (accessed on 1<sup>st</sup> October 2021).

MAREAN, C.W., Y. ABE, P.J. NILSSEN & E.C. STONE 2001. Estimating the minimum number of skeletal elements (MNE) in zooarchaeology: a review and a new image-analysis GIS approach, *American Antiquity* 66(2): 333-348.

MÁRQUEZ-GRANT, N. 2015. An overview of age estimation in forensic anthropology: perspectives and practical considerations, *Annals of Human Biology* 42(4): 308-322.

MARTIN, D.L., N.J. AKINS & H.W. TOLL 2013. Disarticulated and disturbed, processed and eaten? Cautionary notes from the La Plata assemblage (AD 1000–1150), in A.J. OSTERHOLTZ, K.M. BAUSTIAN & D.L. MARTIN (eds) *Commingle and disarticulated human remains: working toward improved theory, method, and data*: 129-147. New York, NY: Springer.

MAYS, S. 2010. *The archaeology of human bones*. Milton: Taylor and Francis.

MCKERN, T.W. & T.D. STEWART 1957. Skeletal age changes in young American males. *U.S. Army Quartermaster Research and Development Command, Technical Report* EP-45.

MEEUSEN, R.A., A.M CHRISTENSEN & J.T. HEFNER 2015. The use of femoral neck axis length to estimate sex and ancestry, *Journal of Forensic Sciences* 60(5):1300-1304.

MEINDL, R.S. & C.O. LOVEJOY 1985. Ectocranial suture closure: a revised method for the determination of skeletal age at death based on the lateral-anterior sutures, *American Journal of Physical Anthropology* 68(1): 57-66.

MERCIECA, S. 2008. The ownership of black slaves in Malta, *The Malta Independent on Sunday*, 15 June 2008, pp. 31-33.

- MOLNÁR, M. 2020. AMS C14 analysis report (HEKAL Project Code:I-2219). Unpublished report, Isotoptech ZRT Debrecen, Hungary. Courtesy of Heritage Malta.
- MOORE, M.K. 2013. Sex estimation and assessment, *Research Methods in Human Skeletal Biology*: 91-116. Elsevier Inc.
- MORAITIS, K. & C. SPILIOPOULOU 2006. Identification and differential diagnosis of perimortem blunt force trauma in tubular long bones, *Forensic Science, Medicine, and Pathology* 2(4): 221-229.
- MORAITIS, K. & C. SPILIOPOULOU 2009. Fracture characteristics of perimortem trauma in skeletal material, *The Internet Journal of Biological Anthropology* 3(2): 1-8.
- MULHERN, D.M. & E.B. JONES 2005. Test of revised method of age estimation from the auricular surface of the ilium, *American Journal of Physical Anthropology* 126:61– 65.
- NAGPRA 1990 Native American Graves Protection and Repatriation Act. Available at <https://www.nps.gov/subjects/nagpra/index.htm> (accessed October 1<sup>st</sup>, 2021).
- OSBORNE, D.L, T. L. SIMMONS & S.P. NAWROCKI 2004. Reconsidering the auricular surface as an indicator of age at death, *Journal of Forensic Sciences* 49(5):1-7.
- OSTERHOLTZ, A.J. & A.L. STODDER 2010. Conjoining a neighbourhood: data structure and methodology for taphonomic analysis of the very large assemblage from Sacred Ridge, *American Journal of Physical Anthropology*: 183.
- OSTERHOLTZ, A.J., K.M. BAUSTIAN, D.L. MARTIN & D.T. POTTS 2013. Commingled human skeletal assemblages: integrative techniques in determination of the MNI/MNE, in A.J. OSTERHOLTZ, K.M. BAUSTIAN & D.L. MARTIN (eds) *Commingled and disarticulated human remains: working toward improved theory, method, and data*: 35-50. New York, NY: Springer New York.
- OSTERHOLTZ, A.J., K.M. BAUSTIAN & D.L. MARTIN (eds) 2014. *Commingled and disarticulated human remains: working toward improved theory, method, and data*. New York, NY: Springer New York.
- OUTRAM, A.K., C.J. KNÜSEL, S. KNIGHT & A.F. HARDING 2005. Understanding complex fragmented assemblages of human and animal remains: a fully integrated approach, *Journal of Archaeological Science* 32(12): 1699-1710.
- PALMIOTTO, A., C.A BROWN & C.B LEGARDE 2019a. Estimating the number of individuals in a large commingled assemblage, *Forensic Anthropology* 2(2): 129–138.
- PALMIOTTO, A., C.A BROWN & M. MEGYESI 2019b. Introduction: commingled human remains special issue, *Forensic Anthropology* 2(2): 61-64.

- PARKER PEARSON, M. 2001. *The archaeology of death and burial*. London: Sutton.
- PARKINSON, J.A. 2018. Revisiting the hunting-versus-scavenging debate at FLK Zinj: A GIS spatial analysis of bone surface modifications produced by hominins and carnivores in the FLK 22 assemblage, Olduvai Gorge, Tanzania, *Palaeogeography, Palaeoclimatology, Palaeoecology* 511: 29-51.
- PÉREZ, V.,R. 2012. The taphonomy of violence: recognizing variation in disarticulated skeletal assemblages, *International Journal of Paleopathology* 2(2-3): 156-165.
- PERIZONIUS, W.R.K. 1979. Non-metric cranial traits: sex difference and age dependence, *Journal of Human Evolution* 8(7): 679-684.
- PERIZONIUS, W.R.K. 1984. Closing and non-closing sutures in 256 crania of known age and sex from Amsterdam (A.D. 1883–1909), *Journal of Human Evolution* 13(2): 201-216.
- PHENICE, T.W. 1969. A newly developed visual method of sexing the os pubis, *American Journal of Physical Anthropology* 30(2): 297-301.
- PINHEIRO, J. 2006. Decay process of a cadaver, in A. SCHMIDT, E. CUNHA, & J. PINHEIRO (eds) *Forensic anthropology and medicine: complementary sciences from recovery to cause of death*: 85-116. Totowa, NJ: Humana Press.
- PLENS, C.R., C.D. DE SOUZA, J. ALBANESE, T.T.L. CAPP & L.A. SAAVEDRA DE PAIVA 2021. Reflections on methods to estimate race and ancestry on reference osteological samples in the Brazilian context, *Ethics, Medicine, and Public Health* 18.
- POKINES, J., S.A. SYMES & C. ROPER 2014. *Manual of forensic taphonomy*. Baton Rouge, FL: CRC Press.
- RAMASWAMY, S. & J. PACE 1979. The medieval skeletal remains from St Gregory's church at Żejtun (Malta): Part 1. Paleopathological Studies, *Archivio Italiano di Anatomia e di Embriologia* lxxxiv.
- RAMASWAMY, S. & J. PACE 1980. The medieval skeletal remains from St Gregory's church at Żejtun (Malta): Part II. Anthropological Studies, *Archivio Italiano di Anatomia e di Embriologia* lxxxv.
- RODRÍGUEZ-MARTÍN, C. 2006. Identification and differential diagnosis of traumatic lesions of the skeleton, in A. SCHMIDT, E. CUNHA, & J. PINHEIRO (eds) *Forensic anthropology and medicine: complementary sciences from recovery to cause of death*: 197-221. Totowa, NJ: Humana Press.
- ROGERS, T. & S. SAUNDERS 1994. Accuracy of sex determination using morphological traits of the human pelvis, *Journal of Forensic Sciences* 39(4):1047-56.
- ROKSANDIC, M. 2002. Position of skeletal remains as a key to understanding mortuary behavior, in W.D. HAGLUND & M.H. SORG (eds) *Advances in*

- forensic taphonomy (method, theory, and archaeological perspectives)*:99-117. Boca Raton, Florida: CRC Press LLC.
- ROSE, J. C., T.J. GREEN, & V.D. GREEN 1996. NAGPRA is forever: osteology and the repatriation of skeletons, *Annual Review of Anthropology* 25: 81-103.
- SCHEUER, L. & S. BLACK 2004. *The juvenile skeleton*. Amsterdam, NL: Elsevier Academic Press
- SNOW, C.C. & E.D. FOLK 1970. Statistical assessment of commingled skeletal remains, *American Journal of Physical Anthropology* 32(3): 423-427.
- SNOW, C.C., S. BARTMAN, E. GILES & F.A. YOUNG 1979. Sex and race determination of crania by calipers and computer: A test of the Giles and Elliot discriminant functions in 52 forensic cases, *National Technical Information Service*: 1-16. Springfield, VA.
- SORG, M.H. 2019. Differentiating trauma from taphonomic alterations, *Forensic Science International (Online)*, 302.
- SPRADLEY, M.K. & R.L JANTZ 2011. Sex Estimation in Forensic Anthropology: Skull versus postcranial elements, *Journal of Forensic Sciences* 56(2): 289-296.
- SPRADLEY, M.K. 2016. History and development of metric and non-metric traits in forensic anthropology: forensic applications of human skeletal biology and variation. *Presented at the 2016 Annual Meeting of the American Association of Physical Anthropologists*: 6-7. Atlanta, GA.
- STAVROVA, T., A. BOREL, C. DAUJEARD & D. VETTESE 2019. A GIS based approach to long bone breakage patterns derived from marrow extraction, *PloS One* 14(5): 1-26.
- STEWART, T.D. 1979. *Essentials of forensic anthropology, especially as developed in the United States*. Springfield, Ill: Charles C Thomas Publisher Ltd.
- The Sunday Times of Malta. Skeletons found in hidden corridor, 15 April 1969, p. 9.
- SWGANTH, 2013. Scientific Working Group for Forensic Anthropology, *Ancestry Assessment: 1-4*. Available at: <http://www.swganth.org> (accessed on October 17<sup>th</sup> 2021).
- TODD, T.W. 1920. Age changes in the pubic bone: I. The white male pubis. *American Journal of Physical Anthropology* 3: 285-334.
- TODD, T.W. 1921. Age changes in the pubic bone: II. The pubis of the male Negro-White hybrid; III. The pubis of the White female; IV. the pubis of the female Negro-White hybrid. *American Journal of Physical Anthropology* 4: 1-70.
- TULLER, H., U. HOFMEISTER & S. DALEY 2008. Spatial analysis of mass grave mapping data to assist in the reassociation of disarticulated and commingled human remains, in B.J. ADAMS, & J.E. BYRD (eds) *Recovery, analysis, and identification of commingled human remains*: 7-29. Totowa, NJ: Humana Press.

- UBELAKER, D.H. & B.J. ADAMS 1995. Differentiation of perimortem and postmortem trauma using taphonomic indicators, *Journal of Forensic Sciences* 40 (3): 509-512.
- UBELAKER, D.H. 2002. Approaches to the study of commingling in human skeletal biology, in W.D. HAGLUND & M.H. SORG (eds) *Advances in forensic taphonomy (method, theory, and archaeological perspectives)*: 331-351. Boca Raton, Florida: CRC Press LLC.
- UBELAKER, D.H. 2008. Methodology in commingling analysis: an historical overview, in B.J. Adams & J.E. Byrd (eds) *Recovery, analysis, and identification of commingled human remains*:1-7. Totowa, NJ: Humana Press.
- URBANOVÁ, P. & A.H. ROSS 2016. Advanced methods in 3-D craniofacial morphological analysis, in M.A. Pilloud, & J.T. Hefner (eds) *Biological distance analysis: forensic and bioarchaeological perspectives*: 61-90. Amsterdam, Netherlands: Elsevier Inc.
- VELLA, F. 2014. L-attakk tat-Torok tal-1614: laqta folkloristika. *L-Imnara* 10 (3): 2-7.
- VELLA, F. 2018. A Curious Discovery, *The Sunday Times of Malta*, 25 March 2018. Available at: <http://fionavella.com/features/2018/03/a-curious-discovery/> (accessed 1<sup>st</sup> March 2021).
- VERTOT, R.A.D., 1989. *The history of the Knights of Malta*. Valletta, Malta: Midsea Books.
- WALKER, P.L. 2008. Sexing skulls using discriminant function analysis of visually assessed traits, *American Journal of Physical Anthropology* 136(1): 39-50.
- WEBB, P. & J. SUCHEY 1985. Epiphyseal union of the anterior iliac crest and medial clavicle in a modern multiracial sample of American males and females, *American Journal of Physical Anthropology* 68(4): 457-466.
- WETTINGER, G. 1969. The militia list of 1419-20: a new starting point for the study of Malta's population, *Melita Historica* 5(2): 80-105.
- WETTINGER, G. 1990. *Burials in Maltese churches:1419-1530s*, HYPHEN IV, 2:39-45, University of Malta.
- WETTINGER, G. 2002. *Slavery in the Islands of Malta and Gozo*. Malta: Publishers Enterprises Group.
- WETTINGER, G. 2006. *Black African slaves in Malta*. Malta University Publishers Ltd.
- WHITE, T.D. & P.A. FOLKENS 2005. *Human bone manual*. San Diego, CA: Elsevier Science & Technology.
- WHITE, T.D., M.T. BLACK & P.A. FOLKENS 2012. *Human osteology*, 3rd ed. Amsterdam, Netherlands: Elsevier Inc.

Żejtun Parish Archives. *Bapt. Mat. et Mort. Lib.I, 1580 -1606*, 509. Malta: Żejtun Parish.

Żejtun Parish Archives. *Baptiz. Lib. II - VI, 1606 - 1766*, 511 - 516. Malta: Żejtun Parish.

**APPENDIX I:** Full Inventory and raw data for analyses (Appendix I.A – I.G)

<https://docs.google.com/spreadsheets/d/1paLT4MuPmIQQJfabkTeHvhdeIWfEZQXk/edit?usp=sharing&oid=101795393457490739138&rtpof=true&sd=true>

**Appendix I.A:** Full Inventory

**Appendix I.B:** Taphonomy and GIS Data

**Appendix I.C:** Ossa Coxae Data

**Appendix I.D:** Crania Data

**Appendix I.E:** Cranial Sutures Data

**Appendix I.F:** Ancestry Data

**Appendix I.G:** Ancestry Worksheet Data



## **APPENDIX II: Glossary**

BMD	Bone Mineral Density
BRI	Bone Representation Index
CHR	Commingle Human Remains
DFA	Discriminant Function Analysis
GM	Geometric Morphometrics
GMI	Grand Minimum Total
ILD	Interlandmark Distance
MLNI	Most Likely Number of Individuals
MMS	Macromorphoscopic Traits
MNE	Minimum Number of Elements
MNI	Minimum Number of Individuals
MSP	Midsagittal Plane
NSIP	Number of Individual specimens
OSSA	Optimised Summed Scoring Attributes
SCH	Superintendence of Cultural Heritage
SOS	Spheno-occipital synchondrosis

### **Landmark Descriptions**

Glabella: most anterior midline point on frontal bone above nasion

Mastoid Process: conical prominence of bone on temporal bones posterior to the external auditory meatus (EAM).

Mental Eminence (or Mental Protuberance): bone protuberance on the midline of the mandible; attachment site for mentalis muscle. Lateral to this are the tubercles which may or may not be present

Nuchal Crest: transverse crest along squamous section of occipital bone; area of muscle and ligament attachment

Occipital Protuberance: section of occipital bone that protrudes below the nuchal crest

Supra-Orbital Margin: superior border of orbit

Supra-Orbital Ridge: brow above supraorbital region

**APPENDIX III:** List of Morphological pelvic traits used for sex determination. Adapted from Bass (2005:215) and Rogers and Saunders (1994:1051).

<b>Os Coxae</b>	<b>Male Expression</b>	<b>Female Expression</b>
1. Subpubic concavity angle	V-shaped	U-shaped
2. Ischiopubic ramus ridge	Ridge absent	Ridge present
3. Ventral Arc	Arc absent	Arc present
4. Shape of Pubic bone	Narrow	Broad
<b>Ilium</b>		
5. Sciatic notch – shape and size	Narrow, deep	Wide, shallow
6. Auricular surface height	Not raised	Raised
7. Preauricular sulcus	Absent /thin grooves	Large, circular depressions
8. Ilium shape	High, vertical	Lateral
<b>Pelvis</b>		
9. Obturator foramen	Large, oval	Small, triangular
10. Acetabulum	Large/directed laterally	Small, directed antero-laterally
11. Muscle markings	Marked, rugged	Gracile, smooth

**APPENDIX IV:** Cranial Landmarks used for non-metric sex estimation.  
Adapted from Bass (2012:81) and Klales and Cole (2018).

<b>Landmark</b>	<b>Male Expression</b>	<b>Female Expression</b>
1. General size	Larger, more robust	Smaller, smoother, gracile
2. Orbit shape	Square	Rounder
3. Supraorbital ridges	Robust, prominent	Gracile
4. Supraorbital margins	Thick and blunt	Sharp and thin
5. Temporal lines & nuchal crest	Robust	Smoother, less evident
6. Occipital protuberance	Robust	Smoother, gracile
7. Glabella	Robust	Slight to no projection
8. Mastoid process	Large, robust	Small, gracile
9. Zygomaticomaxillary process	Does not extend beyond EAM	Extends beyond EAM
10. Palate shape	Large	Smaller
11. Mental Eminence	Square, Tubercles	Rounder or Pointy

**APPENDIX V:** Craniometric Points on the Midsagittal Plane (MSP), following Bass (2005:67-69).

Unpaired Points, Abbreviations, Definitions

Alveolare	ids	Apex of septum between upper central incisors .
Prosthion	pr	Prealveolar point: Most anterior point in the midline on the upper alveolar process.
Nasospinale	ns	Lowest landmark for the measurement of nasal height. Point where a line drawn between lower margins of the right and left nasal apertures is intersected by the MSP.
Nasion	n	Uppermost landmark for the measurement of facial height. Intersection of nasofrontal suture with the MSP.
Glabella	g	Most forward projecting point in the midline of the forehead at the level of the supra-orbital ridges and above the nasofrontal suture.
Bregma	br	Intersection of the coronal and sagittal sutures, in midline.
Opisthocranion	op	Most posterior point on the skull, not on external occipital protuberance, instrumentally determined.
Basion	ba	Midpoint of the anterior margin of the foramen magnum most distant from the Bregma.
Alveolon	alv	Point on hard palate where a line drawn through the termini of the alveolar ridges crosses the median line.
Staphyllion	sta	Point in the midline of the back of the hard palate (interpalatal suture) where it is crossed by a line drawn tangent to the curves of the posterior margin of the palate.
Orale	ol	Point on hard palate where line drawn tangent to the curves in the alveolar margin back of the two medial incisor teeth crosses the MSP; opposite side of bone from the alveolare.

## APPENDIX V: Continued

### Paired Points, Abbreviations, Definitions

Euryon	Eu	Two points on opposite sides of the skull that form the termini of the lines of greatest breadth, instrumentally determined.
Alare	Al	Most lateral point on the nasal aperture taken perpendicular to the nasal height, instrumentally determined.
Zygion	Zy	Most lateral point of the zygomatic arch, instrumentally determined.
Ectomalare	Ecm	Most lateral point on the outer surface of the alveolar margins, usually opposite the middle of the upper second molar tooth.
Endomalare	Enm	Most medial point on the inner surface of the alveolar ridge opposite the middle of the second upper molar tooth.

**APPENDIX VI:** Important Indices used for comparative analysis. Adapted from Bass (2005:75-80).

Index	Calculation	Range		
<b>Bone Representation Index (BRI)</b>	$\frac{\text{MNE} \times 100}{\text{number of the elements in complete skeleton} \times \text{MNI}}$	Example: MNI =80, Expect 160 Femurs $80/160 \times 100 = 50\%$		
<b>Cranial Module (CM)</b>	$\frac{\text{length (gl-op)} + \text{breadth (eu-eu)} + \text{height (br-b)}}{3}$	Provides a numerical value for the size of the skull for comparative analysis.		
<b>Cranial Index (CI)</b>	$\frac{\text{maximum cranial breadth (eu-eu)} \times 100}{\text{maximum cranial length (gl-op)}}$	Dolichocrany Mesocrany Brachycrany Hyperbrachycrany	X - 74.99 75.00 - 79.99 80.00 - 84.99 85.00 - X	narrow or long average or medium broad or round headed very broad
<b>Nasal Index (NI)</b>	$\frac{\text{nasal breadth (al-al)} \times 100}{\text{nasal height (n-ns)}}$	Leptorrhiny Mesorrhiny Platyrrhiny	X to 47.99 48.00 to 52.99 53.00 to X	narrow nasal aperture average to medium broad nasal aperture
<b>Upper Facial Index (UFI)</b>	$\frac{\text{upper facial height (n-ids)} \times 100}{\text{bizygomatic breadth (zy-zy)}}$	Hypereuryeny Euryeny Meseny Lepteny Hyperlepteny	X - 44.99 45.00 - 49.99 50.00 - 54.99 55.00 - 59.99 60.00 - X	very wide of broad face wide or broad face average or medium slender or narrow face very slender or narrow face
<b>Maxilloalveolar Index (MI)</b>	$\frac{\text{maxilloalveolar breadth (ec-ec)} \times 100}{\text{maxilloalveolar length (pros-alv)}}$	Dolichurany Mesurany Brachyurany	X - 109.99 110.00 - 114.99 115.00 - X	long or narrow palate average or medium broad palate
<b>Palatal Index (PI)</b>	$\frac{\text{maximum palatal breadth} \times 100}{\text{maximum palatal length}}$	Leptostaphyline Mesostaphyline Brachystaphyline	X - 79.99 80.00 - 84.99 85.00 - X	narrow palate average of medium broad palate

**APPENDIX VII.A:** Phases of morphological changes in the Pubic Symphysis  
– Age estimation using the Suchey-Brooks Method, following Brooks & Suchey (1990:232-233).

*Phase I*

Symphyseal face has a billowing surface (ridges and furrows) which usually extends to include the pubic tubercle. The horizontal ridges are well-marked and ventral beveling may be commencing. Although ossific nodules may occur on the upper extremity, *a key to the recognition of this phase is the lack of delimitation of either extremity (upper or lower).*

*Phase II*

The symphyseal face may still show ridge development. *The face has commencing delimitation of lower and/or upper extremities occurring with or without ossific nodules.* The ventral rampart may be in beginning phases as an extension of the bony activity at either or both extremities.

*Phase III*

Symphyseal face shows lower extremity and *ventral rampart in process of completion.* There can be a continuation of fusing ossific nodules forming the upper extremity and

along the ventral border. Symphyseal face is smooth or can continue to show distinct ridges. Dorsal plateau is complete. Absence of lipping of symphyseal dorsal margin; no bony ligamentous outgrowths.

*Phase IV*

Symphyseal face is generally fine grained although remnants of the old ridge and furrow system may still remain. *Usually the oval outline is complete at this stage, but a hiatus can occur in upper ventral rim.* Pubic tubercle is fully separated from the symphyseal face by definition of upper extremity. The symphyseal face may have a distinct rim. Ventrally, bony ligamentous outgrowths may occur on inferior portion of pubic bone adjacent to symphyseal face. If any lipping occurs it will be slight and located on the dorsal border.

*Phase V*

*Symphyseal face is completely rimmed with some slight depression of the face itself, relative to the rim.* Moderate lipping is usually found on the dorsal border with more prominent ligamentous outgrowths on the ventral border. There is little or no rim erosion. Breakdown may occur on superior ventral border.

*Phase VI*

*Symphyseal face may show ongoing depression as rim erodes.* Ventral ligamentous attachments are marked. In many individuals the pubic tubercle appears as a separate bony knob. The face may be pitted or porous, giving an appearance of disfigurement with the ongoing process of erratic ossification. Crenulations may occur. The shape of the face is often irregular at this stage.



**APPENDIX VII.B:** Suchey-Brooks method: Associated ages with phases to estimate age - based on descriptions of morphological changes in the pubic symphysis, following Brooks & Suchey (1990:233).

Descriptive Statistics:

Phase	<i>Female (n = 273)</i>			<i>Male (n = 739)</i>		
	Mean	Standard Dev.	95% range	Mean	Standard Dev.	95% range
1	19.4	2.6	15-24	18.5	2.1	15-23
2	25.0	4.9	19-40	23.4	3.6	19-34
3	30.7	8.1	21-53	28.7	6.5	21-46
4	38.2	10.9	26-70	35.2	9.4	23-57
5	48.1	14.6	25-83	45.6	10.4	27-66
6	60.0	12.4	42-87	61.2	12.2	34-86

**APPENDIX VIII.A:** Morphological changes to the auricular surface – Age estimation, following Lovejoy *et al.* (1985) in White *et al.* (2012:401).

Phase 1: Age 20–24; billowing and very fine granularity

Phase 2: Age 25–29; reduction of billowing but retention of youthful appearance

Phase 3: Age 30–34; general loss of billowing, replacement by striae, coarsening of granularity

Phase 4: Age 35–39; uniform coarse granularity

Phase 5: Age 40–44; transition from coarse granularity to dense surface; this may take place over islands on the surface of one or both faces

Phase 6: Age 45–49; completion of densification with complete loss of granularity

Phase 7: Age 50–59; dense irregular surface of rugged topography and moderate to marked activity in periauricular areas

Phase 8: Age 60+; breakdown with marginal lipping, microporosity, increased irregularity, and marked activity in periauricular areas

**APPENDIX VIII.B:** Auricular surface – Scoring to determine age estimation based on revisions by Buckberry and Chamberlain (2002) in White *et al.* (2012:402).

Characteristic	Score	Description
Transverse organization	1	90% or more of surface is transversely organized
	2	50–89% of surface is transversely organized
	3	25–49% of surface is transversely organized
	4	Transverse organization is present on less than 25% of surface
	5	No transverse organization is present
Surface texture	1	90% or more of surface is <i>finely granular</i>
	2	50–89% of surface is <i>finely granular</i> ; replacement of finely granular bone by coarsely granular bone in some areas; no dense bone is present
	3	50% or more of surface is <i>coarsely granular</i> , but no dense bone is present
	4	<i>Dense bone</i> is present, but occupies less than 50% of surface; this may be just one small nodule of dense bone in very early stages
	5	50% or more of surface is occupied by <i>dense bone</i>
Microporosity	1	No microporosity is present
	2	Microporosity is present on one demiface only
	3	Microporosity is present on both demifaces
Macroporosity	1	No macroporosity is present
	2	Macroporosity is present on one demiface only
	3	Macroporosity is present on both demifaces
Apical changes	1	Apex is sharp and distinct; auricular surface may be slightly raised relative to adjacent bone surface
	2	Some lipping is present at apex, but shape of articular margin is still distinct and smooth (shape of outline of surface at apex is a continuous arc)
	3	Irregularity occurs in contours of articular surface; shape of apex is no longer a smooth arc

**APPENDIX IX:** Cranial suture observation sites and definitions, used to estimate age, following Meindl and Lovejoy (1985:59).

Parietomastoid: point on the parieto-mastoid suture lying 1 cm anterior of asterion

Squamosal: point on the squamosal suture lying directly superior to the postglenoid tubercle

Occipitomastoid: point on the occipitomastoid suture at its intersection with a line connecting the apices of the mastoid processes

Zygomatic: midpoint of the external surface of the zygomaticotemporal suture

Malar: point on the zygomaticomaxillary suture directly lateral to the infraorbital foramen

Frontolacrimal: at lacrimale (juncture of the posterior lacrimal crest and frontal bone) on the frontolacrimal suture

Frontoethmoid: midpoint of the frontoethmoid suture

Midlambdoid: midpoint of each half of the lambdoid suture (in "pars intermedia" of the lambdoid suture)

Lambda: at lambda (in "pars lambdica" of sagittal and "pars lambdica" of lambdoid sutures)

Obelion: at obelion (in "pars obelica" of the sagittal suture)

Anterior sagittal: point on the sagittal suture at the juncture of the anterior one third and posterior two-thirds of its length (usually near the juncture of the "pars bregmatica" and "pars verticis" of the sagittal suture)

Bregma: at bregma (in "pars bregmatica" of the coronal and "pars bregmatica" of the sagittal sutures)

Midcoronal: midpoint of each half of the coronal suture (in "pars complicata" of the coronal suture)

Pterion: at pterion, the region of the upper portion of the greater wing of the sphenoid, usually the point at which the parietosphenoid suture meets the frontal bone

Sphenofrontal: midpoint of the sphenofrontal suture

Inferior sphenotemporal: point of the sphenotemporal suture lying at its intersection with a line connecting both articular tubercles of the temporomandibular joint

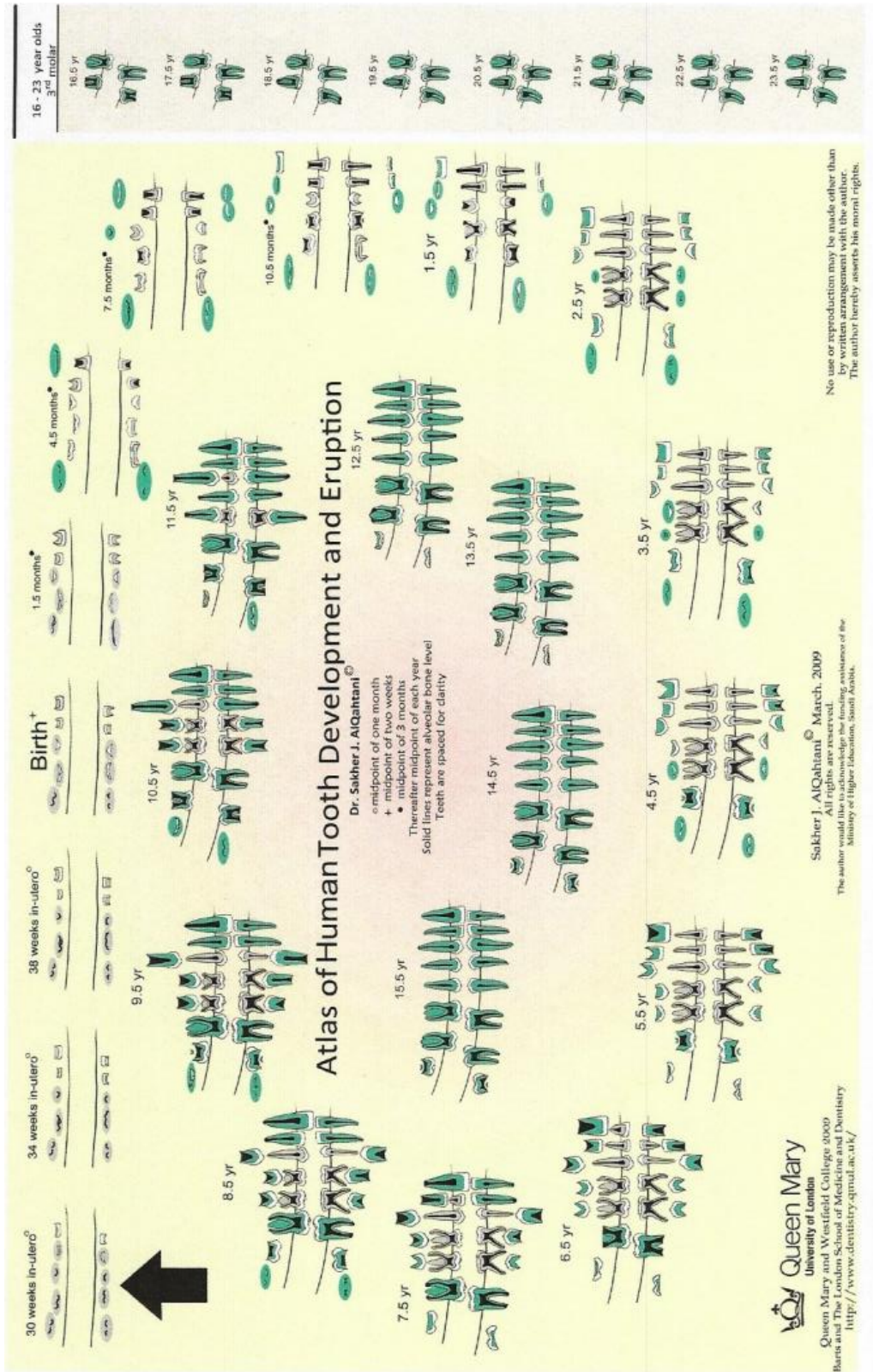
Superior sphenotemporal: point on the sphenotemporal suture lying 2 cm below its juncture with the parietal bone

**APPENDIX X:** Location of cranial sutures and scoring key to determine age following Meindl and Lovejoy (1985:60).

<i>Site</i>	<i>Description</i>
1 Midlambdoid	Midpoint of left lambdoid suture
2 Lambda	Intersection of sagittal and lambdoid sutures
3 Obelion	At obelion
4 Anterior sagittal	One-third the distance from bregma to lambda
5 Bregma	At bregma
6 Midcoronal	Midpoint of left coronal suture
7 Pterion	Usually where the parietosphenoid suture meets the frontal
8 Sphenofrontal	Midpoint of left sphenofrontal suture
9 Inferior sphenotemporal	Intersection of left sphenotemporal suture and line between articular tubercles of the temporomandibular joint
10 Superior sphenotemporal	On left sphenotemporal suture 2 cm below junction with parietal
11 Incisive suture	Incisive suture separating maxilla and premaxilla
12 Anterior median palatine	Score entire length on paired maxillae between incisive foramen and palatine bone
13 Posterior median palatine	Score entire length
14 Transverse palatine	Score entire length
15 Sagittal (endocr.)	Entire sagittal suture endocranially
16 Left lambdoid (endocr.)	Score indicated portion
17 Left coronal (endocr.)	Score indicated portion

Meindl and Lovejoy (1985) "vault" sutural ages (add scores for sites 1-7).			Meindl and Lovejoy (1985) "lateral-anterior" sutural ages (add scores for sites 6-10).		
<i>Composite Score</i>	<i>Mean Age</i>	<i>Standard Deviation</i>	<i>Composite Score</i>	<i>Mean Age</i>	<i>Standard Deviation</i>
0	—	—	0	—	—
1-2	30.5	9.6	1	32.0	8.3
3-6	34.7	7.8	2	36.2	6.2
7-11	39.4	9.1	3-5	41.1	10.0
12-15	45.2	12.6	6	43.4	10.7
16-18	48.8	10.5	7-8	45.5	8.9
19-20	51.5	12.6	9-10	51.9	12.5
21	—	—	11-14	56.2	8.5
			15	—	—

**APPENDIX XI:** Human tooth development following AlQahtani *et al.* (2010:485).



**APPENDIX XII:** Non-metric traits for ancestry determination, following White *et al.* (2012:423) citing Rhine (1990) and Gill (1995).

	Native Americans	European-Americans	African-Americans
<i>Incisors</i>	shovel-shaped	blade-form	blade-form
<i>Zygomastics</i>	robust, flaring	small, retreating	
<i>Prognathism</i>	moderate	very limited	marked alveolar and facial
<i>Palate</i>	elliptic	parabolic	hyperbolic
<i>Cranial sutures</i>	complex	simple	simple
<i>Nasal spine</i>	medium, "tilted"	long, large	small
<i>Chin</i>	blunt, median	square, bilateral, projecting	blunt, median, retreating
<i>Ascending ramus</i>	wide, vertical		narrow, oblique
<i>Palatine suture</i>	straight	jagged	arched
<i>Zygomatic tubercle</i>	present		
<i>Incisor rotation</i>	present		
<i>Nasal profile</i>	concavo-convex	straight	
<i>Sagittal arch</i>	low, sloping		
<i>Wormian bones</i>	present		
<i>Nasals</i>	low, tented	highly arched, steeplelike	low, flat
<i>Nasal aperture</i>	medium		wide
<i>Zygomaticomaxillary suture</i>	angled	curved	curved
<i>Dentition</i>		small, crowded	large molars
<i>Nasal sill</i>		very sharp	very dull or absent
<i>Nasion</i>		depressed	
<i>Cranial vault</i>		high	low
<i>Mandible</i>		cupping below incisors	
<i>Inion hook</i>		present	
<i>Postbregmatic depression</i>		present	

**APPENDIX XIII:** Ancestry determination measurements utilised, following worksheet and form created by Giles and Elliot (1962) and Gill (1984) as outlined in Bass (2005: 89).

Specimen: \_\_\_\_\_ Date: \_\_\_\_\_ Measured by: \_\_\_\_\_

MEASUREMENT	MALE		FEMALE		SEX
	WHT/NEG	WHT/IND	WHT/NEG	WHT/IND	
*1. Basion-Prosthion Ht. _____ x	+ 3.06 = _____	+ 0.10 = _____	+ 1.74 = _____	+ 3.05 = _____	1. _____ x - 1.00 = _____
*2. Glabell-Occip. Ln. _____ x	+ 1.60 = _____	- 0.25 = _____	+ 1.28 = _____	- 1.04 = _____	2. _____ x + 1.16 = _____
3. Maximum Width _____ x	- 1.90 = _____	- 1.56 = _____	- 1.18 = _____	- 5.41 = _____	5. _____ x + 1.66 = _____
4. Basion-Bregma Ht. _____ x	- 1.79 = _____	+ 0.73 = _____	- 0.14 = _____	+ 4.29 = _____	6. _____ x + 3.98 = _____
*5. Basion-Nasion Ht. _____ x	- 4.41 = _____	- 0.29 = _____	- 2.34 = _____	- 4.02 = _____	7. _____ x + 1.54 = _____
*6. Max Diam. Bi-zyg. _____ x	- 0.10 = _____	+ 1.75 = _____	+ 0.38 = _____	+ 5.62 = _____	TOTAL = _____
*7. Prosth-Nasion Ht. _____ x	+ 2.59 = _____	- 0.16 = _____	- 0.01 = _____	- 1.00 = _____	MALE _____ +
8. Nasal Width _____ x	+ 10.56 = _____	- 0.84 = _____	+ 2.45 = _____	- 2.19 = _____	FEMALE _____ -
TOTALS					891.12

\*These measurements are used for calculating sex.

**APPENDIX XIV:** List of Bone Elements for San Girgor assemblage with MNE, MNI and BRI.

R & P = Ramaswamy and Pace (1980) MNE; not idt = not identified

Bone Elements	Left	Right	Unknown	MNI	MNE R&P	MNE	Expected MNE	BRI	
<b>Crania</b>	--	--	--	35		36	35	92	38%
<b>Mandible</b>	--	--	--	29		29	29	92	32%
<b>Maxilla</b>	--	--	--	29		n/a	29	92	32%
<b>Vertebrae (total)</b>	--	--	--	--		197	73	2208	3%
<i>Vertebrae (not idt)</i>	--	--	--	--		--	64	--	--
<i>Cervical</i>	--	--	--	--		37	4	--	--
<i>Thoracic</i>	--	--	--	--		106	5	--	--
<i>Lumbar</i>	--	---	--	--		54	0	--	--
<b>Sacrum</b>		--	--	30		33	30	92	33%
<b>Clavicle</b>	14	23	--	23		32	37	184	20%



Bone Elements	Left	Right	Unknown	MNI	MNE R&P	MNE	Expected MNE	BRI	
<b>Scapula</b>	34	42	2	42		85	78	184	42%
<b>Ribs</b>	--	--	--	--		223	234	2208	11%
<b>Sternum</b>	--	--	--	8		7	8	92	9%
<b>Humerus</b>	92	81	3	92		160	176	184	96%
<b>Radius</b>	34	55	1	55		88	90	184	49%
<b>Ulna</b>	47	47	4	47		90	98	184	53%
<b>Carpals (total)</b>	--	--	--	--		3	8	4968	0.3%
<i>Scaphoid</i>	1			1		--	1	--	--
<i>Lunate</i>	1	1		2		--	2	--	--
<i>Triquetral</i>	1	--		1		--	1	--	--
<i>Capitate</i>	2	--		2		--	2	--	--
<i>Trapezium</i>	1	--		1		--	1	--	--

Bone Elements	Left	Right	Unknown	MNI	MNE R&P	MNE	Expected MNE	BRI
<i>Hamate</i>	1	--	--	1	--	1	--	--
<b>Metacarpals (total)</b>	--	--	--	--	57	58	920	5%
<i>1st Metacarpal</i>	5	--	--	5	--	5	--	--
<i>2nd Metacarpal</i>	12	4	--	16	--	16	--	--
<i>3rd Metacarpal</i>	9	9	--	18	--	18	--	--
<i>4th Metacarpal</i>	10	--	--	10	--	10	--	--
<i>5th Metacarpal</i>	5	4		5	--	9		
<b>Phalanges - Hand</b>			5	5	5	5	2576	0.2%
<b>Os Coxae</b>	43	34	5	43	70	82	184	45%
<b>Femur</b>	74	69	--	74	124	143	184	78%
<b>Patella</b>	1	1	--	2	1	2	184	1%
<b>Fibula</b>	77	72	4	77	156	153	184	83%

Bone Elements	Left	Right	Unknown	MNI	MNE R&P	MNE	Expected MNE	BRI	
<b>Tibia</b>	66	69	--	69		129	135	184	73%
<b>Tarsals (total)</b>	--	--	--	--		58	61	4784	1%
<i>Calcaneus</i>	15	18	--	18		32	33	--	--
<i>Talus</i>	8	12	1	12		20	21	--	--
<i>Navicular</i>	3	--	2	3		--	5	--	--
<i>Cuboid</i>	1	--	1	1		--	2	--	--
<i>Lateral cuneiform</i>	1	--	--	1		--	1	--	--
<i>Other</i>	--	--	--	--		3	--	--	--
<b>Metatarsals (total)</b>		--	--	--		93	99	920	11%
<b>Phalanges - Foot</b>	3	--	--	3		2	3	2576	0.1%
<b>Teeth</b>	--	--	--	--		n/a	115	2944	4%
<i>Loose</i>	--	--	--	--		n/a	29	--	--


Bone Elements	Left	Right	Unknown	MNI		MNE R&P	MNE	Expected MNE	BRI
<i>In Cranium</i>	--	--	--	--		n/a	50	--	--
<i>In Mandible</i>	--	--	--	--		n/a	22	--	--
<i>In Maxilla</i>	--	--	--	--		n/a	14	--	--

**APPENDIX XV:** Results of indices for those determined to be of sub-Saharan Ancestry.

F=Female F? = Probably Female

ID	Sex Metric	Sex Non-Metric	Age Range	CI Range	UFI Range	NI Range	MI Range	PI Range
<b>SGR2019/713</b>	F	F	39.4-41.1	Mesocrany - average or medium	Lepteny - slender or narrow face	Leptorrhiny - narrow nasal aperture	Mesurany - average	Brachystaphyline - broad palate
<b>SGR2019/714</b>	F	F	34.7-41.1	Mesocrany - average or medium	Euryeny - wide or broad face	Platyrrhiny - broad nasal aperture	Brachyurany - broad	Brachystaphyline - broad palate
<b>SGR2019/715</b>	F	F?	45.2-56.2	Mesocrany - average or medium	n/a	Platyrrhiny - broad nasal aperture	Brachyurany - broad	Brachystaphyline - broad palate
<b>SGR2019/754</b>	F	F?	51.5-56.2	Mesocrany - average or medium	Euryeny - wide of broad face	Platyrrhiny - broad nasal aperture	Brachyurany - broad	Brachystaphyline - broad palate
<b>SGR2019/1730</b>	F	F?	45.2-51.9	Dolichocrany - narrow or long	Meseny - average or medium	Mesorrhiny - average to medium	Dolichurany - long narrow palate	Brachystaphyline - broad palate

**APPENDIX XVI:** Radiocarbon dating results of samples taken from the human remains at San Girgor (Molnár 2020: 1-5 and 1-2). Courtesy of Matthew Grima, Heritage Malta and Ruben Abela, Wirt -iż-Żejtun. Note Page 2 of the Stable Isotope Analyses Report is blank and was not inserted below.

 <b>Isotoptech Zrt.</b> H-4025 Debrecen, Piac utca. 53. II/9. Tel: 06-30 206 6999, Fax: 06-52 403 921	<b>I S O T O P T E C H Z R T .</b> H-4025 Debrecen, Piac utca. 53. II/9. Tel: 06-30 206 6999, Fax: 06-52 403 921	
	Page: 1/5 Valid since: 2017.01.15.	<b>Fny08.5-19. AMS <sup>14</sup>C Analyses Report</b>

To:  
 Partner name: **Matthew Grima**  
 Organization/Institution: **Diagnostic Science Laboratories, Heritage Malta**  
 Partner address: **Heritage Malta, Conservation Division, Bighi, Kalkara KKR 1524, Malta**  
 Partner contact (tel/fax): **00356 79206702**  
 e-mail: **matthew.a.grima@gov.mt**

**AMS <sup>14</sup>C analyses report (HEKAL project code: I/2219)**

Dear Matthew Grima,

We have completed the AMS radiocarbon age determination on your 7 bone samples. The results are given below:

AMS <sup>14</sup> C Lab Code	HEKAL Sample Nr.	Sample name (sample material dated)	Conventional <sup>14</sup> C age (BP) (± 1σ)	Calibrated calendar age (cal) (1σ)
DeA-22630	I/2219/1	SGR2019/714.17	237 ± 25	AD 1640-1800
DeA-22631	I/2219/2	SGR2019/716.27	254 ± 26	AD 1640-1800
DeA-22632	I/2219/3	SGR2019/725.17	203 ± 26	AD 1650-1950*
DeA-22633	I/2219/4	SGR2019/755.27	164 ± 26	AD 1660-1950*
DeA-22634	I/2219/5	SGR2019/756.27	382 ± 26	AD 1440-1620
DeA-22635	I/2219/6	SGR2019/757.17	279 ± 26	AD 1520-1660
DeA-22636	I/2219/7	SGR2019/760.17	229 ± 25	AD 1640-1950*
	I/2219/8	SGRSRef-Soil sample		

Ranges marked with a \* are suspect due to impingement on the end of the calibration data set.

Pretreatment: collagen extraction, sealed tube combustion, sealed tube graphitization, AMS analyses  
 Quality control samples (accompanied with your samples during the whole preparation and C-14 analyses):


Internal lab standard, bone (HEKAL I/1277/1): conv. C-14 age: ~ 6800 yr BP

Internal lab standard, bone (HEKAL I/1703/3): conv. C-14 age: blank.

The results are quoted as their radiocarbon age in years before present (yr BP). The values are quoted corrected to -25‰ for δ<sup>13</sup>C. The radiocarbon age is the conventional uncalibrated <sup>14</sup>C age and is quoted in years "before present (BP)", where "present" has been defined as the expected natural level for -1950AD.



ISO 9001:2015, ISO 14001:2015 certified laboratory

 <b>Isotoptech Zrt.</b>	<b>I S O T O P T E C H Z R T .</b> H-4025 Debrecen, Piac utca. 53. II/9. Tel: 06-30 206 6999, Fax: 06-52 403 921	
	Page: 2/5 Valid since: 2017. 01. 15.	<b>Fny08.5-19. AMS <sup>14</sup>C Analyses Report</b>

We have also quoted the calibrated age by comparing the <sup>14</sup>C content to known-age tree-ring information, which is attached. I have attached a printout from Calib 7.0.4 ([www.calib.org](http://www.calib.org)).

Publications which might be cited when you publish the results above:

Molnár M, Rinyu L, Veres M, Seiler M, Wacker L, Snyal HA. 2013. EnvironMICADAS: a mini <sup>14</sup>C AMS with enhanced Gas Ion Source Interface in the Hertelendi Laboratory of Environmental Studies (HEKAL), Hungary. Radiocarbon 55 (2-3): 338-344.

Molnár M, Janovics R, Major I, Orsovszki J, Gőnczi R, Veres M, Leonard AG, Castle SM, Lange TE, Wacker L, Hajdas I, Jull AJT. 2013. Status report of the new AMS C-14 preparation lab of the Hertelendi Laboratory of Environmental Studies, Debrecen, Hungary. Radiocarbon 55 (2-3): 665-676.

Major I, Dani J, Kiss V, Melis E, Patay R, Szabó G, Hubay K, Túri M, Futó I, Huszánk R, Jull AJT, Molnár M. 2019. Adoption and evaluation of a sample pretreatment protocol for radiocarbon dating of cremated bones at HEKAL. Radiocarbon 61 (1): 159-171.

Major I, Futó I, Dani J, Cserpák-Laczi O, Gasparik M, Jull AJT, Molnár M. 2019. Assessment and development of bone preparation for radiocarbon dating at HEKAL. Radiocarbon 61 (5): 1551-1561.

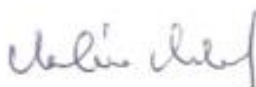
Please, contact us if you have any question.

Yours sincerely,

**Date:**

Debrecen, 14-02-2020

**Signature:**




Dr. Mihály Molnár PhD.  
(C-14 specialist)



Mihály Veres  
(CEO)



ISO 9001:2015, ISO 14001:2015 certified laboratory

 <b>Isotoptech Zrt.</b>	<b>I S O T O P T E C H Z R T .</b> <b>H-4025 Debrecen, Piac utca. 53. II/9.</b> <b>Tel: 06-30 206 6999, Fax: 06-52 403 921</b>	
	Page: 3/5	<b>Fny08.5-19. AMS <sup>14</sup>C Analyses Report</b>
Valid since: 2017.01.15.		

CALIB RADIOCARBON CALIBRATION PROGRAM\*  
 Copyright 1986-2017 M Stuiver and PJ Reimer

\*To be used in conjunction with:  
 Stuiver, M., and Reimer, P.J., 1993, Radiocarbon, 35, 215-230.

DeA-22630  
 I/2219/1  
 Radiocarbon Age 237±25  
 Calibration data set: intcal13.14c  
 # Reimer et al. 2013  
 1 Year moving average  
 One Sigma Ranges: [start:end] relative area  
                   [cal AD 1648: cal AD 1665] 0.691886  
                   [cal AD 1785: cal AD 1795] 0.308114  
 Two Sigma Ranges: [start:end] relative area  
                   [cal AD 1533: cal AD 1536] 0.003056  
                   [cal AD 1636: cal AD 1679] 0.617073  
                   [cal AD 1764: cal AD 1800] 0.339532  
                   [cal AD 1939: cal AD 1949\*] 0.04034

DeA-22631  
 I/2219/2  
 Radiocarbon Age 254±26  
 Calibration data set: intcal13.14c  
 # Reimer et al. 2013  
 1 Year moving average  
 One Sigma Ranges: [start:end] relative area  
                   [cal AD 1641: cal AD 1665] 0.843391  
                   [cal AD 1785: cal AD 1793] 0.156609  
 Two Sigma Ranges: [start:end] relative area  
                   [cal AD 1523: cal AD 1559] 0.133099  
                   [cal AD 1563: cal AD 1570] 0.007881  
                   [cal AD 1631: cal AD 1670] 0.680657  
                   [cal AD 1779: cal AD 1799] 0.166774  
                   [cal AD 1943: cal AD 1949\*] 0.011589

DeA-22632  
 I/2219/3  
 Radiocarbon Age 203±26  
 Calibration data set: intcal13.14c  
 # Reimer et al. 2013  
 1 Year moving average  
 One Sigma Ranges: [start:end] relative area  
                   [cal AD 1658: cal AD 1678] 0.305751  
                   [cal AD 1765: cal AD 1773] 0.105822  
                   [cal AD 1776: cal AD 1800] 0.430801  
                   [cal AD 1940: cal AD 1949\*] 0.157626  
 Two Sigma Ranges: [start:end] relative area  
                   [cal AD 1650: cal AD 1683] 0.286494  
                   [cal AD 1739: cal AD 1805] 0.570325  
                   [cal AD 1931: cal AD 1949\*] 0.143182



ISO 9001:2015, ISO 14001:2015 certified laboratory




DeA-22633  
 I/2219/4  
 Radiocarbon Age 164±26  
 Calibration data set: intcal13.14c  
 # Reimer et al. 2013  
 1 Year moving average  
 One Sigma Ranges: [start:end] relative area  
     [cal AD 1669: cal AD 1685] 0.167029  
     [cal AD 1731: cal AD 1780] 0.543592  
     [cal AD 1798: cal AD 1808] 0.111662  
     [cal AD 1927: cal AD 1945] 0.177717  
 Two Sigma Ranges: [start:end] relative area  
     [cal AD 1664: cal AD 1697] 0.177529  
     [cal AD 1724: cal AD 1789] 0.434019  
     [cal AD 1791: cal AD 1816] 0.11598  
     [cal AD 1834: cal AD 1878] 0.083718  
     [cal AD 1916: cal AD 1949\*] 0.188755

DeA-22634  
 I/2219/5  
 Radiocarbon Age 382±26  
 Calibration data set: intcal13.14c  
 # Reimer et al. 2013  
 1 Year moving average  
 One Sigma Ranges: [start:end] relative area  
     [cal AD 1451: cal AD 1497] 0.739228  
     [cal AD 1507: cal AD 1511] 0.052878  
     [cal AD 1601: cal AD 1616] 0.207894  
 Two Sigma Ranges: [start:end] relative area  
     [cal AD 1445: cal AD 1523] 0.705923  
     [cal AD 1560: cal AD 1560] 0.001613  
     [cal AD 1572: cal AD 1630] 0.292464

DeA-22635  
 I/2219/6  
 Radiocarbon Age 279±26  
 Calibration data set: intcal13.14c  
 # Reimer et al. 2013  
 1 Year moving average  
 One Sigma Ranges: [start:end] relative area  
     [cal AD 1525: cal AD 1556] 0.507434  
     [cal AD 1632: cal AD 1655] 0.492566  
 Two Sigma Ranges: [start:end] relative area  
     [cal AD 1517: cal AD 1595] 0.543455  
     [cal AD 1618: cal AD 1665] 0.444959  
     [cal AD 1786: cal AD 1792] 0.011587

DeA-22636  
 I/2219/7  
 Radiocarbon Age 229±25  
 Calibration data set: intcal13.14c  
 # Reimer et al. 2013  
 1 Year moving average  
 One Sigma Ranges: [start:end] relative area  
     [cal AD 1649: cal AD 1667] 0.575908  
     [cal AD 1783: cal AD 1796] 0.424092  
 Two Sigma Ranges: [start:end] relative area  
     [cal AD 1641: cal AD 1680] 0.531431  
     [cal AD 1740: cal AD 1742] 0.002689  
     [cal AD 1763: cal AD 1801] 0.404119  
     [cal AD 1938: cal AD 1949\*] 0.061761




 <b>Isotoptech Zrt.</b>	<b>I S O T O P T E C H Z R T .</b> H-4025 Debrecen, Piac utca. 53. II/9. Tel: 06-30 206 6999, Fax: 06-52 403 921	
	Page: 5/5	<b>Fny08.5-19. AMS <sup>14</sup>C Analyses Report</b>
Valid since: 2017. 01. 15.		

Ranges marked with a \* are suspect due to impingment on the end of the calibration data set

† Reimer PJ, Bard E, Bayliss A, Beck JW, Blackwell PG, Bronk Ramsey C, Buck CE  
 † Cheng H, Edwards RL, Friedrich M, Grootes PM, Guilderson TP, Haflidason H,  
 † Hajdas I, Hatté C, Heaton TJ, Hogg AG, Hughen KA, Kaiser KF, Kromer B,  
 † Manning SW, Niu M, Reimer RW, Richards DA, Scott EM, Southon JR, Turney CSM,  
 † van der Plicht J.  
 † IntCal13 and MARINE13 radiocarbon age calibration curves 0-50000 years calBP  
 † Radiocarbon 55(4). DOI: 10.2458/azu\_js\_rc.55.16947



ISO 9001:2015, ISO 14001:2015 certified laboratory

 <b>Isotoptech Zrt.</b> H-4025 Debrecen, Piac utca. 53. II/9. Tel: 06-30 206 6999, Fax: 06-52 403 921	<b>I S O T O P T E C H Z R T .</b>	
	Page: 1/1 Valid since: 2018. 10. 15.	<b>Fny08.5-65. Stable Isotope Analyses Report</b>

Partner name **Matthew Grima**  
 Organization/Institution: **Heritage Malta, Conservation Division**  
 Partner address **Bigħi, Kalkara KKR 1524, Malta**  
 e-mail: [matthew.a.grima@gov.mt](mailto:matthew.a.grima@gov.mt)

**$\delta^{13}\text{C}$ ,  $\delta^{15}\text{N}$  and C/N analyses report (HEKAL project code: I/2219)**

Dear Matthew Grima,

We have completed the  $\delta^{13}\text{C}$ ,  $\delta^{15}\text{N}$  and C/N determination of your 7 samples. The results are given below:

HEKAL Sample Nr.	Sample name (sample material)	$\delta^{13}\text{C}$ vs. PDB (‰) ( $\pm 0.15\%$ )	C content (%) ( $\pm 1\%$ )	$\delta^{15}\text{N}$ vs. air (‰) ( $\pm 0.15\%$ )	N content (%) ( $\pm 1\%$ )	C/N ratio
I/2219/1	SGR2019/714.17	-20.4	37.5	12.1	13.5	3.2
I/2219/2	SGR2019/716.27	-19.1	37.7	10.9	14.5	3.0
I/2219/3	SGR2019/725.17	-18.9	37.6	10.4	13.8	3.2
I/2219/4	SGR2019/755.27	-18.9	31.6	9.3	11.0	3.3
I/2219/5	SGR2019/756.27	-18.6	38.2	11.4	13.7	3.2
I/2219/6	SGR2019/757.27	-18.7	33.0	10.8	12.1	3.2
I/2219/7	SGR2019/760.17	-18.6	38.7	10.6	13.7	3.3

Please, contact us if you have any question.

Publications which might be cited when you publish the results above:


Majó I, Dani J, Kiss V, Melis E, Patay R, Szabó G, Hubay K, Tóti M, Futó I, Huszár R, Jull AJT, Molnár M. 2019. Adoption and evaluation of a sample pretreatment protocol for radiocarbon dating of cremated bones at HEKAL. *Radiocarbon*, 61 (1): 159-171.

Majó I, Futó I, Dani J, Csérik-Laczi O, Gasparik M, Jull AJT, Molnár M. 2019. Assessment and development of bone preparation for radiocarbon dating at HEKAL. *Radiocarbon* 61 (5): 1551-1561.

Yours sincerely,

Date:  
Debrecen, 28.01.2020

Signature:



Dr. István Futó  
(Stable isotope specialist)



Mihály Veres  
(CEO)

**APPENDIX XVII:** Baptisms and confirmation of enslaved persons 1586 -1693. Listed as noted in Żejtun Parish Archives and females are highlighted.

Date	Name	Status	Age	Sex	Owner
<b>Baptism</b>					
13/09/1586	Andreanna	Slave	--	F	Leonardo Tabuni di Casal Pasqualino
03/03/1587	Ursula	Black slave	Adult	F	Miser Masi Mizzi
12/04/1587	Juliana	Black slave	--	F	Blasco Habela di casal Pasqualino
24/12/1588	Lucia	Slave	Adult	F	Antonio Hablea
24/12/1588	Mario	Slave	Adult	M	--
24/12/1588	Marco	Slave	Adult	M	Leonardo Tabuni di Casal Pasqualino
26/12/1589	Juliana	Black slave	--	F	Miser Masi Tabuni
1589	Juliana	Black	--	F	Blasco Habela
10/09/1589	Albino	Slave	Adult	M	Gusman Bonichi
03/03/1589	Christoforo	Slave	Adult	M	Chierico Masi Bonichi
30/09/1591	Filippo	Black	Adult	M	Pietro Tabuni
03/10/1596	Gratio	Son of ? Black di A Habela	Child	M	A Habela
17/09/1598	Jacobo	Black	Adult	M	--
27/09/1598	Angelo	Black	Adult	M	Alessandro Tabuni di Casla Pasqualino
26/07/1599	Francesco	Black	--	M	Paulucio Habela di casal Pasqualino

Date	Name	Status	Age	Sex	Owner
<b>Baptism</b>					
06/1601	Vittoria	Black slave	--	F	Signora Isabella of Valletta and Gabriel Cassar casal Pasqualino
28/03/1605	Joannesdi di Machometto	Slave	Child?	M	--
01/06/1621	Martino	Black slave	--	M	Alessandro Tabuni
1622	Clemente	Slave	--	M	Sign. Mathiolo Delia
19/11/1622	Hieronymus Cagliares	Slave	--		Bishop Baldassare Cagliares
1686	Mattheo	Black	--	M	Signa. Angeluzza Habela
<b>Confirmation</b>					
?	Martino	Black slave	--	M	Sign. Alessandro Habela
1686	Mattheo	Black	--	M	Signora Angeluzza Habela
1686	Domenica	Daughter of Barbara the Black woman belonging to Habela	--	F	--
1686	Mariettina	Black slave	--	F	Sign. Gregorio Bonici
1686	Giorgio	Black slave	--	M	Sign. Chierico Marco Antonio Bonichi (Bonnici)
1686	Giorgio	Slave	--	M	Chierico Angelo Bonichi
1686	Angelo	White slave	--	M	Don Pietro sacerdote Busuttil
1693	Anna Maria	Slave	--	F	Sign. Thomaso Habela